

2004

Molecular Basis of Vertebrate Embryonic Migration

Paris A. Skourides

Follow this and additional works at: http://digitalcommons.rockefeller.edu/student_theses_and_dissertations

 Part of the [Life Sciences Commons](#)

Recommended Citation

Skourides, Paris A., "Molecular Basis of Vertebrate Embryonic Migration" (2004). *Student Theses and Dissertations*. Paper 37.



Molecular Basis of Vertebrate Embryonic Migration

**A thesis presented to the faculty of
The Rockefeller University
In partial fulfillment of the requirements for
the Degree of Doctor of Philosophy**

by

Paris A. Skourides

Acknowledgements

Many people have been a part of my graduate education- as friends, teachers, and colleagues. Without these people I would have never reached this stage for reasons too numerous to mention. Thanks to all the people who have helped me through my graduate career, including the following:

From the Brivanlou Lab:

I would like to thank my advisor, Dr. Ali Brivanlou for his continued guidance, support and understanding during the preparation of this dissertation and my entire tenure in his lab. I am most grateful to Ali for allowing me to follow my interests and for his ability to act as a mentor, a friend, a boss and a colleague depending on the circumstance. I would also like to thank, Dr. Curtis Altman for our numerous discussions and for his guidance, Dr. Francesca Spagnoli, Blaine Cooper, Mike Heke, Dr. Alin Vonica, Dr. Esther Bell, Dr. Ignacio Munoz, Dr. Daniel Besser and Alice Dyer.

Collaborators

The work on QD lineage tracing would not have been possible without our collaboration with the lab of Dr. Albert Libchaber. I would like to thank, Dr. Libchaber, Dr. Benoit Dubertret and Dr. Vincent Noireaux for countless discussions and giving me the opportunity to work with quantum dots.

My Thesis Committee

I am grateful to the members of my thesis committee, Dr. Robert Roeder and Dr. Robert Darnel for their advice and support. I would also like to thank Dr. Alexander Schier for taking the time and accepting to be my external committee member.

Other

Besides scientific help and guidance, a large number of people have contributed to my mental and emotional health and stability that, as it turns out, is just as important if one is to successfully finish a Phd! I would like to thank Dr. Malinda Stefanou for her unyielding support for the past two years, Stavros Papastavrou for his musical genius without whom I would have never had the courage to perform in professional music clubs let alone consider myself a singer, Christos Roushias for being there even at 5:00am when I needed him, Joel Lopez for being a great friend, and last but not least, my family which from thousands of miles away has always supported me more than one would deem possible.

CONTENTS

GENERAL INTRODUCTION – page 1

SECTION 1

Molecular Basis of the Morphogenetic Movements in *Xenopus*.

INTRODUCTION – page 3

CHAPTER 1

**Active Mesoderm Migration Requires the Focal Adhesion Kinase Activity During
Gastrulation in *Xenopus laevis*.**

Introduction – page 10

Results – page 13

Discussion – page 28

CHAPTER 2

Rap1b is Required for Morphogenetic Movements in *Xenopus laevis*.

Introduction – page 33

Results – page 34

Discussion – page 37

CHAPTER 3

Unbiased Screen for Factors Influencing Mesoderm Migration

Introduction – page 38

Results – page 38

CHAPTER 4

A Study of the Localization of Akt in Directionally Migrating Mesoderm

Introduction – page 43

Results - page 45

Discussion – page 50

SECTION 2

Quantum Dots in Biology

INTRODUCTION – page 52

CHAPTER 1

In Vivo use of micelle encapsulated QD nanocrystals

Introduction – page 54

Results – page 54

Discussion – 68

CHAPTER 2

QD accumulation in the nucleus at mid blastula transition

Results – page 71

Discussion – page 77

CHAPTER 3

Introduction – page 80

Results – page 83

Discussion – page 97

MATERIALS & METHODS

Page 99

REFERENCES

Page 104

GENERAL INTRODUCTION

Embryology aims at understanding how a single fertilized cell develops into a complex multicellular organism. Initially the embryo is no more than a ball of cells where the three primordial layers, the ectoderm, mesoderm and the endoderm are one on top of the other. The three germ layers will go on to form all the tissues and organs of the embryo. For example, the ectoderm will give rise to epidermis and the nervous system; the mesoderm to muscles, the skeletal system, the dermis or inner layer of the skin, the circulatory, excretory, and reproductive systems; and, finally, the endoderm will give rise to the inner lining of the alimentary canal and the structures derived from it, such as lungs, the liver, pancreas, and the bladder. Correct positioning of the germ layers paves the way for the inductive interactions that are the hallmark of both axis determination and organogenesis. Therefore, the formation of the body plan requires highly integrated and regulated cell movements. The study of these movements is central to the field of embryology.

Historically, the amphibian gastrula became one of the predominant models for experimental embryologists. This was partially due to the major influence of studies that lead to the eventual discovery of the organizer by Spemann and Mangold in 1924. After decades of research there is an imposing literature on the subject of inductive interactions in the amphibian and other embryos but the investigation of the movements leading from the relatively simple architecture of a blastula to the advanced and highly complex architecture of the late gastrula has been lacking. Perhaps it is not surprising, given the difficulties of studying these movements, that after almost a century of research fundamental questions still have not been answered. Haeckel first proposed the name “gastrula” in 1872, and although there was a long debate concerning the movements leading to the formation of the gastrula structures, the first experimental evidence for epiboly and inward morphogenetic movements was provided by Kopsch in 1895. Epiboly refers to the intercalation of cells in the animal cap ([Figure 1A, B and D](#)) while inward movements are the movements that lead to the internalization of the mesoderm, which is now referred to as involution ([Figure 1](#) compares the location of the orange

colored mesoderm at F stage 9 with that of G stage 10). The morphogenetic movements involved in gastrulation were later described by Vogt (1925, 1929) and then studied by Holtfreter (1943, 1944) and, more recently, by Keller (Gerhart and Keller 1986; Keller 1991; Weliky, Minsuk et al. 1991; Wilson and Keller 1991; Keller, Shih et al. 1992). The vast majority of this work was descriptive and only recently have we begun to gain some molecular insight regarding the pathways that are involved in specific morphogenetic movements.

This study will focus on cellular movements occurring during the gastrulation of the amphibian embryo by using *Xenopus laevis* as a model system. The amphibian gastrula is still a prevailing model for the study of morphogenesis and gastrulation today. Among the advantages that *Xenopus* offers are the large number of embryos, their size and the rate of development. Another major advantage is the fact that the blastulae can be dissected and the resulting explants can still undergo morphogenesis and they do so in complete temporal agreement with intact sibling embryos. This is an ideal property because an understanding of the individual movements is necessary in order to understand gastrulation. Breaking down the movements of gastrulation into their component events is very useful when attempting an interpretation of a complex change in the shape of an embryo.

The first section describes our efforts to uncover molecular components involved in one of the major gastrulation movements and integrating this movement in the gastrulation process. We have identified FAK as the first protein selectively involved in mesoderm migration and have shown that it is necessary for successful gastrulation. We have also identified a number of other genes involved in morphogenesis and we discuss their involvements in different movements. In the second section we describe work done to advance biological imaging using Quantum Dots (QD's), the inorganic nanocrystals that have been recently introduced as alternatives to existing fluorophores. We report the first successful use of QD's as lineage tracers in *Xenopus* and other biological models, discuss their intracellular behavior during the *Xenopus* development and describe the first *in situ* hybridization using QD nanocrystals.

SECTION 1

Molecular Basis of the Morphogenetic Movements in *Xenopus laevis*

Introduction

As discussed previously, the earliest stages of embryonic development require the formation of the three embryonic germ layers, establishment of cell fates and organ primordia, as well as highly coordinated cell movements that will ultimately establish the functional architecture of a mature embryo. While in the past decades, tremendous progress has been made in elucidating the molecular aspects of germ layer and cell type formation in the developing embryos, our knowledge about the molecular aspect of cell movements remains sparse. In vertebrates the first movements of embryogenesis (also called morphogenetic movements) occur at the onset of gastrulation.

Gastrulation is a process involving highly integrated and regulated cell movements, which result in the correct placement of tissues and the formation of the basic body plan of the embryo. In the frog *Xenopus laevis*, where these movements have been studied extensively at the cellular level, five major morphogenetic movements have been characterized. The first is a process called epiboly, in which the cells of the prospective ectoderm located on top of the spherical embryo (or animal pole) move downward toward the equator (Keller 1980). Epiboly, is mediated at the cellular level by radial intercalation of the deep layers of the animal cap cells (Figure 1B and E). The animal cap, which is made of three cell layers during gastrulation, becomes a two-layered structure. The cells of the lower layer intercalate into the layers above. This creates a larger surface area, which pushes the cells down toward the equatorial region. While fibronectin has been suggested to be required for this process (Marsden and DeSimone 2001), nothing is known about the molecular mechanism underlying this active intercalation behavior.

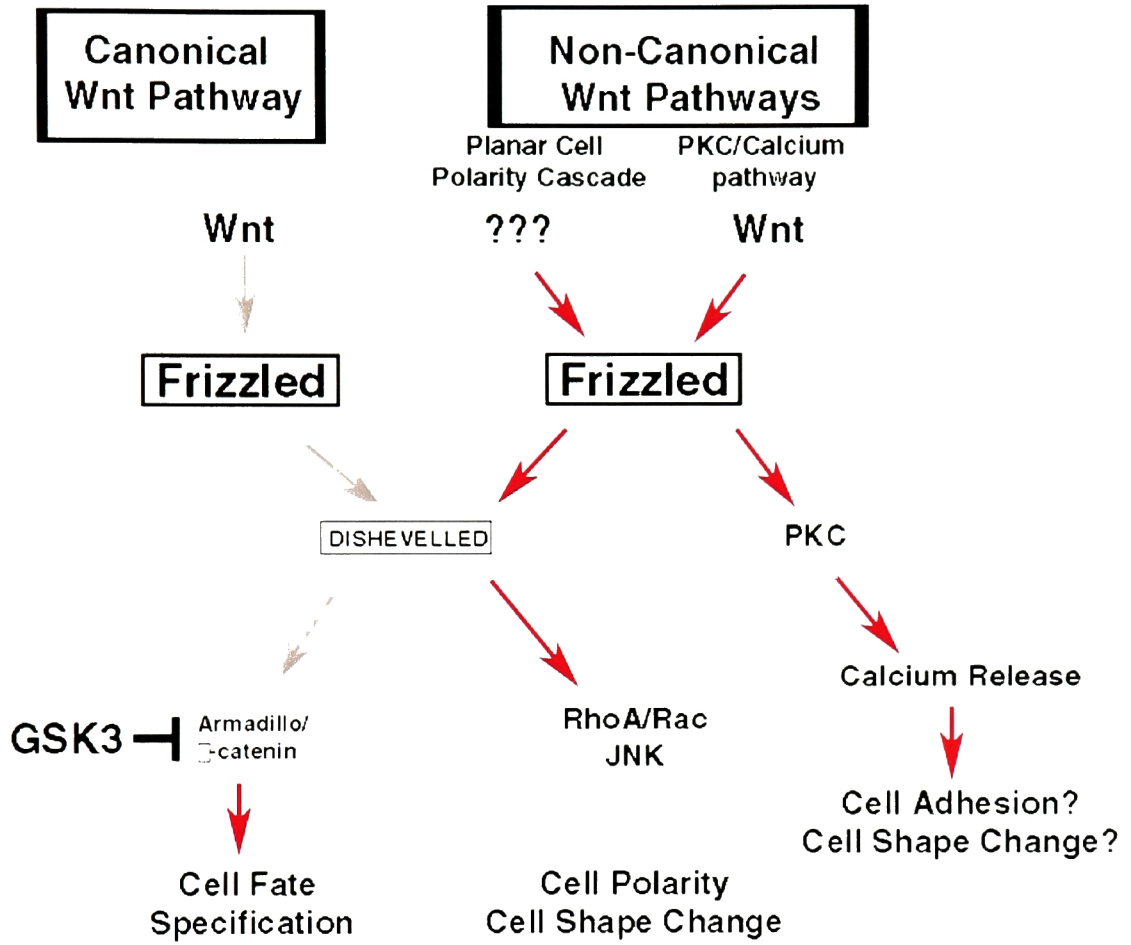
The second movement, convergent extension (Figure 1C and E), is a movement whereby the cells located in the dorsal region of the equatorial region (or marginal zone)

converge and extend toward the dorsal midline (Keller, Danilchik et al. 1985). Convergent extension is mediated at the cellular level by active movement of dorsal equatorial cells providing convergence and mediolateral intercalation, which ultimately gives rise to the extension of the anteroposterior axis (Keller, Danilchik et al. 1985). The cells adapt a clear polarity in their morphology during these movements. At the molecular level, while the pathways involved in the regulation of these movements are not well understood, experiments performed in *Xenopus* and Zebrafish have demonstrated that the Wnt pathway (Panel 1A), mediated by Disheveled (Dsh), plays a crucial role in the establishment of cell polarity (Tada and Smith 2000; Wallingford and Harland 2001). JNK was also shown to be part of the non-canonical Wnt pathway and is involved in convergent extension movements (Yamanaka, Moriguchi et al. 2002).

The third movement is involution (Figure 1 C), a process during which cells become internalized by invaginating and rolling over the blastopore lip. The first site of involution is directly below the dorsal marginal zone. The first pioneering cells that become internalized will form the prechordal plate (or head mesoderm) and are immediately followed by the cells of the axial mesoderm, contributing to the notochord. Involution then expands mediolaterally and, finally, ventrally until the invaginating cells form a full circle called the blastopore. Involution is preceded by the formation of bottle cells, which demarcate the site of invagination initially in the dorsal side (Keller 1981). The activin/nodal pathway, as well as the activation of the Wnt pathway, have been shown to induce the formation of ectopic bottle cells, but no additional molecular information is available about involution (Hardin and Keller 1988; Kurth and Hausen 2000).

In the fourth morphogenetic movement the cells of the endoderm located at the lower part of the embryo (vegetal pole), undergo upwelling movements (Figure 1D). These endodermal cell movements are assumed to occur in order to push and maintain the mesodermal precursors juxtaposed to the ectoderm. Nothing is known about the molecular aspect of endodermal movements (Winklbauer and Schurfeld 1999).

PANEL 1



Finally, once the cells invaginate inside the embryo and become apposed to the animal cap (with the help of vegetal rotation), the cells of the prechordal plate and notochord adhere to the fibronectin (FN) rich extracellular matrix (ECM) and start moving toward the animal pole by crawling on the blastocoel roof (Nakatsuji, Gould et al. 1982; Nakatsuji and Johnson 1982; Nakatsuji and Johnson 1983; Smith, Symes et al. 1990; Winklbauer 1990). This fifth discernable morphogenetic movement is called mesoderm migration (Figure 1C). Mesoderm migration has not been molecularly characterized and its role and importance during gastrulation have been debated. There are no known proteins that are selectively involved in this type of movement and no molecular pathways that are either required or inhibitory to it. Despite the lack of molecular information there is an abundance of descriptive work. Mesodermal cells, once involuted, adhere to the ECM of the blastocoel roof (Figure 1A and C), become flat, create a shingled arrangement, and extend numerous filopodia and lamellipodia. While active migration on fibronectin is cell autonomous (dissociated single cells will flatten adhere to the ECM and start migrating at the same time as explants would), the directionality of migration is not (Winklbauer 1990; Winklbauer and Nagel 1991; Winklbauer and Selchow 1992; Niehrs, Keller et al. 1993; Winklbauer, Nagel et al. 1996; Nagel and Winklbauer 1999). Directionality requires a community effect, since only mesodermal explants and not individual cells are able to migrate directionally on the ECM secreted by animal caps. Community effect is the requirement of a threshold number of cells in order to achieve the normal *in vivo* behavior.

The study of mesoderm migration, like the study of other morphogenetic movements, is complicated by the fact that any protein that has an effect on cell fate determination will inadvertently influence the morphogenesis of the tissue in which it is expressed. Different types of tissues undergo different morphogenetic movements, and in isolating pathways involved in movements, care needs to be taken to ensure no cell fate changes are brought about by activation or blockage of these pathways. An elegant example of such a pathway the Wnt pathway as mentioned before (Panel 1A) is involved in convergent extension (Sokol 1996; Wallingford and Harland 2001). The authors showed that, although the canonical Wnt pathway is involved in cell fate determination a

non-canonical pathway, goes through Disheveled (Dsh) just like the canonical pathway, leads to the polarization of mesodermal cells (which is required for convergent extension), it does so without affecting cell fate (Sokol 1996; Wallingford and Harland 2001).

We chose to study mesoderm migration due to the lack of any molecular information on this movement and because its role in gastrulation has not been determined. Our goal was to start revealing molecular aspects of the movement and ideally address its function during gastrulation in *Xenopus laevis*. To do this, two main approaches were taken. Firstly, a number of candidate genes were selected. We chose genes based on findings concerning their role in development of other models. Secondly, we performed an unbiased screen of gastrula stage cDNA libraries using gain of function, loss of function, and modifier screens. Our screens involved a number of assays we developed or adopted from previous studies using both explants as well as dissociated cells. These types of assays have been used in the past for the *in vitro* study of movements during the *Xenopus* gastrulation, and a general outline is shown in [Figure 1E](#) and [F](#) (Nakatsuji and Johnson 1982; Nakatsuji and Johnson 1983; Winklbauer 1990; Winklbauer and Nagel 1991; Wallingford and Harland 2001; Davidson, Hoffstrom et al. 2002). The chapters that follow deal with our efforts to start unveiling the molecular aspects of mesoderm migration in *Xenopus*.

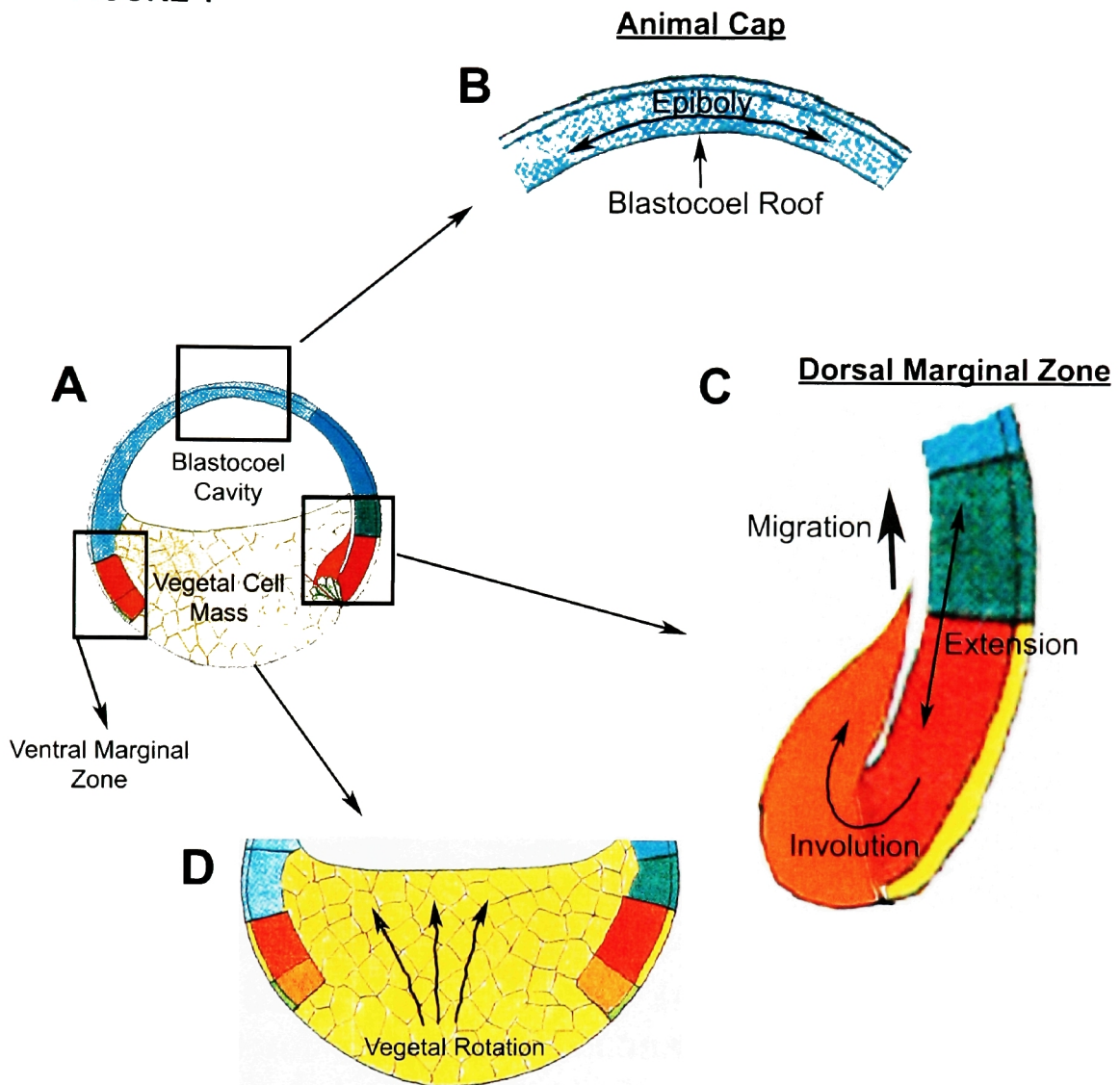
Finally, once the cells invaginate inside the embryo and become apposed to the animal cap (with the help of vegetal rotation), the cells of the prechordal plate and notochord adhere to the fibronectin (FN) rich extracellular matrix (ECM) and start moving toward the animal pole by crawling on the blastocoel roof (Nakatsuji, Gould et al. 1982; Nakatsuji and Johnson 1982; Nakatsuji and Johnson 1983; Smith, Symes et al. 1990; Winklbauer 1990). This fifth discernable morphogenetic movement is called mesoderm migration (Figure 1C). Mesoderm migration has not been molecularly characterized and its role and importance during gastrulation have been debated. There are no known proteins that are selectively involved in this type of movement and no molecular pathways that are either required or inhibitory to it. Despite the lack of molecular information there is an abundance of descriptive work. Mesodermal cells, once involuted, adhere to the ECM of the blastocoel roof (Figure 1A and C), become flat, create a shingled arrangement, and extend numerous filopodia and lamellipodia. While active migration on fibronectin is cell autonomous (dissociated single cells will flatten adhere to the ECM and start migrating at the same time as explants would), the directionality of migration is not (Winklbauer 1990; Winklbauer and Nagel 1991; Winklbauer and Selchow 1992; Niehrs, Keller et al. 1993; Winklbauer, Nagel et al. 1996; Nagel and Winklbauer 1999). Directionality requires a community effect, since only mesodermal explants and not individual cells are able to migrate directionally on the ECM secreted by animal caps. Community effect is the requirement of a threshold number of cells in order to achieve the normal *in vivo* behavior.

The study of mesoderm migration, like the study of other morphogenetic movements, is complicated by the fact that any protein that has an effect on cell fate determination will inadvertently influence the morphogenesis of the tissue in which it is expressed. Different types of tissues undergo different morphogenetic movements, and in isolating pathways involved in movements, care needs to be taken to ensure no cell fate changes are brought about by activation or blockage of these pathways. An elegant example of such a pathway the Wnt pathway as mentioned before (Panel 1A) is involved in convergent extension (Sokol 1996; Wallingford and Harland 2001). The authors showed that, although the canonical Wnt pathway is involved in cell fate determination a

non-canonical pathway, goes through Disheveled (Dsh) just like the canonical pathway, leads to the polarization of mesodermal cells (which is required for convergent extension), it does so without affecting cell fate (Sokol 1996; Wallingford and Harland 2001).

We chose to study mesoderm migration due to the lack of any molecular information on this movement and because its role in gastrulation has not been determined. Our goal was to start revealing molecular aspects of the movement and ideally address its function during gastrulation in *Xenopus laevis*. To do this, two main approaches were taken. Firstly, a number of candidate genes were selected. We chose genes based on findings concerning their role in development of other models. Secondly, we performed an unbiased screen of gastrula stage cDNA libraries using gain of function, loss of function, and modifier screens. Our screens involved a number of assays we developed or adopted from previous studies using both explants as well as dissociated cells. These types of assays have been used in the past for the *in vitro* study of movements during the *Xenopus* gastrulation, and a general outline is shown in [Figure 1E](#) and [F](#) (Nakatsuji and Johnson 1982; Nakatsuji and Johnson 1983; Winklbauer 1990; Winklbauer and Nagel 1991; Wallingford and Harland 2001; Davidson, Hoffstrom et al. 2002). The chapters that follow deal with our efforts to start unveiling the molecular aspects of mesoderm migration in *Xenopus*.

FIGURE 1



E

The Process of Cell Intercalation



Figure 1. The major morphogenetic movements in *Xenopus*. (A) The embryo at the initial stages of gastrulation. Involution has begun on the dorsal side (right side) but not on the ventral side. (B) Epiboly through radial intercalation leads to the increase of the ectodermal surface. (C) On the dorsal side convergent extension, involution and mesoderm migration are all taking place simultaneously leading to the internalization of the mesoderm. (D) Upwelling movements of the vegetal pole cells constitutes the movement of vegetal rotation which helps the internalization of the vegetal cell mass. (E) A schematic depicting how cell intercalation takes place. Intercalation is responsible for, epiboly and convergent extension.

FIGURE 1

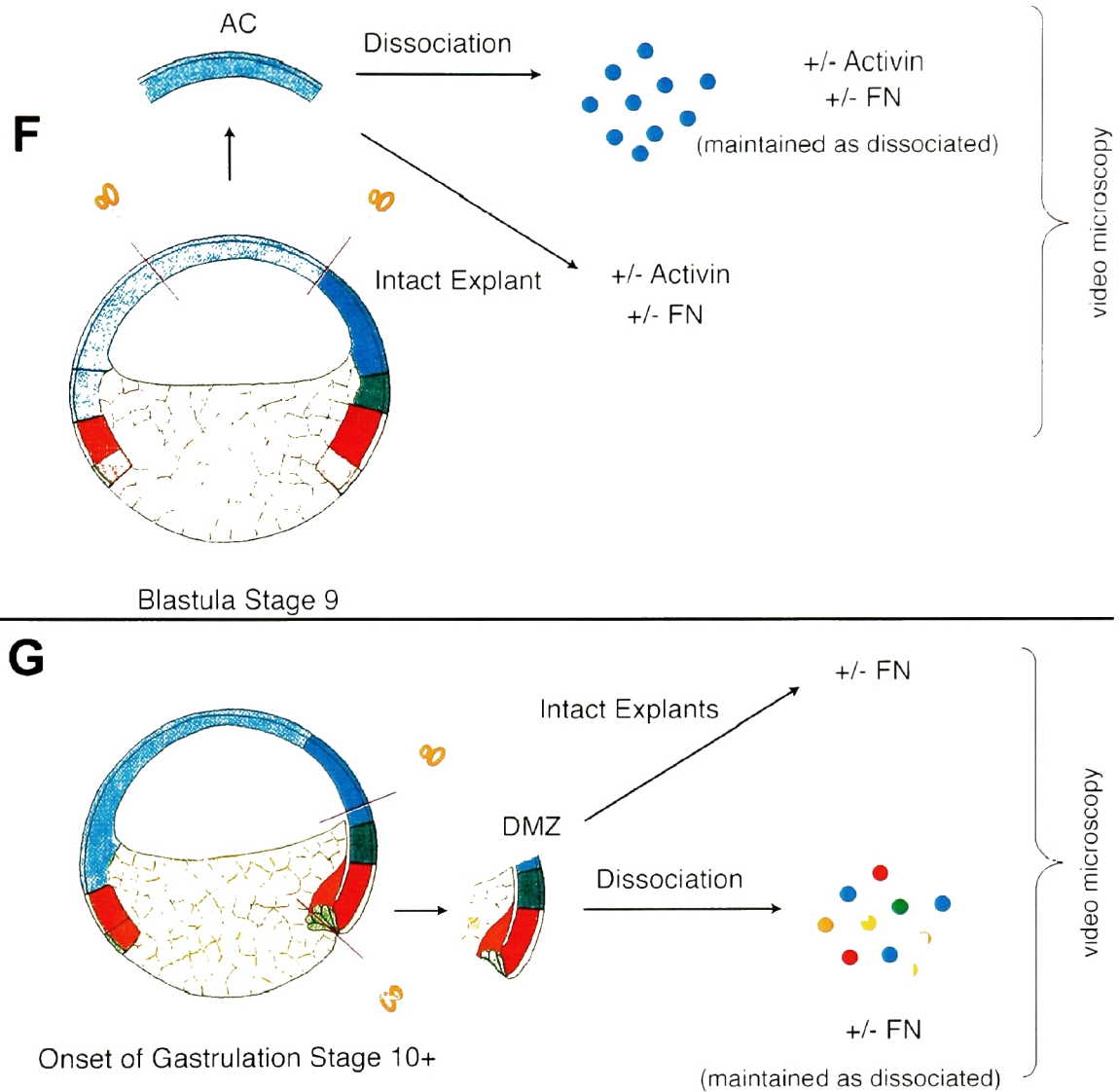


Figure 1 : A schematic diagram depicting the assays used to test motility as well as convergent extension. (top) Ectodermal explants from stage 9 embryos were dissected and placed on slides covered with FN or BSA. The solution in which they were plated either contained buffer or buffer + activin to induce mesoderm. These explants were then monitored using time lapse microscopy. Ectodermal explants were also used after being dissociated in $Ca^{2+}Mg^{2+}$ free buffer and were then plated on FN coated wells. These cells were either directly plated after dissociation or were treated with activin prior to plating. (bottom) DMZ explants were taken from stage 9 embryos and plated on FN coated slides or wells. They were also monitored by time lapse microscopy DMZ explants were also used after being dissociated in $Ca^{2+}Mg^{2+}$ free buffer In this case the DMZ explant was further trimmed to primarily contain anterior mesoderm. They were then plated on FN coated wells and time lapse microscopy was used to monitor their motility.

CHAPTER 1

Active Mesoderm Migration Requires the Focal Adhesion Kinase Activity During Gastrulation.

Introduction

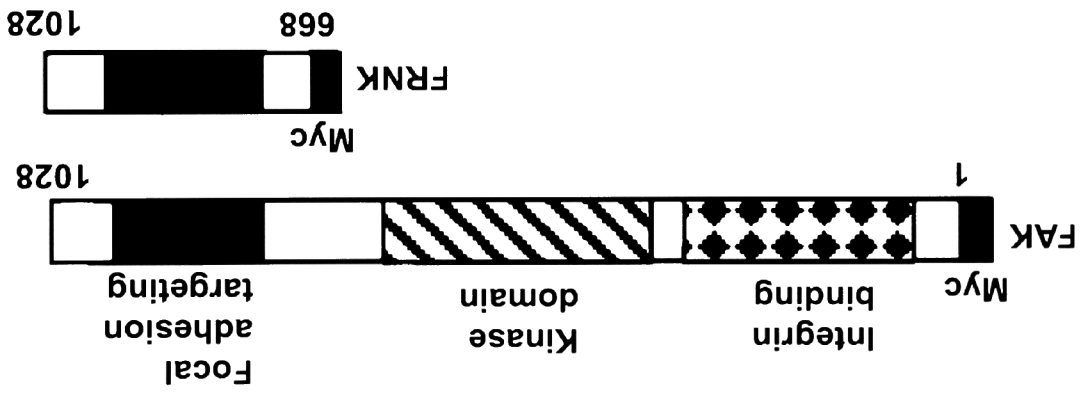
As mentioned above, the molecular pathways involved in active mesoderm migration are unknown. This has been mostly due to the inability to specifically inhibit active mesoderm migration without affecting other morphogenetic movements or cell fate. The assays used to address the role of active mesoderm migration in the past relied on blocking adhesion of mesodermal cells extracellularly using antibodies against fibronectin or peptides containing the RGD sequence (a sequence present in fibronectin's type III repeats and is responsible for cell adhesion onto FN), which were injected in the blastocoel cavity (Ramos and DeSimone 1996; Ramos, Whittaker et al. 1996; Winklbauer and Keller 1996; Marsden and DeSimone 2001). The aim of these experiments was to block the FN-Integrin interactions, and, as a result, block mesoderm migration. While these studies are suggestive and informative, they fall short in addressing two issues.

First there is no direct evidence that active mesoderm migration is inhibited *in vivo* when adhesion to fibronectin is blocked. Although it is clear that in such experiments the anterior-most of the migrating mesoderm becomes detached from the ECM, it is not clear whether posterior mesoderm still in contact with the ECM is migrating (Marsden and DeSimone 2001). Recent findings show that if the leading cells of a spreading mesodermal explant are blocked, and even become detached, the explant itself keeps moving forward, suggesting that inhibition of the anterior of a migrating explant would not block mesoderm migration (Davidson, Hoffstrom et al. 2002). Incomplete inhibition of mesoderm migration by blocking Integrin-FN interactions might also be explained by postulating that adhesion to fibronectin is blocked effectively, but adhesion to other ECM components is sufficient for migration.

Second, the specificity of the inhibition has not been proven as other morphogenetic movements that require an intact ECM (Epiboly for example), are also affected. The comparison of the phenotypes resulting from experiments where researchers are interfering with the FN-Integrin interactions lead to the conclusion that morphogenesis is disrupted in many ways (Ramos and DeSimone 1996; Ramos, Whittaker et al. 1996; Winklbauer and Keller 1996; Marsden and DeSimone 2001). These specificity issues with the use of antibodies had already been described following their use in other species, but in the absence of a better approach they were again used in *Xenopus* (Johnson, Darribere et al. 1993)..

We therefore aimed at identifying essential molecular components that would enable us to specifically inhibit mesoderm migration and overcome some of the shortcomings of previous attempts. A combination of three different assays were used encompassing dissociated cells, embryonic explants, and whole embryos with the help of high-resolution video microscopy (Figure 1F and G). We first demonstrate by loss of function studies that while the non-canonical *Wnt* pathway mediated by *disheveled* is essential for convergent extension, it has no input in active mesoderm migration, suggesting that the two movements have different molecular mechanisms. In asking what is involved molecularly, we provide direct evidence that *Xenopus* migrating mesodermal cells adhere to the ECM through highly dynamic focal adhesion complexes. The failure to detect such complexes in the migrating *Xenopus* mesoderm in previous studies appears to be due to their small size and weak fluorescence. In agreement with a role of the focal adhesions in mesoderm migration, we demonstrate that a specific non-receptor tyrosine kinase: the Focal Adhesion Kinase (FAK) is not only present in these focal adhesion complexes, but is also necessary for active mesoderm migration. This is the first protein to be implicated specifically in this morphogenetic movement. We show that inhibition of FAK activity at the focal adhesions with a splice variant form of FAK, called FRNK (Focal Adhesion related Non-Kinase), blocks active mesoderm adhesion spreading and migration. *FRNK* contains the C-terminus portion of *FAK* but lacks the kinase domain while at the same time maintains the focal adhesion localization sequence (panel 2). By competing with FAK at the focal adhesions, it acts as a strong negative

PANEL 2



regulator of focal adhesion formation (Schaller, Borgman et al. 1993; Gilmore and Romer 1996; Heidkamp, Bayer et al. 2002). FRNK finally enabled us to cell autonomously inhibit active mesoderm migration without affecting other morphogenetic movements or ECM assembly. We show that inhibition of active mesoderm migration by FRNK does not affect convergent extension and is specific, once again highlighting the molecular differences between the two types of gastrulation movements. Finally, we show that specific inhibition of active mesoderm migration leads to failure of blastopore closure. These results provide the first molecular characterization of this important morphogenetic movement and at the same time emphasize its importance for gastrulation.

Results

Dsh is not involved in active mesoderm migration.

Experiments in *Xenopus* embryos have demonstrated that mesodermal explants derived at blastula stages will either undergo convergent extension and elongate or will undergo active migration if placed on a fibronectin matrix (Figure 1F, movie7). *Disheveled* (*Dsh*) has been shown to be essential for convergent extension. A dominant negative form of *Dsh*, *Xddl*, has been shown to specifically block convergent extension movements by affecting cell polarity without affecting mesoderm induction (Tada and Smith 2000; Wallingford and Harland 2001).

In order to address the molecular pathways involved in mesoderm migration, we began by investigating the role of the Wnt pathway in this morphogenetic movement. Figure 2B shows that injection of *Xddl* at the dorsal marginal zone, in agreement with published observations, leads to curved embryos with the tailbud and the head juxtaposed due to inhibition of convergent extension on the dorsal side (Sokol 1996; Wallingford and Harland 2001). Anterior mesoderm explants from *Xddl+GFP* and *GFP* injected embryos were then dissected, dissociated in calcium magnesium free media (CMFM), and then plated onto FN coated wells. The *Xddl* injected cells showed no reduction of migratory activity as determined by average speed of migration, which was

FIGURE 2

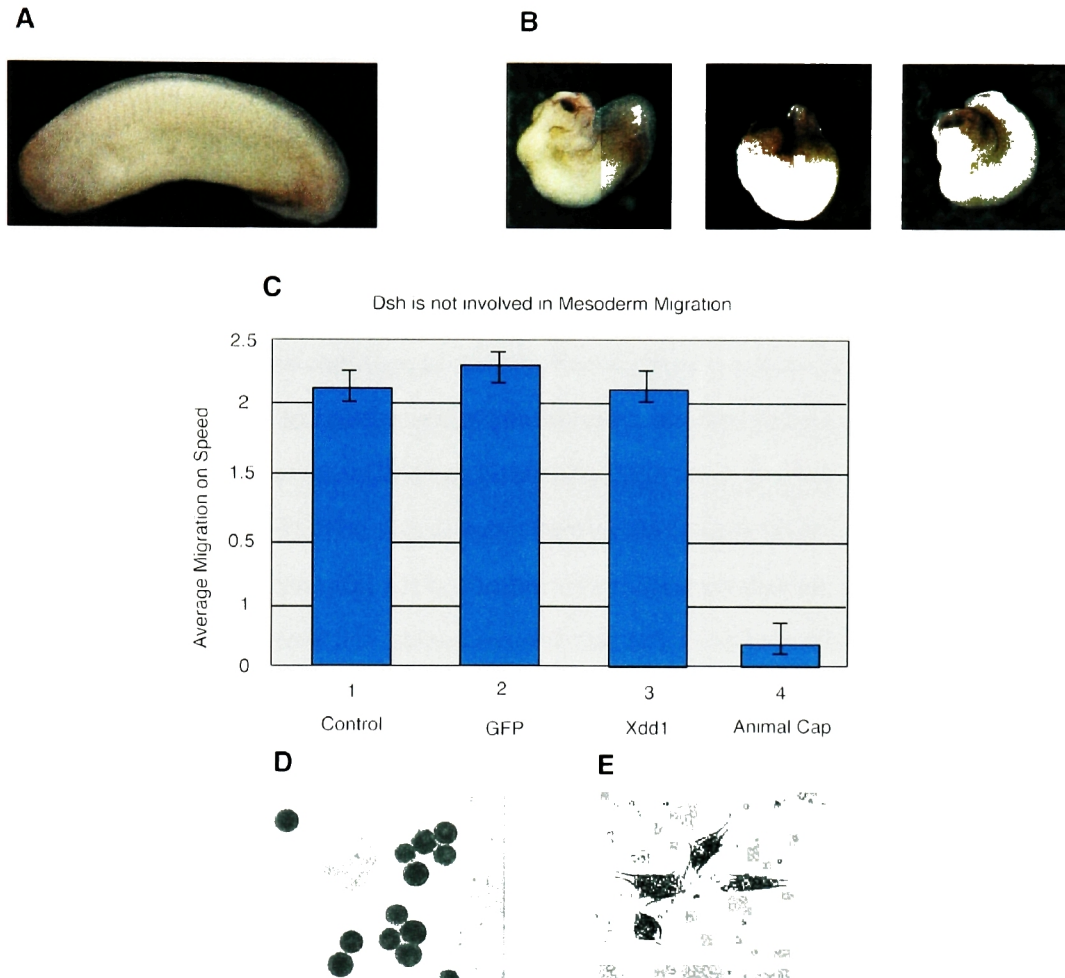


Figure 2. Dominant negative Dsh (Xdd1) injection at the dorsal marginal zone (DMZ) results in the inhibition of convergent extension (B) but has no effect on mesoderm migration on FN (C). Injection of Xdd1 at the DMZ (1.5ng) inhibits dorsal mesoderm elongation leading to the characteristic curved embryos where the head and the tailbud are in close proximity (B) compared to the control embryos (A). The histogram shows the average speed of migration of dissociated anterior mesoderm from DMZ's which were injected with the mRNA's indicated and that of animal cap cells as a control. Injection of Xdd1 does not reduce the migratory activity of dorsal mesoderm and injected cells display a migratory phenotype (E) compared to control (D).

calculated by time-lapse microscopy ([Figure 2C](#)). *Xddl* injected cells were phenotypically, identical to *GFP* injected cells, and showed a migratory morphology ([Figure 2E](#)). This result suggests that active mesoderm migration might have an entirely different basis compared to convergent extension.

Anterior mesoderm forms focal adhesions during migration on a FN matrix.

Attachment of mammalian cells to the extracellular matrix (ECM) is primarily mediated by the integrin family of receptors (Hynes 1992; Hynes, George et al. 1992). Engagement of heterodimeric integrin receptors leads to the clustering of integrins and recruitment of a large number of proteins to form multi-protein complexes on the cytoplasmic face of the plasma membrane termed focal adhesions (BurrIDGE, FATH et al. 1988). Focal adhesions serve to anchor actin cytoskeleton to the plasma membrane and to provide linkage between the extracellular environment and the cytoplasm (BurrIDGE and Chrzanowska-Wodnicka 1996). The recruitment of cytoskeletal proteins and the assembly of focal adhesions are vital for a number of cellular processes, including cell migration, survival, and proliferation, depending on the cell type in question (Lauffenburger and Horwitz 1996; Palecek, Schmidt et al. 1996). Previous studies have concluded that *Xenopus* mesoderm does not form focal adhesions during active migration and spreading on FN (Selchow and Winklbauer 1997). Adherent mammalian cells are known to attach to the extracellular matrix through these complexes and a large number of proteins like the focal adhesion kinase (FAK) have been identified which are consistently localized at focal adhesions (vinculin, talin, and paxillin). These proteins are often used to visualize focal adhesion complexes. Use of antibodies against tyrosine phosphorylated proteins also stains focal adhesions in adherent mammalian cells due to the high number and concentration of tyrosine phosphorylated proteins at these sites (Maher, Pasquale et al. 1985). Using a monoclonal anti phosphotyrosine (a-py) antibody we examined the phosphotyrosine (py) distribution of *Xenopus* ectoderm, as well as that of adherent mesodermal cells. Although the bulk of the staining in the ectoderm and most other tissues (including the eye Fig 3I, J and K) was concentrated at the sites of cell contact ([Figure 3A](#)), in adherent cells we observed a punctate pattern that resembled focal

adhesions (Figure 3B). Double labeling with texas red phalloidin to visualize the actin cytoskeleton revealed a closely matching pattern between f-actin and the py staining (Figure 3D). Close examination showed that the focal adhesion complexes formed at the ends of actin cables (Figure 3E) in a similar fashion as described in mammalian adherent cells (Maher, Pasquale et al. 1985; Yap, Stevenson et al. 1995). To further confirm the presence of focal adhesions in migrating mesodermal cells we used monoclonal antibodies directed against a number of well characterized focal adhesion proteins and fluorescent secondary and tertiary antibodies to increase the signal-to-noise ratio. We detected focal adhesions in migrating as well as stationary adherent mesodermal cells that were plated on FN coated coverslips. Figure 3 shows that these focal adhesions were present in both dissociated cells (B, F, G), small explants (H), and contained FAK, paxillin and vinculin. In both cases, they were mainly concentrated at the cell periphery and were much weaker and smaller than the ones seen on mammalian cells grown on FN. The weak staining and their small size might be the reason they had not been detected before. The presence of focal adhesions in migrating mesodermal cells strongly suggests that it is through these complexes that mesoderm adheres and migrates on the BCR (Figure 3). This makes focal adhesions good targets to inhibit active cell migration, which relies on cell-ECM interactions without affecting other morphogenetic movements that depend on cell-cell interactions like convergent extension.

FRNK localizes to the focal adhesion complexes and inhibits the tyrosine phosphorylation of FAK.

FAK has been shown to be expressed in migrating mesodermal cells (Hens and DeSimone 1995; Zhang, Wright et al. 1995) and we have shown that it is localized at the focal adhesions that these cells form. In order to examine the role of FAK in active mesoderm migration we used influenza hemagglutinin (HA) tagged versions of both FAK and a dominant negative splice variant called FRNK. FRNK, as mentioned before, contains the C-terminal domain of FAK and lacks catalytic activity (Schaller, Borgman et al. 1993). We first established by microinjection that ectopic FRNK localizes correctly to the focal adhesions, ensuring that the tag did not alter the subcellular distribution of the

FIGURE 3

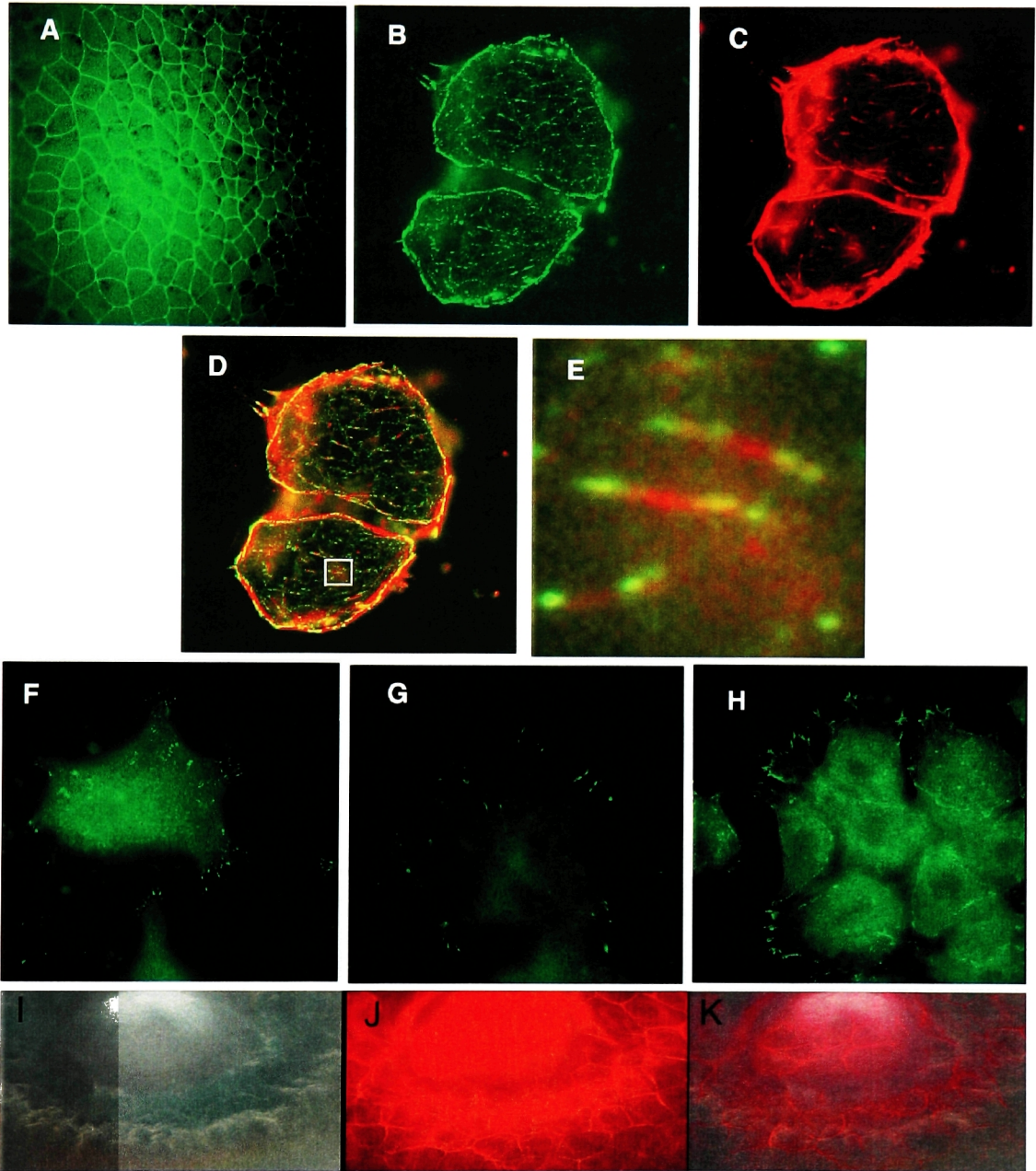


Figure 3. Anterior mesoderm forms focal adhesion complexes on fibronectin during gastrulation. The phosphotyrosine (py) distribution in the ectoderm of a gastrulating *Xenopus* embryo as determined using a monoclonal anti phosphotyrosine (a-py) antibody (A). The dorsal lip is at the lower left corner. The distribution of the tyrosine phosphorylated proteins changes when looking at migrating mesodermal cells attached on Fibronectin (B) and seems to correspond closely to the staining pattern of actin as seen using Texas red phalloidin (C). Superimposition of the images reveals that even though the phosphotyrosine staining parallels the actin pattern it does not overlap with it (D). Close examination (E) shows that the a-py antibody (Green) stains focal adhesion like complexes at the ends of actin filaments as previously seen in mammalian adherent cells (E is a magnification of the area in the white square of D). Staining with a-paxillin (F), a-FAK and a-vincullin (H) confirms that migrating mesoderm forms focal adhesions.

protein. A-C of [Figure 4](#) show that FRNK-HA (50pg injection) co-localizes with the endogenous FAK to the focal adhesions of mesodermal cells plated on FN. The endogenous FAK was visualized using a phospho-specific antibody that recognizes FAK(Tyr397), but not FRNK.

We then addressed the effect that over-expression of FRNK had on the tyrosine phosphorylation levels of FAK in *Xenopus*. Tyrosine phosphorylation of FAK is a good indicator of its activity, and cycles of phosphorylation and dephosphorylation are believed to be essential for migration (Du, Ren et al. 2001; Leu and Maa 2002). Because endogenous levels of phosphorylated FAK (FAK-py) were very low and FRNK overexpressing cells did not adhere well, we first over-expressed HA-FAK in order to elevate the FAK-py level. [Figure 4D](#) shows *Xenopus* ectodermal cells stained with a specific antibody against Tyr397 FAK-py (red). The green staining is memGFP, which was injected as a lineage tracer of injected cells. Over-expression of HA-FAK significantly increased the level of FAK-py indicating that the HA-FAK construct is active in the context of *Xenopus* ectoderm. We then over-expressed HA-FAK in adherent mesodermal (activin induced) cells ([Figure 4E and F](#)) and a similar result was obtained. The injected cells (stained with anti-HA antibody) showed significantly elevated levels of FAK-py ([Figure 4F](#)) compared to non-injected surrounding cells used as control. Co-injection of HA-FRNK together with HA-FAK lead to the reduction of the FAK-py levels of the injected cells to levels similar to those in non-injected cells (compare F and H). The fact that FRNK correctly localizes to the focal adhesions and reduces FAK's phosphorylation level shows that it is, as suggested before, functioning as a bona fide dominant negative (Richardson and Parsons 1996; Leu and Maa 2002).

In order to address the effects the FRNK has on endogenous levels of Tyr397 FAK phosphorylation we over-expressed FRNK in *Xenopus* ectodermal cells and then

FIGURE 4

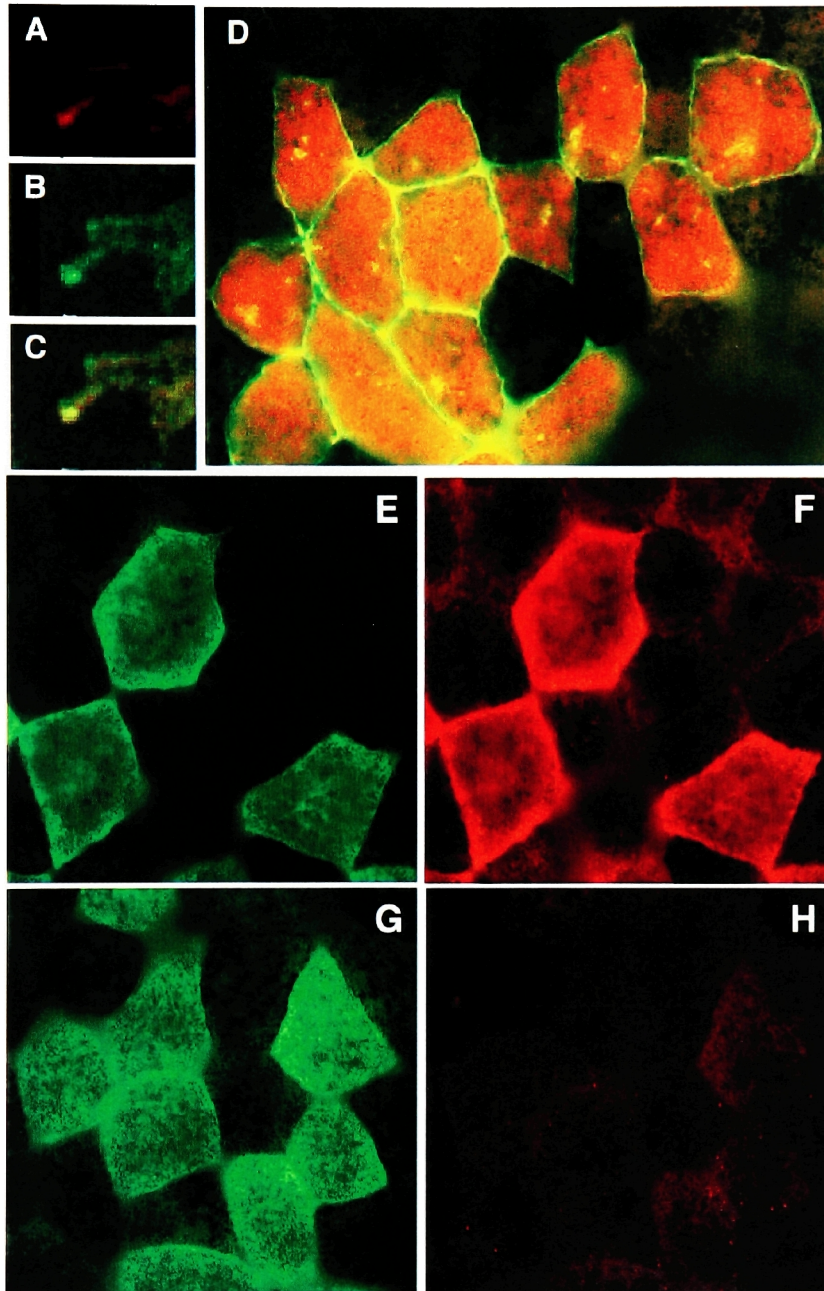


Figure 4. Exogenously expressed HA-FRNK (200pg) localizes to the focal adhesions of Xenopus mesoderm and is able to inhibit FAK autophosphorylation. A, B and C are magnified views of a mesodermal cell extension were microinjected HA-FRNK (A, red) is shown to colocalize (C, yellow) with endogenous phosphorylated FAK (B, green) at a focal adhesion complex. Injection of FAK (50pg) in the ectoderm (D) as well as in the mesoderm (E and F) of Xenopus will increase the level of phosphorylated FAK (red) significantly. In D memGFP was coinjected with FAK to indicate the injected cells (green) while in E FAK was HA tagged and stained with an α -HA antibody. Overexpression (1ng) of HA-FRNK (G) with the same amount of HA-FAK as in E in mesodermal cells leads to a dramatic reduction of autophosphorylated FAK (compare F and H).

followed by staining with a phosphospecific antibody. Despite the fact that the tyrosine phosphorylated FAK levels are very low, there was a clear reduction of the fluorescent signal from the FRNK expressing cells (Figure 5B and C). The low endogenous levels of Tyr397 phosphorylated FAK are in agreement with results in zebrafish where very little Tyr397 FAK-py was observed in the enveloping cell layer (Crawford, Henry et al. 2003). This is not surprising considering that Tyr397 has been shown to be the major site of phosphorylation in response to beta 1 integrin-mediated cell adherence and ectodermal cells are non-adherent (Chan, Kanner et al. 1994). The fact that FRNK can reduce FAK autophosphorylation in the context of ectodermal cells suggests that FRNK competes FAK from active complexes formed in these cells. Using a FAK antibody, we observed that endogenous FAK localized in the sites of cell contact in the epithelial layer of the animal cap (Figure 5A). This type of localization was not seen in mesodermal explants and is consistent with findings in zebrafish where FAK was reported to be localized in cell boundaries (Henry, Crawford et al. 2001) and with results showing FAK and Paxillin complexes localized at the boundaries of epithelial cells (Crawford, Henry et al. 2003). The proposed function of these FAK containing complexes is signaling to the cytoskeleton through cadherin-based adherens junctions (Crawford, Henry et al. 2003). FRNK expression leads to the redistribution of FAK from these complexes to the cytoplasm (Figure 5D, E and F). This is in agreement with findings that FRNK expression leads to the redistribution of FAK from the focal adhesions to the cytoplasm in rat myocytes (Heidkamp, Bayer et al. 2002), and also supports the hypothesis that FRNK functions by competing FAK off its signaling complexes (Richardson and Parsons 1996; Crawford, Henry et al. 2003). It is also the first time that FRNK has been shown to disrupt non-ECM based FAK containing complexes.

Overall, these experiments established the specificity of FRNK and provided an insight into the way FRNK might regulate FAK in the context of *Xenopus*. They also set the stage to explore the role of FAK in the context of active mesoderm migration *in vivo* and *in vitro*.

FRNK inhibits active mesoderm migration in a cell autonomous manner

FIGURE 5

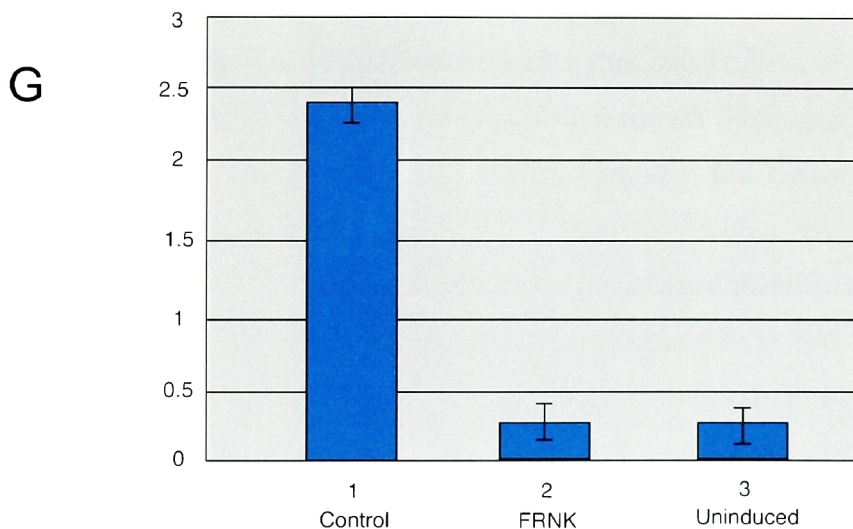
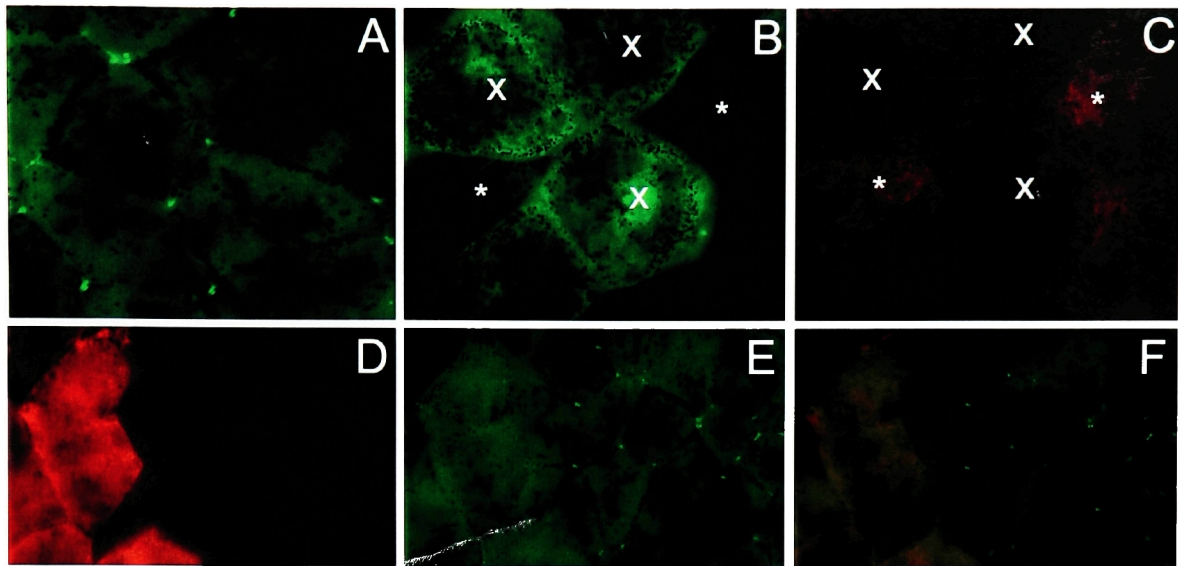


Figure 5. FRNK acts as a dominant negative reducing endogenous FAK phosphorylation as well as competing endogenous FAK from its complexes. (A) FAK localizes in cell-cell boundaries in the epithelium of the animal cap ectoderm. (B-C) FRNK-HA overexpression in *Xenopus* ectoderm (green cells, labeled with X) reduces the endogenous levels of tyrosine phosphorylated FAK (red). Cells without FRNK expression (labeled with *) have significantly higher endogenous levels of phosphorylated FAK. (D-F) FRNK-HA expression (red cells) can compete FAK from its signaling complexes. FRNK-HA was stained with an HA specific antibody while endogenous FAK (green) was visualized using a FAK polyclonal antibody raised against the N-terminus of FAK which does not recognize FRNK. (G) Dominant negative FAK (FRNK) can inhibit cell spreading and migration of dissociated *Xenopus* mesoderm on FN in a cell autonomous manner. Cells from the animal caps of FRNK injected (1ng) and uninjected embryos were dissociated and then mixed. memGFP was coinjected with FRNK as a marker for injected cells. The mixed population of cells was then plated onto FN and mesoderm was induced using activin. The movements were recorded using time-lapse video microscopy. The histogram shows the average speed of migration of control (GFP negative), FRNK injected (GFP positive) and uninduced ectodermal cells. FRNK expressing cells showed a non migratory phenotype with an average migration speed similar to uninduced cells

The presence of focal adhesions on migrating mesodermal cells raises the possibility that FAK is involved in adhesion and migration of *Xenopus* mesoderm. Previous studies in mammalian cells have shown that FAK overexpression can induce migration in mammalian fibroblast cells, while FRNK can block spreading and migration (Schaller, Borgman et al. 1993; Gilmore and Romer 1996). We found that injection of HA-FAK in ectodermal cells does not induce a migratory phenotype, nor does it increase the rate of migration of mesodermal cells ([movie 1](#)). To examine the role of FAK in the process of mesoderm migration, FRNK was coinjected with mem-GFP in the DMZ of four cell stage embryos. In this manner, the cells of the head mesoderm, which are migratory, were specifically targeted. Following injection embryos were allowed to develop to late blastula stages and then the DMZ was dissected and dissociated. A mixture of injected and uninjected DMZ cells were then plated on a FN coated well where they were filmed. [Movie 2](#) is a portion of such a time-lapse movie were FRNK expressing cells (GFP positive) clearly fail to migrate and spread whereas non-expressing cells (three of them indicated with red arrows) migrate normally. Individual cells were followed and their migration rates determined. We went on to calculate the average speed of migration for GFP positive and GFP negative cells. Dissociated FRNK over-expressing cells fail to spread and their migration rate is comparable to that of ectodermal cells ([Figure 5G](#)). The same is true for small dorsal marginal zone explants, which remain rounded and do not spread on FN ([Figure 6 A-C](#)). This data is in agreement with previous findings in mammalian cells and is supported by the fact that FAK is present in the right tissue at the right time to play a role in active mesoderm migration (Hens and DeSimone 1995; Zhang, Wright et al. 1995). Furthermore, co-injection of *FAK* together with *FRNK* rescues the spreading phenotype, and most of the FAK + FRNK expressing cells exhibit a migratory morphology ([Figure 6 J, K and L](#)). Our results demonstrate that FRNK can specifically and cell autonomously inhibit active mesoderm migration and suggest that FAK is necessary for this morphogenetic movement. Our results using FAK over-expression in ectodermal cells indicate that FAK is not sufficient for the induction of a motile phenotype in this cell type.

FIGURE 6

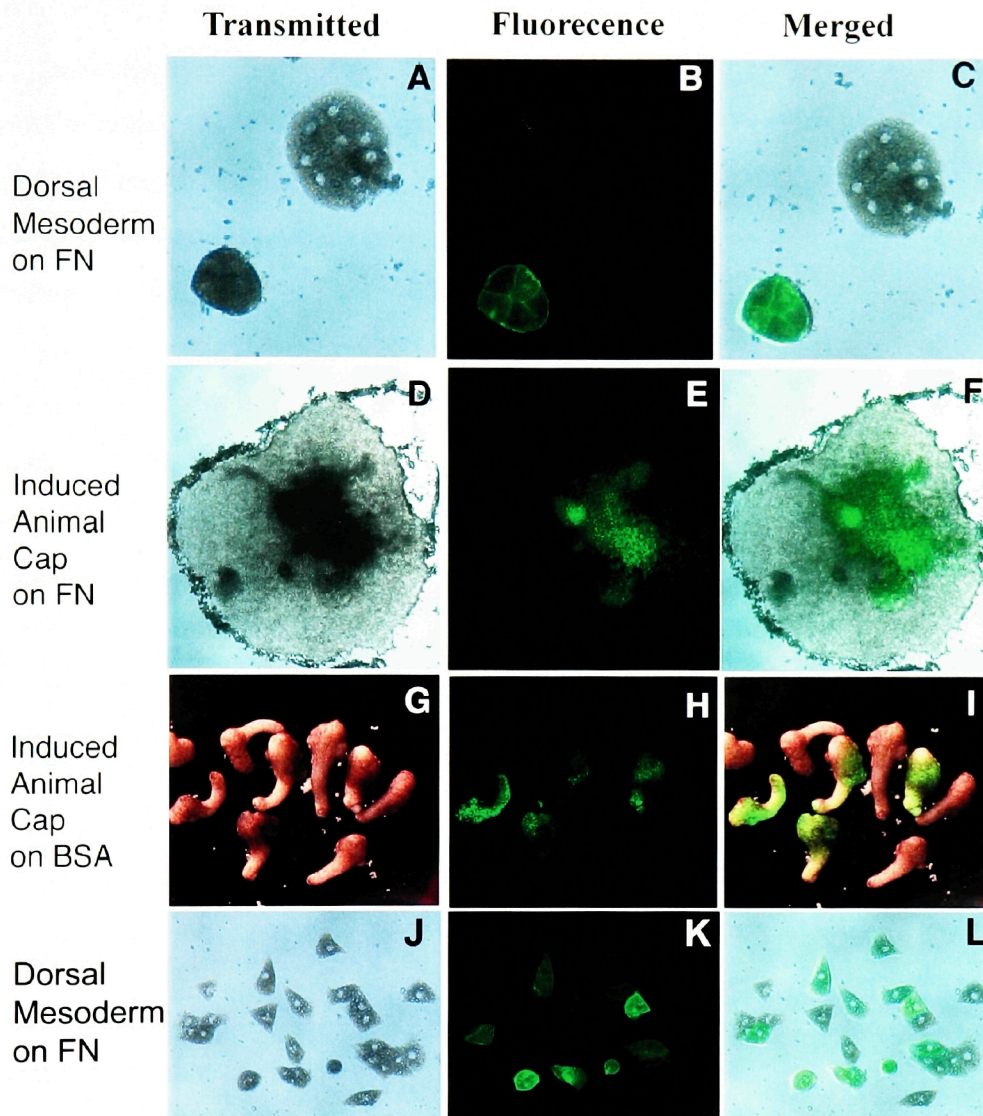


Figure 6. FRNK can inhibit cell spreading and migration of induced animal cap explants as well as that of dorsal mesoderm explants but has no effect on convergent extension movements. (A-C) Small dorsal marginal zone explants are inhibited from spreading by FRNK overexpression. MemGFP coinjected with FRNK serves as a marker for injected cells. Notice the rounded phenotype of the GFP positive cells compared to the flattened GFP negative cells. (D-F) Activin induced animal caps were inhibited from spreading on FN after being injected with FRNK (1ng) together with mem-GFP as a marker. The lack of spreading is clear by the phase dense nature of cells positive for GFP. (G-I) Injection of FRNK at the same amounts was on the other hand unable to block convergent extension and GFP positive explants elongated like the controls. (J-L) Co-injection of FAK can rescue the FRNK phenotype. The majority of cells express both FAK and FRNK together with mem-GFP as a marker spread and migrate like un-injected cells

FRNK blocks induced mesoderm spreading without affecting convergent extension.

We next addressed the specificity of FRNK vis-à-vis other morphogenetic movements. Embryos were injected with *FRNK* and *memGFP* as a lineage tracer at the animal pole at the two cell stage, and animal caps were cut at late blastula. The animal caps were then either placed in wells that had been coated with FN followed with BSA (to block non specific binding), or BSA alone. The media in both cases contained activin-B protein. Activin is a type-beta transforming growth factor (TGF-beta) and has the ability to induce ectodermal explants to form mesoderm. Induced explants undergo morphogenetic movements and have been used extensively to test the effects of different factors on mesoderm morphogenesis (Sokol 1996; Winklbauer and Keller 1996). The explants were allowed to develop until sibling controls reached late neurula. [Figure 6D](#) through [F](#) shows that explants placed in the FN coated wells adhered on the substrate and started spreading forming a monolayer. The explant spread to a monolayer except in the regions positive for GFP where it was inhibited from spreading. On the other hand, explants in BSA coated wells healed and then underwent convergent extension movements leading to their elongation, which was identical in extent to that of uninjected control explants ([Figure 6G, H and I](#)). These results demonstrate that FRNK can efficiently inhibit active mesoderm migration and spreading without affecting convergent extension. The selective inhibition of mesoderm migration establishes FRNK as a tool to specifically inhibit this morphogenetic movement *in vivo* in order to address its role in gastrulation.

FAK inhibition at the DMZ *in vivo* leads to failure of blastopore closure.

Since FRNK can inhibit active mesoderm migration *in vitro*, we next tested the activity of FRNK *in vivo* as a means of measuring the contribution of active mesoderm migration in gastrulation movements. The dorsal mesoderm is the tissue most actively engaged in this type of morphogenetic movement (Wacker, Brodbeck et al. 1998), we therefore injected *FRNK* at the dorsal marginal zone of four cell stage embryos in both dorsal blastomeres (the injections were made at the dorsal most region of the embryo as close to the cell boundary as possible). Despite the fact that FRNK injection inhibits

mesoderm migration *in vitro*, it is impossible to monitor the behavior of mesodermal cells *in vivo* due to the opacity of the *Xenopus* embryo. Fixation and dissection of *FRNK* injected embryos revealed that the anterior mesoderm of these embryos was attached to the ECM, but the cells were rounded, indicating that migration was indeed blocked but adhesion was not. Injected embryos were allowed to develop until sibling stage controls reached the tailbud stages. [Figure 7](#) shows that the phenotype of injected embryos was a failure of blastopore closure. 83% (n=31) of *FRNK* injected embryos failed to reach blastopore closure compared to 0% (n=27) of *mem-GFP* injected embryos ([Table 1](#)). The *FRNK* injected embryos which gastrulated normally were morphologically normal. Evidence of specificity of the *FRNK* phenotype was established by co-injection of *FAK* which can rescue the *FRNK* phenotype and significantly reduce (but not eliminate) the number of embryos failing to reach the tadpole stage. 43% (n=44) of *FAK* co injected embryos failed to reach blastopore closure compared to 83% (n=31) of *FRNK* alone ([Table 1](#) and [Figure 7A](#) inset). The partial rescue of the *FRNK* phenotype by co-expression of *FAK* is consistent with the partial rescue observed in dissociated cells. Since head mesoderm is active in this type of morphogenetic movement, we postulated that inhibition in less active tissues would be predicted to be less detrimental to the gastrulation process. This prediction was tested by lateral injections of *FRNK* in four cell stage embryos. Lateral injections did not lead to failure of blastopore closure and produced normal embryos further supporting the specificity of the phenotype of the DMZ injections. Overall, our data supports a role for *FAK* in mesoderm migration *in vivo* and shows that this movement is essential for normal gastrulation in *Xenopus*.

Focal adhesion formation is essential for active mesoderm migration but does not inhibit convergent extension.

Mesoderm is morphogenetically dimorphic. As we demonstrated, the same explants can either undergo convergent extension or active migration. Two distinct morphogenetic movements are involved: one primarily dependent on cell-ECM interactions and one dependent on cell-cell interactions. Both processes are essential for gastrulation, but only active migration requires the formation of focal adhesions. Since in

FIGURE 7

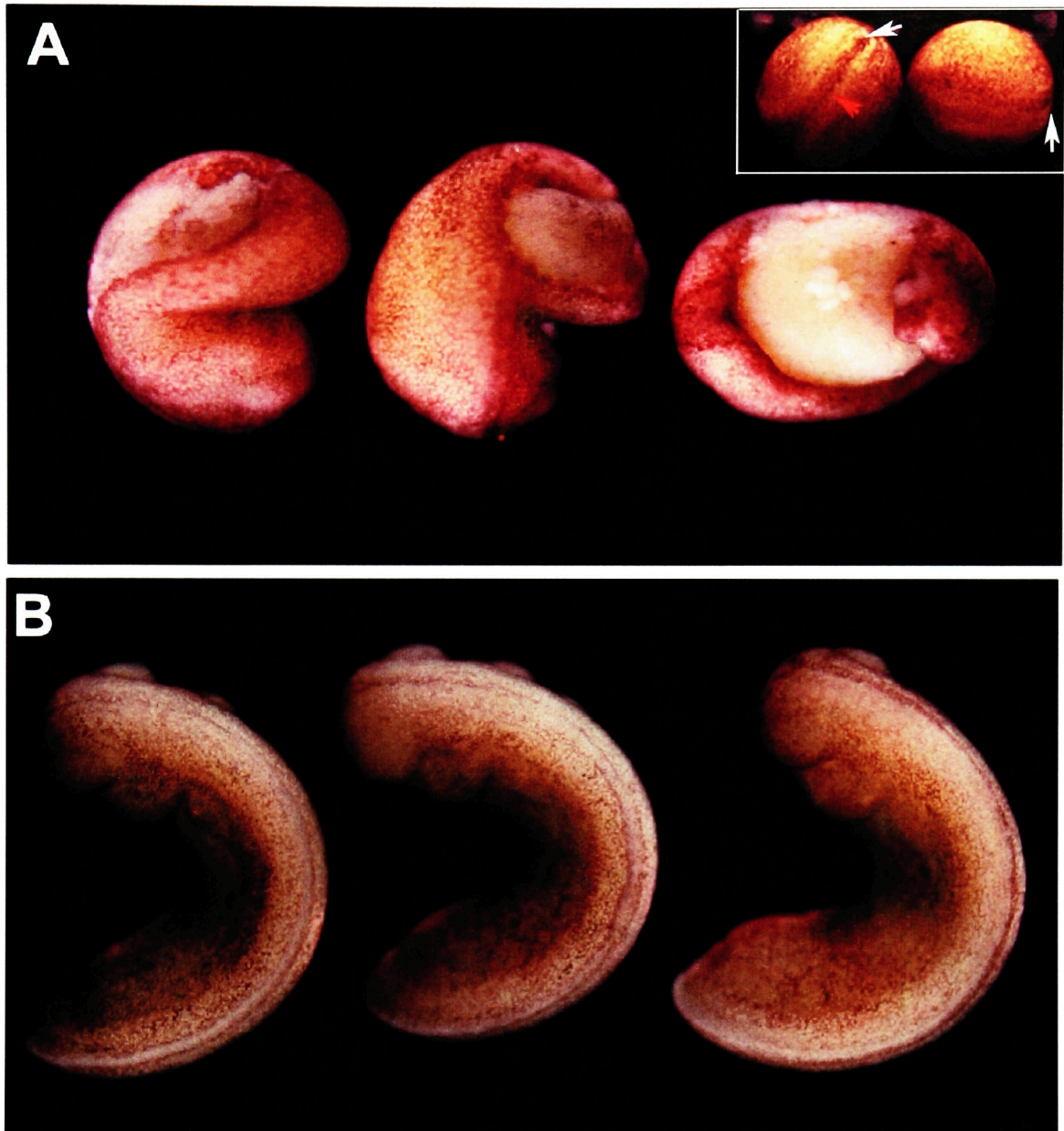


Figure 7. FRNK injection inhibits mesoderm migration and results in failure of blastopore closure which often prevents neural tube closure. FRNK injected (1ng) embryos fail to close their blastopore (A) compared to uninjected sibling embryos(B). This often leads to failure of closure of the posterior regions of the neural tube. FAK coinjection rescues the blastopore phenotype(inset of A) and the blastopore closes completely in the majority of embryos(white arrows). As a result the neural tube closes completely as well(red arrow).

Table 1

	mem GFP	FRNK+memGFP	FRNK+FAK+memGFP
Normal	27 / 100%	5 / 17%	25 / 67%
Gastrulation failure due to Blastopore closure failure	0 / 0%	26 / 83%	19 / 43%
Total Number injected	27 / N/A	31 / N/A	44 / N/A

Table1. FAK (100pg) can rescue the FRNK (1ng) induced blastopore closure failure.

the presence of ECM mesoderm invariably undergoes active migration and convergent extension seems to be blocked, we wanted to test whether signaling from the focal adhesions was responsible for this inhibition. In order to test this we coated glass beads with FN and placed them on top of activin-induced animal caps (animal pole facing down). The explant cells adhered to the beads and the explants healed with the beads inside. If signaling from the formed focal adhesions was responsible for pushing the explant towards active migration and blocked convergent extension, there should be no elongation. If on the other hand, focal adhesions were not responsible for the change of mesodermal behavior, but some mechanistic effect due to tension created within the explant pulling on the ECM these explants should elongate normally. Repeated experiments showed that mesodermal explants bound on FN coated beads underwent convergent extension and elongated to the same extent as control explants containing uncoated beads. Even though these explants adhere to the coated beads, they are unable to generate traction on the beads and as a result no tension is created within the explants. In order for spreading to occur, cells in the explant need to directionally intercalate towards the substrate while the intercalation that leads to convergent extension is toward a point of convergence. Our results suggest that even though formation of focal adhesions is essential for active mesoderm migration and induction of intercalation towards the ECM, this is not sufficient for inhibition of convergent extension if the adhering cells can not generate tension within the explant. Tension within the explant -- created when marginal cells of the explant start pulling away from it -- appears to be essential in order to change the direction of intercalation and thus cause an explant to spread rather than elongate. This interpretation is in agreement with published data showing that tension applied to ectodermal explants (another intercalating tissue) alters the direction of intercalation. Cell intercalation in such explants becomes perpendicular to the stretching force, in complete agreement with our observations in mesodermal explants (Belousov, Luchinskaia et al. 1999; Beloussov, Louchinskaia et al. 2000).

Discussion

In this study, we have demonstrated a role for the Focal Adhesion Kinase in the process of mesoderm migration during the *Xenopus* gastrulation. More importantly, we have for the first time managed to block this process in a cell autonomous manner and addressed its role in gastrulation independent of other morphogenetic movements.

Of the two major morphogenetic movements of the mesoderm, convergent extension is considered the most important and is responsible for the anterior to posterior axis elongation of the embryo (Keller, Danilchik et al. 1985). Despite the fact that the same mesodermal explant can undergo either movement, mesoderm migration appears to be independent of pathways essential for convergent extension. Our results indicate that a dominant form of Dsh, extremely competent at blocking convergent extension, fails to block mesoderm migration.

We have presented evidence that FRNK can displace FAK from non-Integrin-based complexes assembled at epithelial cell-cell contact sites. We have not examined whether these complexes are still present, but the fact that convergent extension is not inhibited in FRNK injected explants leads us to believe that cell-cell contacts are not compromised. It is possible that the kinase activity of FAK is not necessary for its role in these types of complexes, and thus FRNK can substitute without adverse effects in this context. Injection of FRNK in mesodermal cells, on the other hand, can cell autonomously inhibit cell spreading on FN and inhibit both individual cell migration, as well as the spreading of mesodermal explants on this substrate. While FAK is necessary for mesoderm migration, gain of function experiments using FAK overexpression in non-migratory and non-adherent ectodermal cells show that FAK is not sufficient for the initiation of spreading and active cell migration in *Xenopus*. Our results suggest that FAK is necessary for this process, and are supported by FAK's spatiotemporal expression during *Xenopus* development. FAK is expressed in the marginal zone at the time of gastrulation, perfectly coinciding with the mesodermal tissues that undergo active mesoderm migration (Hens and DeSimone 1995; Zhang, Wright et al. 1995). We have also provided evidence that the inhibition of mesoderm migration by FRNK is not due to toxicity or nonspecific blockage of mesoderm morphogenesis because FRNK injections,

as discussed, fail to inhibit or reduce convergent extension. Further evidence of this specificity is demonstrated by results showing that co injection of FAK with FRNK can rescue the majority of injected cells. Overall, our results identify FRNK as the first cell autonomous and specific inhibitor of mesoderm migration.

Injections of FRNK at the DMZ of four cell stage *Xenopus* embryos result in failure of blastopore closure in the majority of embryos. Blastopore closure failure is a very common phenotype when the RNA injected is toxic but *mem-GFP* tracer coinjected with the *FRNK* RNA indicates that the injected cells show no sign of toxicity and that other morphogenetic movements like convergent extension are not affected. Furthermore coinjection of *FAK* together with *FRNK* rescues the phenotype providing further evidence that it is a specific effect. This phenotype is also consistent with results from previous reports (Winklbauer 1990; Winklbauer, Selchow et al. 1992; Kuhl and Wedlich 1996; Ramos and DeSimone 1996; Winklbauer, Nagel et al. 1996) where delay of blastopore closure was observed after peptide and antibody injections. Despite the observed delay, a complete failure of blastopore closure was not common when the integrin-FN interaction was disrupted. It has been shown that the assembly of the FN matrix is also essential for epiboly. Epiboly continues during convergent extension, pushing the marginal zone and, in effect, the non-involuting mesoderm (Figure 1C red and green) down towards the vegetal pole. The internalized mesoderm, on the other hand, is in fact moving upwards towards the top of the BCR by means of mesoderm migration and convergent extension. During this movement the substrate of the migrating mesoderm is the FN matrix on the BCR, which is moving downwards due to epiboly, and is acting like a treadmill opposing the upward push pull movement of the mesoderm. A possible interpretation of the discrepancy between the observed phenotypes would be that the role of mesoderm migration is to counteract the downward movement of the substrate due to epiboly.

The kind of phenotype resulting from FRNK injections is very similar to that of the dominant negative FGF receptor (Amaya, Musci et al. 1991). It is tempting to speculate that since FRNK inhibits FAK phosphorylation, and since FGF (through the

MAP kinase pathway) can phosphorylate FAK, the open blastopore is due to inhibition of the end player (FAK) of one of the signaling pathways activated by FGF. Close observation of the phenotype produced by dominant negative FGF receptor (dn-FGFR) and its comparison to the FRNK phenotype reveals differences between the two that should be noted. In the case of dn-FGFR, the blastopore forms dorsally, but often does not extend ventrally. Thus involution does not begin on the ventral side of the embryo. In the case of FRNK, the formation of the dorsal lip, as well as the formation of the blastopore ring, occurs normally and the timing of these events is identical to control embryos. This suggests that the underlying cause leading to the open blastopore phenotype in each case might be different. At the same time, one would expect any inhibitor of mesoderm induction, and, as a result, convergent extension and mesoderm migration would lead to this type of phenotype. If the mediolateral intercalation responsible for the constriction of the blastopore ring does not take place, the blastopore will not close. These observations, together with the fact that injection of peptides and antibodies blocking mesoderm adhesion on the ECM mimic the observed phenotype (and they by no means affect FGF signaling), lead us to conclude that the phenotype we observe is unrelated to that of dn-FGFR.

The observed FRNK phenotype is also consistent with studies done in other species. FAK knockout mice implant and initiate gastrulation normally, but show abnormalities in subsequent stages of development (Furuta, Ilic et al. 1995). The mouse phenotype is in agreement with what we observe in *Xenopus*, but more severe. This should be expected because with the use of a dominant negative in the form of RNA, injections inhibition is never complete and is eventually relived with the gradual degradation of the injected RNA. Late functions of FAK, or even potential early functions unrelated to cell-ECM interactions (for example convergent extension), are not affected. In *Drosophila* and chick the expression pattern of FAK suggests that it is involved in cell-ECM interactions as well (Fox, Rebay et al. 1999; Palmer, Fessler et al. 1999; Ridyard and Sanders 1999; Ridyard and Sanders 2000; Ridyard and Sanders 2001).

In summary, our experiments show that mesoderm migration is an integral part of the gastrulation process, and that it relies on a different molecular basis than convergent extension. We also show that mesoderm can undergo both movements and provide data suggesting that the decision to undergo one or the other is mechanical and not based on signaling from the focal adhesions. Finally, we show that FAK is necessary for mesoderm migration and, as a result, for normal gastrulation in *Xenopus laevis*. While this study provides the first molecular component specifically involved in mesoderm migration, a more detailed analysis of the pathways involved is essential for a global temporal and spatial understanding of its integration in the gastrulation process.

CHAPTER 2

Rap1b is Required for Morphogenetic Movements in *Xenopus*

Introduction

Ras proximate (Rap) proteins (de Gunzburg 1993; Noda 1993) are GTPases that belong to the Ras superfamily of G proteins (Boguski and McCormick 1993). They were originally identified by GTP γ S³⁵ binding (Nagata, Itoh et al. 1989), low stringency hybridization by using Ras probes (Pizon, Lerosey et al. 1988), and by expression cloning as a Ras revertant clone (Kitayama, Sugimoto et al. 1989; Nagata, Itoh et al. 1989; Noda, Kitayama et al. 1989). Although Rap shares only about 50% overall sequence identity with Ras, their effector domain regions are identical (Valencia, Chardin et al. 1991), raising the possibility that both proteins might have similar or even antagonistic functions. Having identical effector domains at the biochemical level, together with the ability of Rap1 to revert Ras-mediated cellular transformation at the biological level, led to the current notion that Rap1 is an antimutagenic protein that functions by antagonizing Ras action (Valencia, Chardin et al. 1991).

Aside from their role in antagonizing Ras signaling, both Rap1 and Rap2 were shown to be necessary for the migration of B-cells towards a chemoattractant, the chemokine stromal cell-derived factor-1 (McLeod, Li et al. 2002). Rap1b was also shown to have an early embryonic role in *Drosophila melanogaster*. Rap1b was shown to be involved in morphogenesis in the fly (Asha, de Rooter et al. 1999; Bos, de Rooij et al. 2001). Signaling pathways involved in morphogenesis are often conserved between the fly and vertebrates. One recent example is the involvement of the *Drosophila* planar cell polarity (PCP) pathway in convergent extension. The PCP pathway of *Drosophila* is a conserved signaling pathway that regulates the coordinated orientation of cells or structures within the plane of an epithelium and has been shown to be necessary for the oriented polarization of mesodermal cells during the intercalation process that gives rise

to elongation in the antero-posterior axis. We thus decided to investigate a possible role for Rap1b in the *Xenopus* morphogenesis. Using a constitutive active, a wild type (WT), a dominant negative (dn) form of Rap1b, and assays described in the previous chapter, we tested the potential involvement of Rap1b in morphogenesis during the *Xenopus* gastrulation. We show that Rap1b can influence both convergent extension and mesoderm migration and that an activated form is capable of enhancing convergent extension, achieving greater elongation on the injected side of the embryo. These results are suggestive of a possible role for Rap1b in general mesoderm morphogenesis, but further studies will be required to rule out effects on cell proliferation, as well as cell fate specification.

Results

Rap1b is involved in mesoderm migration

Rap1bV12 a constitutively active form of the small G-protein as well as *Rap1bN17* a dominant negative form and WT *Rap1* were independently injected into the animal pole of two cell stage *Xenopus* embryos. *Mem-GFP* was injected together with each construct as a marker of the injected cells. The embryos were left to develop normally up to late blastula and the animal caps were then dissected and induced to form mesoderm with activin. The caps were then placed onto a FN coated dish and were observed using video microscopy. This assay, which tests the ability of the injected explants to spread on FN, has been described in the previous chapter. The explants expressing Rap1bN17 were partially inhibited from spreading while those expressing the constitutively active form spread substantially more (Figure 8). Despite the fact that the dominant negative Rap1b seemed to block mesoderm spreading, Rap1bv12 does not enhance and even seems to slightly inhibit mesoderm migration at high expression levels. These results suggest that Rap1b might be involved in mesoderm migration and raise the possibility that tight regulation of its activity is necessary for efficient cell migration.

FIGURE 8

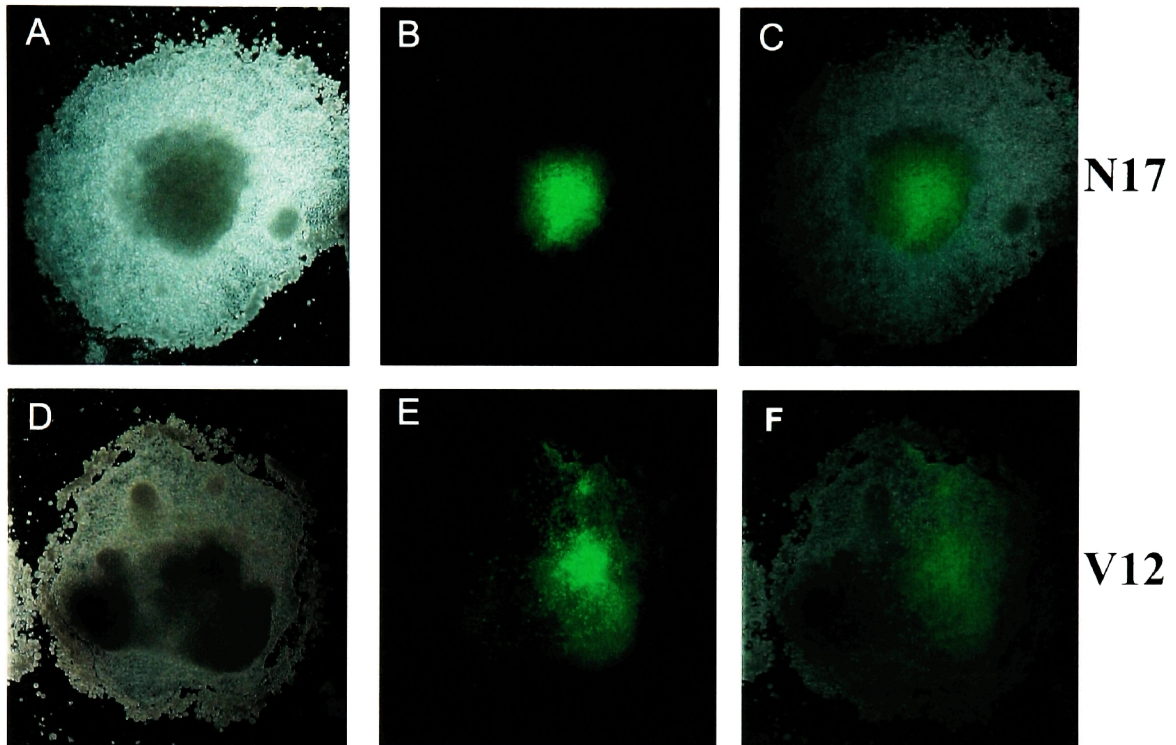


Figure 8. Dominant negative Rap1b blocks spreading and migration when expressed in induced ectodermal explants (A-C) while a constitutively active form also appears to negatively influence this process(D-F). The two constructs were injected on both animal cap blastomeres of two cell stage embryos together with GFP to mark the recipient cells. Animal caps were dissected at late blastula, induced with activin and were plated on fibronectin coated dishes where they were allowed to adhere and spread. Rap1bN17 expressing cells remained within a clump and did not spread or mix with the uninjected cells(A-C) while Rap1bV12 cells did(D-E).

FIGURE 9

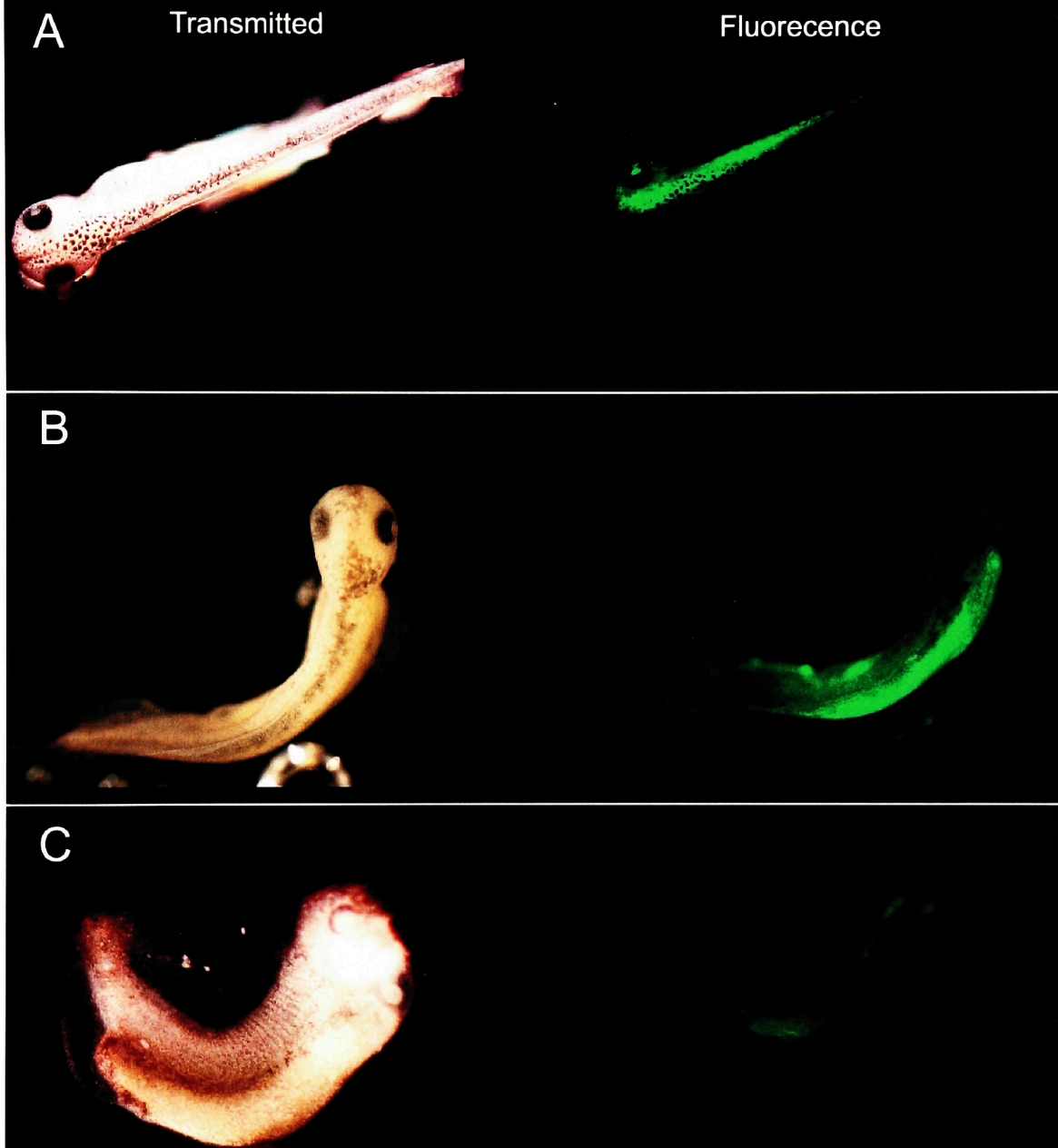


Figure 9. Overexpression of Rap1bV12(20pg) can enhance convergent extension movements while Rap1bN17(500pg) has an inhibitory effect. Despite the fact that overexpression of wild type Rap1b (200pg injected in the form of RNA together with GFP as a marker of the injected cells) had no effect on the elongation of axial and paraxial tissues and gave rise to normal embryos (injection of one out of two dorsal marginal zone blastomeres), overexpression of constitutively active Rap1bV12 lead to increased elongation of axial and paraxial tissues which resulted in embryos which curved away from the injected site(A-B). Overexpression of the dominant negative Rap1bN17 in both dorsal marginal blastomeres(injected in the form of RNA together with GFP as a marker of the injected cells) lead to inhibition of elongation and embryos curved towards the site of injection indicating abnormal convergent extension movements.

Rap1b can both inhibit and enhance convergent extension

Since our aim was to identify genes selectively involved in mesoderm migration after determining that Rap1b was involved in this movement we tested whether Rap1b can interfere with other morphogenetic movements. Blocking convergent extension leads to highly characteristic phenotypes as seen in Chapter 1 (Figure 9). Embryos become curved towards the area where convergent extension is inhibited due to reduced elongation of the tissue in question. Injection of *Rap1bN17* at the DMZ had an inhibitory effect on convergent extension and led to the formation of dorsally curved embryos while injection of the WT mRNA led to normal embryos (Figure 9A and C). On the other hand *Rap1bv12*, expressing embryos surprisingly showed increased elongation at the site of injection. When the left blastomere of a four cell stage embryo was injected with *Rap1bv12* together with GFP as a tracer the expressing side elongated more than the non-expressing side leading to a bend towards the right side of the embryo (Figure 9B). These data suggest that Rap1b might be required for convergent extension and that excessive Rap1b activity leads to an enhancement of this movement.

Discussion

We have shown that Rap1b is involved in morphogenesis during the *Xenopus* gastrulation. The fact that it can modulate both convergent extension as well as mesoderm migration leads to the conclusion that Rap1b is a factor generally required for cell movements. Both major morphogenetic movements that mesodermal cells undergo are blocked by the dominant negative form of Rap1b and the constitutively active form has been shown to enhance convergent extension movements in *Xenopus*. The same constitutively active construct failed to enhance mesoderm spreading and migration and might even inhibit this type of movement. This could be interpreted as either non-specific toxicity or a requirement for precise control of the activation level of Rap1b during mesoderm migration.

CHAPTER 3

Unbiased Screen for Factors Influencing Mesoderm Migration

Introduction

As mentioned in the introduction for Section 1, two main approaches were used in an effort to address the molecular basis of mesoderm migration. One was a screen of candidate genes out of which a number of proteins were identified that are important for this movement. The other was an unbiased screen of RNA pools from a gastrula stage expression library. Screening of this library resulted in the identification of one pool (665), which exhibited a potent morphogenetic activity that was further characterized. Despite repeated efforts, the gene responsible for the activity was not successfully isolated. Pool 665 blocked induced animal cap adhesion to FN during the early stages of gastrulation, during which time the explants elongated and allowed late stage adhesion and mesoderm migration. These results demonstrate that an explant can display temporally distinct morphogenetic movements.

Results

Spreading of induced mesoderm on fibronectin is inhibited by clone 665.

In a screen for the identification of genes involved in mesoderm, migration pools of RNA from a gastrula cDNA library were injected in the animal pole of two cell stage *Xenopus* embryos together with GFP as a marker of the expressing cells. The animal caps were then dissected prior to gastrulation, induced with activin, and placed in FN coated dishes to test spreading and migration. Compared to a control pool (664), cells injected with pool 665 remained in a concentrated mass of the explant and did not spread (Figure 10). In the areas of the explant where spreading was inhibited, elongated structures were observed (arrows Figure 10D). Despite the strong phenotype produced when 665 was injected in explants, it did not have any effect when these explants were dissociated and then plated on FN. These cells adhered quickly and their migration rates were

FIGURE 10

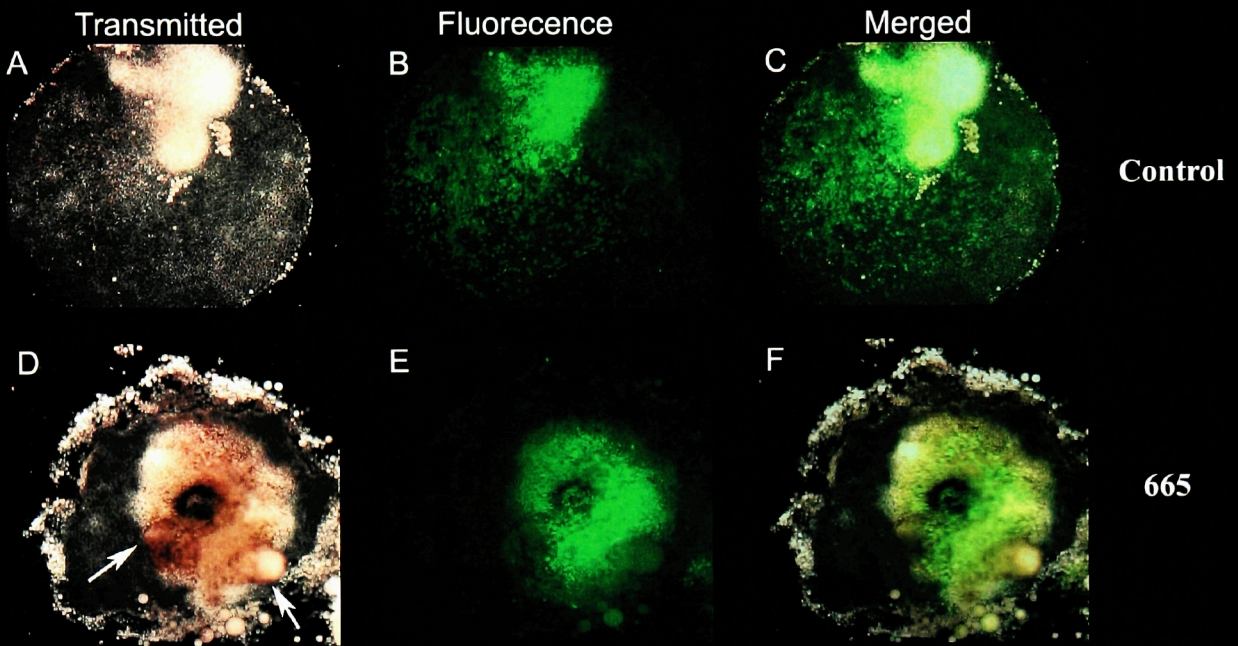


Figure 10. Pool 665 expressing explants fail to spread and migrate normally on fibronectin. Pool 665 and a control pool of RNA's (664) were injected on both animal cap blastomeres of two cell stage embryos together with GFP to mark the recipient cells. Animal caps were dissected at late blastula, induced with activin and were plated on fibronectin coated dishes where they were allowed to adhere and spread. While the control explant spread extensively (A-C) and GFP expressing cells were found throughout the explant the 665 injected explant failed to spread. Only the non GFP positive areas of the perimeter spread while the GFP positive cell mass remained concentrated in the middle(D-F). Abnormal elongated nodules can be seen within the GFP positive cell mass(arrows) indicating that convergent extension might have taken place instead of mesoderm migration.

comparable to those of GFP injected cells and cells injected with a control pool (664) that showed no phenotype in explant assays ([movie 3](#)). The lack of a phenotype in this assay would suggest that the activity of pool 665 does not alter the cell autonomous aspect of mesoderm migration but it only affects the non cell autonomous aspects of this movement.

We went on to analyze the behavior of 665 expressing explants using time-lapse microscopy. These recordings demonstrated that pool 665 can at low levels delay explant spreading in favor of convergent extension ([movie 4](#)). 665 expressing explants at early stages do not exhibit enough flexibility to spread, and they continuously rebound ([movie 5](#)), unlike control explants, which spread smoothly ([movie 6](#)). In order for spreading to occur, cells in the explant need to directionally intercalate towards the substrate, allowing the leading edge to proceed and the explant to spread into a monolayer sheet of cells. This can be seen in [movie 7](#), where the time-lapse recording was made from the bottom of a glass slide on which the explant was spreading. New cells keep appearing from deeper layers of the explant and come into contact with the ECM, at which point they adhere and start migrating outwards. While the intercalation needed for explant spreading is directed towards the ECM, in order for an explant to elongate the cells need to intercalate towards the midline. This type of intercalation gives rise to elongated explants of controls when they are not in contact with the ECM, and this type of intercalation is what 665 expressing explants exhibited during the initial phases of gastrulation ([movie 4](#), [movie 8](#)). At later times, these explants do spread on fibronectin, nearly dissolving the elongated structures formed by convergent extension ([movie 8](#), [movie 9](#)). This data shows that 665 can induce morphogenetic movements, but can also modulate movements induced by another factor, in this case activin. The fact that the modulatory effects were only observed in whole explants and not in dissociated cells suggests that 665 might function by modifying cell-cell interactions rather than cell-ECM interactions. Most importantly, the behavior of 665 injected explants shows that the same tissue can undergo both convergent extension and mesoderm migration, albeit at different times, something that has until now been rejected (Davidson, Hoffstrom et al. 2002).

Phenotype of pool 665.

When 665 was injected at the DMZ of four cell stage embryos, a range of mild phenotypes were observed at tailbud stage. Occasionally, a small part of the vegetal pole was not internalized (arrow [Figure 11A](#)) and reduced anterior structures (eyes, head). The protruding vegetal mass indicates a failure of the blastopore to close and is in agreement with previous data showing that inhibition of mesoderm migration by FRNK leads to the failure of blastopore closure ([Figure 7](#)). Co-injection with memGFP demonstrated that the expressing cells were viable, underwent convergent extension, and were found at the expected tissues according to the site of injection ([Figure 11A](#)). Expression of pool 665 in progenitor cells of axial and paraxial mesoderm did not alter their behavior and gastrulation proceeded normally, as evidenced by the elongated fluorescently labeled structures in 665 injected embryos. Injection of pool 665 at the animal pole of four cell *Xenopus* embryos induced abnormal morphogenetic movements on the animal cap at the onset of gastrulation, and 80% of the embryos developed posterior axis duplications at later stages. Co-injection with *mem-GFP* as a cell autonomous marker showed that both 665 expressing and non-expressing cells were found in the ectopic tail ([Figure 11B](#)). This leads to the conclusion that 665 can induce the formation of a number of tissues directly and indirectly. The phenotype of 665 is identical to that of *Laloo*, a Src family tyrosine kinase that was shown to be a mesoderm inducer, and injections of this gene also lead to posterior axis duplications (Weinstein, Marden et al. 1998). *Laloo* RNA injections also give rise to posterior axis duplications, and the injected cells contribute to the secondary axis, which contains both axial and paraxial tissues. The possibility of 665 being *Laloo* was eliminated by PCR amplification of the pool using *Laloo*-specific primers. The exact identity of the clone(s) responsible for the activity of pool 665 remains elusive.

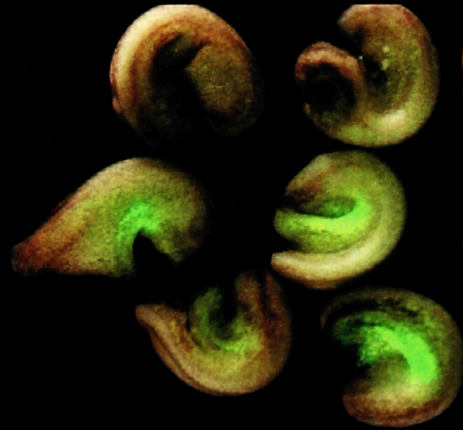
FIGURE 11

A



665 DMZ

B



665 AC

Figure 11. Phenotype of pool 665. (A) Injection of pool 665 together with GFP at the dorsal marginal zone of four cell *Xenopus* embryos typically lead to normal embryos with the expressing axial tissues elongating without problems as well as normal heads. In agreement with partial inhibition or delay of mesoderm migration occasionally the blastopore failed to close entirely preventing the complete internalization of the vegetal pole (arrow). (B) Animal cap injections of 665 with GFP lead to posterior duplications in the injected embryos. The secondary axis contains both GFP positive as well as negative cells.

CHAPTER 4

Akt

Introduction

Akt/PKB is part of the regulatory network required for sensing and responding to the chemoattractant gradients that mediate chemotaxis (Meili, Ellsworth et al. 1999; Servant, Weiner et al. 2000). The eukaryotic chemotaxis pathway begins with a receptor responsible for binding the chemoattractant (for example the formylated peptide receptor). The receptor, upon activation, sends a signal that generates PIP3 at the leading edge of the cell, or if the cell is not migrating yet, at the site where the chemoattractant is at its highest concentration. Subsequently, Pleckstrin Homology (PH) domain proteins like Akt (Protein Kinase B, PKB) are recruited to PIP3 through their PH domain where they catalyze the formation of actin filaments that push out the leading edge. The protein responsible for PIP3 accumulation is PI3K, and it has been shown that PI3K together with Akt control both cell polarity and chemotaxis (Chung, Potikyan et al. 2001). It is believed that directional movement of fibroblasts and other cells, as well as their radial membrane activity, are controlled by local generation and rapid degradation of 3' phosphoinoside second messengers (Haugh, Codazzi et al. 2000).

The migration of mesodermal tissue during *Xenopus* gastrulation has been shown to be directional (Winklbauer and Nagel 1991). The cues for this directional movement have not been identified, but a diffusible factor has been ruled out by experiments showing that the animal cap secreted ECM contains everything required for the directionality of the migration (Winklbauer 1990; Winklbauer and Nagel 1991; Nagel and Winklbauer 1999). The FGF pathway was shown to be essential for the animal cap to acquire the polarity, leading to directionality of migration and intact FN fibrils were also shown to be essential (Winklbauer 1990; Winklbauer and Nagel 1991; Nagel and Winklbauer 1999). More recently, the importance of directional cues has been challenged

citing sufficient polarity within the mesoderm itself to account for the directionality of mesodermal migration *in vitro* (Davidson, Hoffstrom et al. 2002).

The cues responsible for the directional movement of the mesoderm are believed to be immobilized within the ECM of the animal cap (Winklbauer 1990; Winklbauer and Nagel 1991; Nagel and Winklbauer 1999). This, however, does not rule out the involvement of the pathway leading to chemotaxis for the sensing of a potential gradient formed by immobilized cues within the ECM. In order to test this, the localization of Akt in directionally migrating mesoderm was determined. As mentioned before, Akt is an integral part of the chemotactic pathway. It has also been shown that it is recruited to the leading edge of chemotactic cells (Meili, Ellsworth et al. 1999; Servant, Weiner et al. 2000). Akt is a mitogen-regulated protein kinase involved in the protection of cells from apoptosis, the promotion of cell proliferation and diverse metabolic responses (Whiteman, Cho et al. 2002; Chang, Lee et al. 2003; Scheid and Woodgett 2003). Furthermore PKA overexpression was shown to block morphogenesis in a non-specific manner interfering with both mesoderm migration and convergent extension (Song, Choi et al. 2003). Because of its numerous activities, using a GFP-Akt fusion construct to monitor the dynamics of Akt would be complicated. The Akt's PH domain fused to GFP has been used before to identify the site of AKT activation within cells (Meili, Ellsworth et al. 1999; Servant, Weiner et al. 2000), and even more advanced constructs have been used to monitor the activation state of the entire protein (Sasaki, Sato et al. 2003). This construct has no enzymatic activity and was chosen as a less invasive way to monitor in real time the dynamics of Akt *in vivo*.

Injections of the Akt-PH-GFP construct into *Xenopus* embryos resulted in perfectly normal embryos independent of the site of injection, proving that our construct did not interfere with morphogenetic movements or the normal developmental process. Akt-PH-GFP was detected at the sites of cell contact *in vivo*, in agreement with previously published *in vitro* studies (Watton and Downward 1999). Its localization became polarized in response to diffusible agents originating from immobilized mesodermal cells, but was not polarized in the direction of migration in directionally

migrating mesoderm. These results indicate that directional mesoderm migration is unlikely to be a canonical chemotactic process.

Results

Xenopus mesoderm migrates directionally on animal cap deposited FN matrix.

Polarity within mesodermal explants was reported to be sufficient for the directional migration of mesoderm *in vitro* (Davidson, Hoffstrom et al. 2002). These results challenge previous publications that reported that the ECM of the animal cap contains guidance cues, necessary and sufficient, for the directional migration of explants (Winklbauer 1990; Winklbauer and Nagel 1991; Nagel and Winklbauer 1999). We wanted to test whether non-polar ectodermal explants induced with activin were capable of directional migration when cultured on animal cap secreted matrix. These explants were placed on a plastic dish where an animal cap was previously placed and allowed to “condition” a demarcated area. If an animal cap explant is cultured in direct contact with a petri dish, it secretes ECM components that coat the plastic surface rendering it capable to support adhesion and migration. The position of the top of the animal cap was demarcated and explants were placed on the conditioned matrix after the plate was washed with Marc's Modified Ringer's (MMR) buffer and coated with FN to ensure that the explant could adhere to the entire surface and not only the conditioned area. The experiment was monitored using time-lapse video microscopy. Repeated experiments using this setup confirmed that induced ectodermal explants were able to move directionally towards the site over which the top of the animal cap was located during conditioning ([movie 13](#) the top of the AC demarcated with a star). These results confirm that guidance cues are indeed present in the matrix secreted by the AC and that non-polar explants can sense these cues. They also confirm that single cells and very small explants are unable to sense these cues, and that they migrate randomly, pointing towards a need for a community effect for the sensing to be effective ([movie 13](#) arrow tips). Because the cues in the secreted matrix were not washed away by MMR washes, we also conclude that they are not diffusible, but rather embedded in the secreted matrix.

AKT's Pleckstrin Homology(PH) Domain fused to GFP is efficiently recruited to the membrane in gastrulating *Xenopus* mesoderm.

Since Akt was shown to be necessary for directional migration of chemotactic cells, we wanted to test its involvement in the directional migration of mesodermal explants. To test the feasibility of using Akt-PH-GFP in *Xenopus* as a marker of Akt's activity, we observed its localization in injected embryos. The Akt-PH-GFP construct was previously described in mammalian cultured cells where it localized at the sites of cell contact (Watton and Downward 1999). Akt-PH-GFP was localized at the cell-cell contact areas in all regions of the embryo including the animal cap, the marginal zone, and the vegetal pole (Figure 12A, B and C). In order to examine the localization of AKT-PH-GFP in mesodermal cells, embryos were injected at the four cell stage at both blastomeres of the dorsal marginal zone, and the marginal zone was subsequently dissected at blastula and dissociated. The cells were then seeded on a FN coated dish and observed with an epifluorescence microscope. Akt-PH-GFP was consistently localized to the membrane at the sites of cell-cell contact, but no membrane localization was observed in cells that were not in contact with any of their neighboring cells (Figure 12D and E). The movement from the cytoplasm to the membrane was rapid when cells came in contact, and also would quickly disappear when contact was broken during random migration showing a very fast activation deactivation cycle (movie 10). These data show that the Akt-PH-GFP construct can be rapidly recruited to the membrane in response to signaling from cell-cell contacts indicating an activation of Akt at these sites.

Polarization of Akt in directionally migrating mesoderm

Akt's polarization in response to chemoattractant in chemotactic cells occurs very rapidly and is maintained during the cells migration. In order to test whether this pathway is involved in the directional migration of mesodermal explants, Akt expressing embryos were dissected at early gastrula and were mounted with the epithelial cells facing down

FIGURE 12

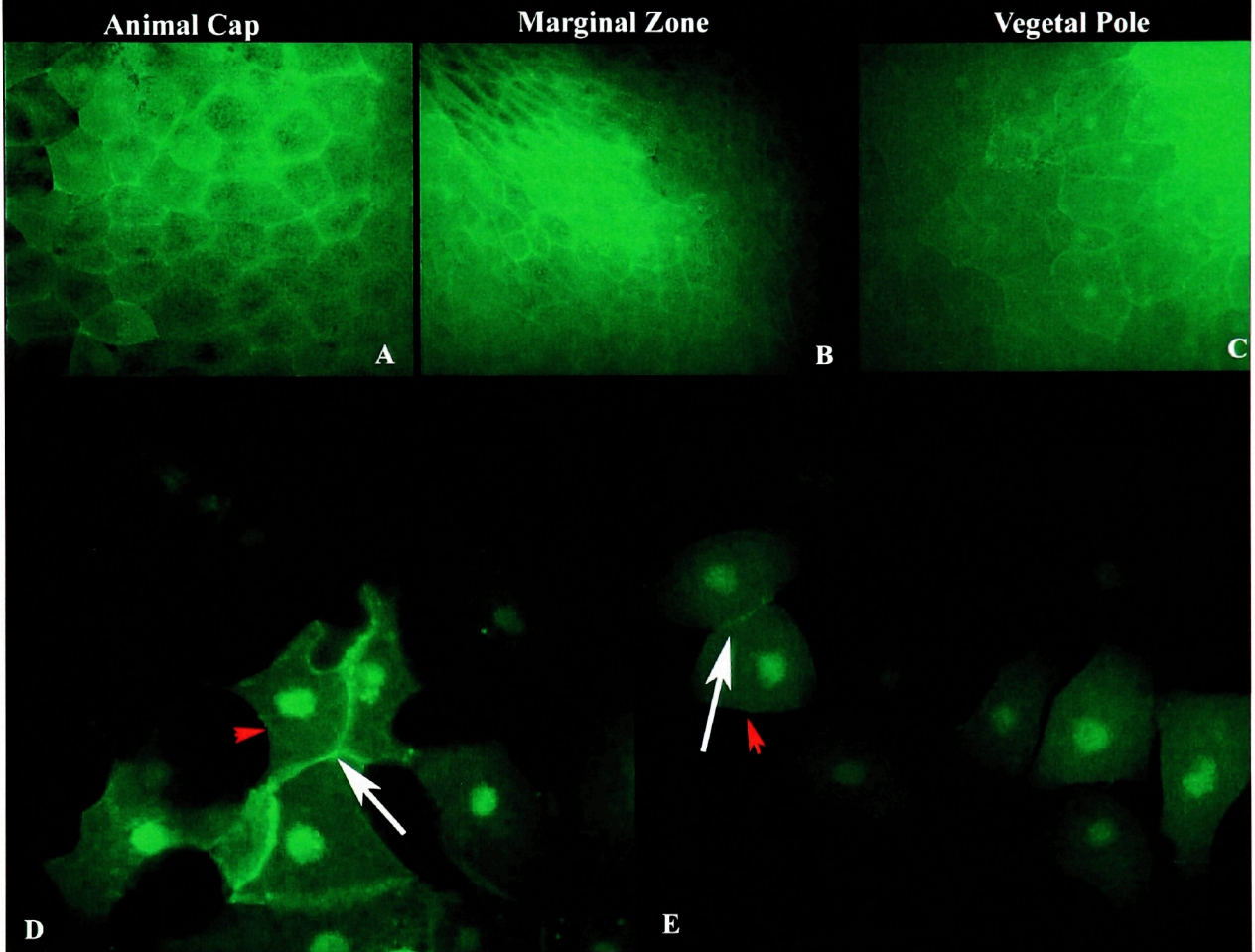


Figure 12. Akt-PII-GFP localizes at the membrane of the cell-cell contact areas in all regions of intact embryos including the animal cap, the marginal zone and the vegetal pole(A-C). A similar pattern is observed in dissociated mesodermal cells spread on fibronectin(D-E). Membrane localization of the Akt-PII-GFP construct is only seen at the areas of cell-cell contact(white arrows) while there is no Akt-PII-GFP at the free edges(red arrows). Cells that are in no contact with other cells have no membrane localized Akt-PII-GFP(E).

and a coverslip was placed onto the explant in order to keep it from rounding up and healing. This way, the directionally migrating mesoderm could be observed under a fluorescent microscope and the dynamics of the Akt-PH-GFP construct assessed ([Figure 13A](#)). Despite the constant recruitment of Akt to the membrane of these cells, no polarization in relation to the direction of movement was observed ([Figure 13B](#)). Akt was seen becoming localized on the membrane both on the side as well as the rear (in relation to the direction of movement) of the migrating cells at the areas of cell-cell contact. Movies made during directional migration of mesoderm failed to detect any transient or persistent polarization in the direction of migration, and AKT-PH-GFP was often absent from the leading edge of the explants ([movie 12](#)). This observation leads to the conclusion that the directional migration of mesodermal tissues during gastrulation does not depend on the chemotactic mechanisms employed by most cells. The cues present in the ECM, which are responsible for the directionality of the movement, are not diffusible and mesoderm might employ a novel mechanism to sense these cues.

Diffusible factors originating from mesodermal cells can activate the Akt pathway

Mesodermal cells migrating on FN show localized activation of Akt at cell-cell contact points. We wanted to also see if Akt is activated in these cells by secreted diffusible agents. In order to test this, we seeded Akt-PH-GFP expressing mesodermal cells on polylysine coated wells at very low densities, sealed the wells, and allowed the cells to settle for about one hour. By sealing the well, we prevent any mixing of the media from taking place, thus allowing the establishment of potential gradients of secreted factors. The polylysine coating allows non-specific adhesion and immobilizes the cells at their locations. The localization of Akt in these cells was observed by time-lapse fluorescent microscopy and the localization of Akt in cells that were close to each other compared to isolated ones. We observed polarization of the Akt-PH-GFP construct in cells that were in close proximity versus isolated cells where Akt was found evenly distributed around each cell ([Figure 13D and E](#) and [movie 11](#)). Filopodia and lamellipodia extensions were also polarized in cells where Akt was polarized, while they

FIGURE 13

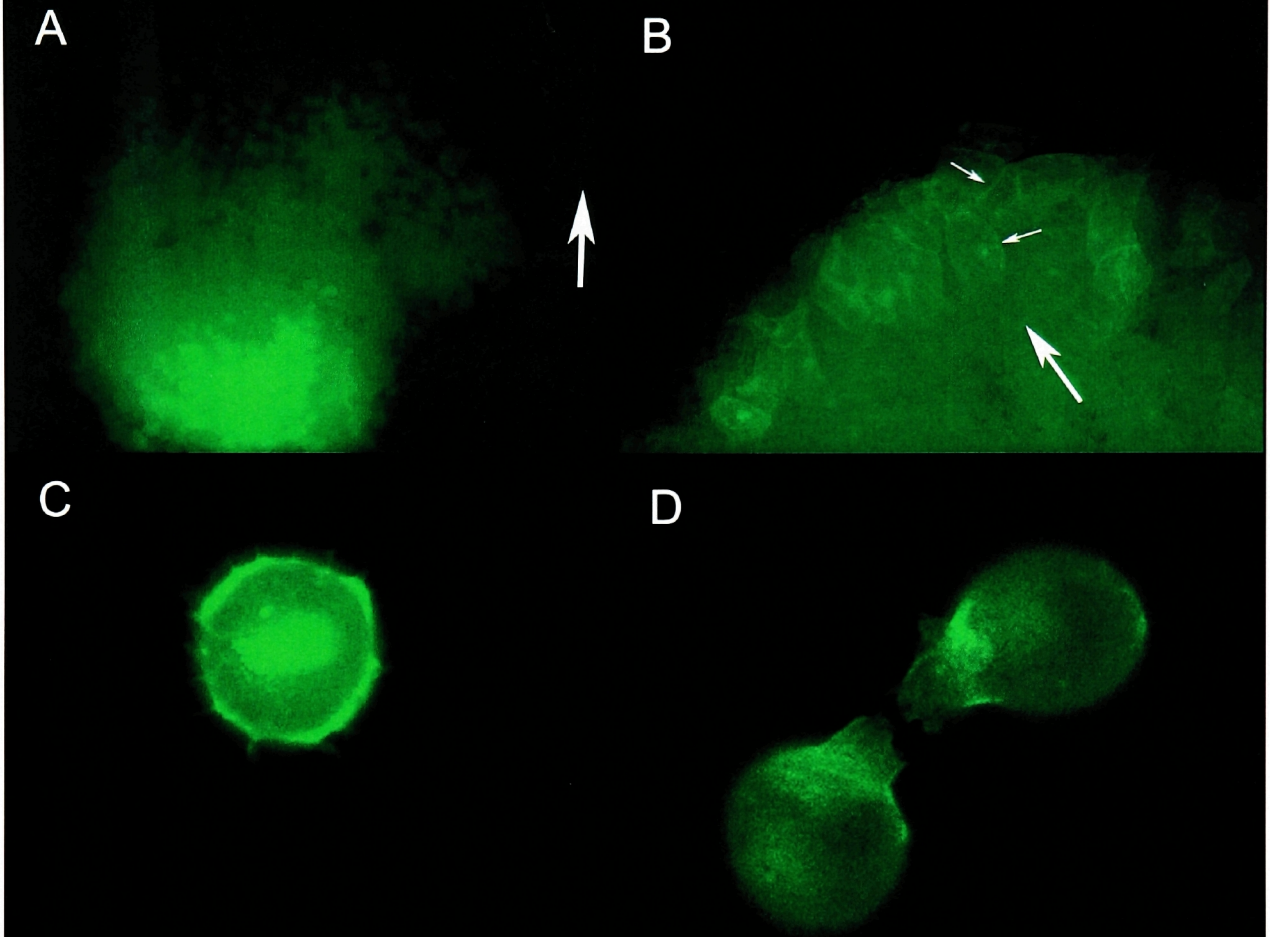


Figure 13. Akt-PH-GFP is not polarized in directionally migrating mesoderm but it does polarize in reaction to signaling between mesodermal cells. (A) An explant conating the dorsal marginal zone and the animal cap from a stage ten embryo was dissected and placed under a coverslip in a plastic dish. Akt-PH-GFP was injected at the dorsal marginal zone at the four cell stage. The explant was then observed under the microscope during the directional migration (arrow shows the direction of migration) and the localization of Akt-PH-GFP determined. (B) No polarization in relation to the direction of migration (large arrow) is observed and Akt-PH-GFP is recruited to the membrane at the rear and sides of migrating cells (small arrows). (C-D) Akt-PH-GFP polarizes in response to signals from mesodermal cells. Cells were seeded on a polylysine coated well were they adhered and became immobilized. The well was sealed and the localization of Akt-PH-GFP determined after one hour. Cells in close proximity (D) showed a polarization of the Akt-PH-GFP construct towards each other while isolated cells showed a uniform distribution (E).

were not in cells where Akt was not polarized (compare D and E of Figure 13). The direction of polarization was always towards the closest cell. These data indicate that diffusible factors secreted by mesodermal cells can activate the Akt pathway in neighboring cells in an oriented manner. The directionality of Akt's polarization suggests that mesodermal cells can orient themselves by detecting gradients of diffusible factors.

Discussion

The directional migration of *Xenopus* mesoderm was first described by Winklbauer (Winklbauer 1990). Although the need of having directional cues present in *Xenopus* has been debated (Davidson, Hoffstrom et al. 2002), the fact that mesodermal explants migrate directionally, and that this migration depends on the ECM secreted by the animal cap, is well established both in *Xenopus* and other amphibians (Winklbauer and Nagel 1991; Johnson, Darribere et al. 1993). We have now shown that induced ectodermal explants are also able to migrate directionally on animal cap conditioned substrates and that the directionality of migration requires a community effect as previously reported for mesodermal explants (Winklbauer, Nagel et al. 1996).

Guidance cues were postulated to be responsible for the directional migration of mesoderm in gastrulating amphibians. Revisiting this issue, haptotaxis was ruled out by the fact that the ability and strength of mesodermal adhesion does not change throughout the animal cap matrix (Winklbauer 1990; Winklbauer and Nagel 1991). The formation of FN fibrils has been shown to be necessary for directional migration. Both adhesion and migration occur when the fibril formation is disrupted but movement is no longer directional (Winklbauer and Nagel 1991). Despite the sufficiency of FN for adhesion and migration, other extracellular matrix components are present in animal cap ECM as well. Directionality of migration might be due to the polarized distribution of other ECM components or due to a gradient of an immobilized signaling molecule. One possibility is that the same pathways resulting in the polarization of chemotactic cells are employed in this type of directional cell movement as well. Akt specifically was previously shown to concentrate in cell-ECM contact areas (Watton and Downward 1999), which raises the possibility that Akt could potentially sense cues embedded in the ECM and not only

diffusible agents. Our data suggests that Akt is not involved in the directional migration of mesodermal explants, but indicate that Akt is involved in the sensing of diffusible factors originating from these cells. The directional polarization of Akt in cells that are in close proximity but not in contact reveals an ability of these cells to locate each others' position. In light of the fact that directional migration requires a community effect (Winklbauer and Nagel 1991, and data presented here) Akt might be involved in the polarization of the explant as a whole by mediating long distance cell-cell communication.

SECTION 2

Quantum Dots In Biology

Introduction

Nanometer-scale semiconductor crystallites (known as nanocrystals or quantum dots) (Murray, Norris et al. 1993; Alivisatos 1996; Hines and Guyot-Sionnest 1996) could dramatically improve the use of fluorescent markers in biological imaging (Bruchez, Moronne et al. 1998; Chan and Nie 1998). Since these colloidal particles act as robust, broadly tunable nano-emitters that can be excited by a single light source, they could provide significant advantages over current *in vitro* and *in vivo* markers (e.g., fluorescent proteins and organic dyes). However, before nanocrystals can be widely used as bio-labels, they must maintain three properties under aqueous biological conditions: efficient fluorescence, colloidal stability, and low non-specific adsorption. Unfortunately, despite recent advances (Bruchez, Moronne et al. 1998; Chan and Nie 1998; Mikulec 1999; Mattoussi, Mauro et al. 2000; Aldana, Wang et al. 2001; Gerion, Pinaud et al. 2001; Gerion, Parak et al. 2002; Goldman, Anderson et al. 2002; Parak, Boudreau et al. 2002), these conditions have not been simultaneously satisfied, limiting the development of *in vivo* applications of non-aggregated (or individual) semiconductor nanocrystals.

The main challenge is that the quantum dots (QD's), as synthesized, have hydrophobic organic ligands coating their surface (Murray, Norris et al. 1993; Hines and Guyot-Sionnest 1996). To make the QD's water soluble, these organophilic surface species are in general exchanged with more polar species, and both monolayer (Chan and Nie 1998; Mikulec 1999) and multilayer (Bruchez, Moronne et al. 1998) ligand shells have been pursued. While the monolayer method is reproducible, rapid, and produces QD's with a regular, well-oriented, thin coating, their colloidal stability is poor (Aldana, Wang et al. 2001). In contrast, the multilayer method yields QD's that are stable *in vitro* (Gerion, Pinaud et al. 2001), but the process is long and the coating is difficult to control. Another concern is that both approaches still produce QD's that tend to aggregate and

adsorb non-specifically. In an attempt to solve this issue, two additional coatings have been performed. First, the outer ligand shell of the QD has been overcoated with proteins adsorbed through hydrophobic or ionic interactions (Mattoussi, Mauro et al. 2000). Other layers can then be added to allow conjugation with specific biomolecules. Indeed, this method has provided new reagents for fluoro-immunoassays (Goldman, Anderson et al. 2002). Second, the outer ligand shell has been overcoated with surfactants or polymers to prevent non-specific adsorption of biomolecules while still permitting bioconjugation. For example, silica-coated QD's have been further modified with small monomers of poly(ethylene glycol) to reduce non-specific adsorption (Gerion, Parak et al. 2002).

Despite these efforts, non-specific adsorption and aggregation still occurs when QD's are used in biological environments. Studies of cellular uptakes of QD's report large aggregate formation inside the cell (Chan and Nie 1998; Dahan, Laurence et al. 2001). The same aggregation problems are reported when QD's are used for fluorescence *in situ* hybridization (Pathak, Choi et al. 2001), or as markers for molecular recognition on cell surfaces (Winter, Liu et al. 2001; Rosenthal, Tomlinson et al. 2002). Consequently, the use of QD's in biological applications is still limited and primarily confined to *in vitro* studies. Use of QD's in biology was restricted because there were no commercially available water soluble QD's and individual researchers had to attempt solubilization on their own. The recent description of water soluble QD's and their successful application in a living organism described in the following chapter and the use of commercially available water soluble QD's to perform non amplified fluorescent *in situs* in Chapter 2 of this section demonstrate that QD's are finally becoming integrated in biological research. The following chapters also demonstrate the immense potential QD's have to revolutionize biological imaging.

Chapter 1

In vivo use of micelle encapsulated QD nanocrystals

Introduction

Solubilizing QD's in an aqueous environment has been the primary challenge for researchers attempting to integrate this tool in biological research. Despite many attempts a method that would efficiently and effectively create water soluble QD's has been elusive. We found, however, that, without any surface modifications, individual ZnS-overcoated CdSe QD's (Murray, Norris et al. 1993; Hines and Guyot-Sionnest 1996) may be encapsulated (Material) in the hydrophobic core of a micelle composed of a mixture of n-poly(ethylene glycol) phosphatidylethanolamine (PEG-PE) and phosphatidylcholine (PC). These QD-micelles were effectively used *in vitro* to label DNA as well as *in vivo* for lineage tracing in a number of biological models. Our results show that encapsulating QD's in micelles is an effective and efficient way of creating water soluble and biocompatible QD's.

RESULTS

QD solubilization using phospholipids Micelles

Individual ZnS-overcoated CdSe QD's (Murray, Norris et al. 1993; Hines and Guyot-Sionnest 1996) can be encapsulated (Material) in the hydrophobic core of a micelle composed of a mixture of n-poly(ethylene glycol) phosphatidylethanolamine (PEG-PE) and phosphatidylcholine (PC) (Fig. 1A). PEG-PEs are micelle-forming hydrophilic polymer-grafted lipids (Hristova and Needham 1995; Belsito, Bartucci et al. 2000) that can be compared to naturally occurring carriers such as lipoproteins and viruses (Kataoka, Kwon et al. 1993). They have been used for drug delivery (Jones and Leroux 1999) and diagnostic imaging (Torchilin 2002). The advantage of these micelles

is that they are very regular in size, shape, and structure (Johnsson, Hansson et al. 2001). In addition, their outer surface is a dense layer of PEG polymers that is poorly immunogenic and antigenic and acts as excellent repellent for biomolecules (Golander, Herron et al. 1992). Further, both the PEG content and length can be adjusted precisely.

By transmission electron microscopy (TEM), the QD-micelles appear spherical and fairly monodisperse (Figure 14B and C). Their size was measured between 10 and 15 nm; however, this range probably reflects the different conformations that the PEG molecule can adopt as the QD-micelles lay down on the TEM grid. In any event, the size is very similar to the diameter of empty micelles formed with 100% PEG-PE phospholipids previously measured in solution (Lasic, Woodle et al. 1991; Johnsson, Hansson et al. 2001). The encapsulation of the QD inside the micelle does not significantly perturb its geometry or size. This is reasonable since, according to measurements of the micelle core (Johnsson, Hansson et al. 2001), one would expect QD's with diameters <3nm to fit loosely inside the micelle. QD's larger than 3nm should slightly overfill the micelle core and provide a solid hydrophobic surface that further stabilizes the structure. We observed that aqueous suspensions with 4nm ZnS-overcoated CdSe QD's were stable for months (even in 1M salt), whereas empty micelles degraded and formed aggregates after several days. Further, we observed that at 4nm, the vast majority of QD-micelles contained only one particle, while at smaller sizes (below 3nm) they contained multiple QD's, as one might expect. The fluorescence quantum yield of these QD-micelles in water was 24% without any optimization.

The ability to encapsulate single QD's depended critically on the properties of the PEG-PE block-copolymer. Both the PEG block and the two alkyl chains linked to the PE block seem necessary. Surfactants with a single alkyl chain did not form single QD-micelles, even if they contained PEG (e.g., Brij78 from Sigma). Conversely, surfactants with two alkyl chains that lack PEG, like bis(2-ethylhexyl) sulfosuccinate (AOT), allowed single QD's to be suspended in water, but failed to prevent aggregation when salt was added to the solution. Micelles also failed to form when PC alone was used. However, with PEG-PE phospholipids, QD-micelles could be formed with various PEG

FIGURE 14

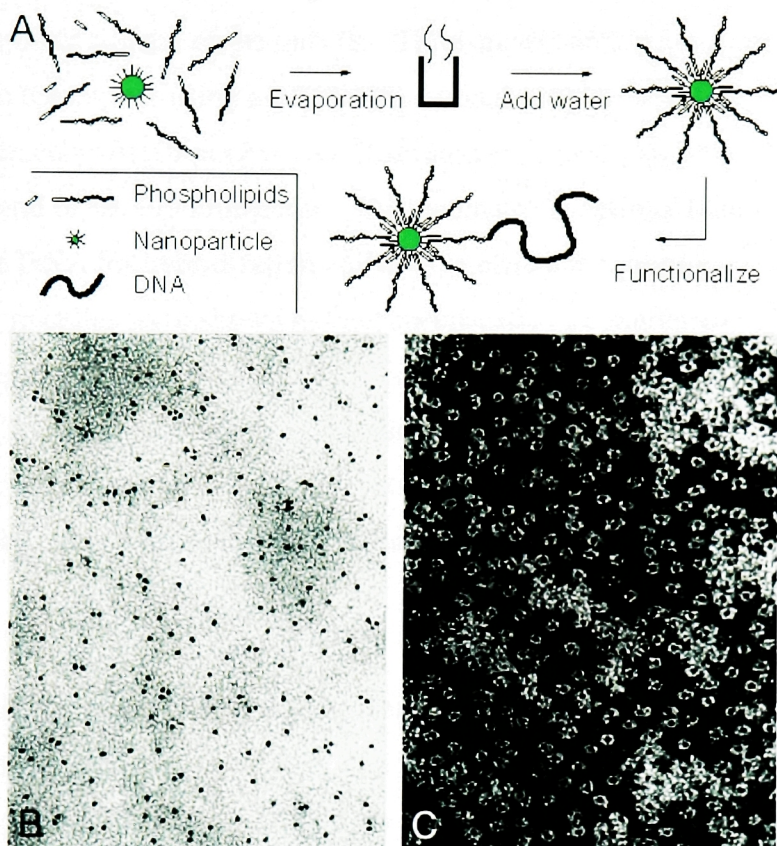


Figure 14. QD-micelle formation and characterization. (A) Schematic of single-QD encapsulation in a phospholipid block-copolymer micelle. (B) TEM image of QD-micelles dried on a carbon-Formvar-coated 200-mesh nickel grid. Only the QDs inside the micelle core are visible. The particles appear evenly spread on the surface. Although some clusters of two to four QDs are visible, most of the QDs are isolated, suggesting that a majority of micelles contain a single QD. (C) TEM image of the phospholipid layer obtained by negative staining with 1% PTA (phosphotungstic acid) at pH 7. With this technique, both the QD and the micelle can be visualized at the same time. The QD (dark spot) appears surrounded by a white disk of unstained phospholipids that stands out against the stained background. A JEOL 100CX TEM was operated at 80 kV.

lengths. QD-micelles similar in shape and stability were obtained from PEG chains with molecular weights of 550, 2000, and 5000. The results reported here are for PEG-2000.

Labeling of DNA Using micelle encapsulated QD's

The QD-micelles could be attached to DNA by replacing up to 50% of the PEG-PE phospholipids with an amino PEG-PE during the micelle formation, thus introducing a primary amine to the outer surface of the micelle. Thiol-modified DNA was then covalently coupled to the amines using a heterobifunctional coupler, with non-coupled DNA removed by ultracentrifugation (17). As illustrated in [Figure 15A](#), the DNA is coupled at the outer end of the PEG molecule. This geometry is optimal both to preserve the availability of the DNA for hybridization and to give efficient coupling. Oligonucleotide-QD-micelles were shown to bind specifically to complementary DNA, immobilized in 4% agarose beads, but not to non-complementary oligonucleotides ([Figure 15B](#) and [C](#)). This demonstrates that QD-micelles attached to the oligos do not prevent their specific hybridization to DNA targets. This process was also very rapid, as incubation times as low as 10 minutes yielded highly fluorescent agarose beads ([Figure 15C](#)).

These results compare favorably with those from silica-coated QD's. Our fluorescence signal to background ratio was above 150, compared to about four for silica-coated QD's (Gerion, Parak et al. 2002), due to the low non-specific adsorption offered by the PEG-2000. After a single PBS wash, we observed no fluorescence in the agarose beads decorated with non-specific targets ([Figure 15B](#)). In addition, our approach offers excellent conjugation yields. When the number of DNA-QD-micelles was smaller than the number of binding sites, all QD-micelles were immobilized in the agarose beads, suggesting that at least one DNA molecule was linked to each micelle. Moreover, compared to silica-coated QD's (Gerion, Parak et al. 2002), our QD-micelles are viable over a much broader range of QD and salt concentration.

FIGURE 15

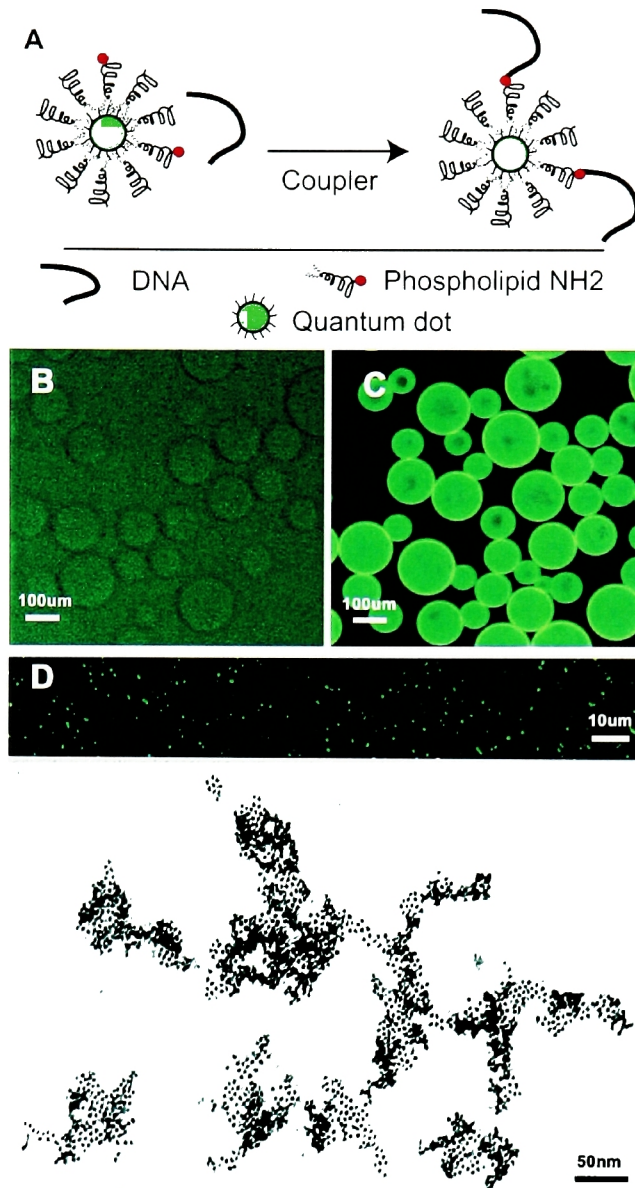


Figure15. Conjugation of QD-micelles with DNA. (A) Schematic of the QD-micelle conjugation with single-stranded DNA (ssDNA). (B and C) Hybridization of QD-micelles conjugated with DNA to surface-bound ssDNA. 5'-Biotin-modifiedssDNA (5'-TTACTCGAGGGATCCTAGTC-3') was attached to streptavidin-modified 4% agarose beads. A PBS solution containing QDmicelles conjugated with 20-base-long ssDNA was added to the bead solution and incubated at room temperature for more than 10 min. After rinsing once with PBS, the bead fluorescence is measured with an optical microscope. In (B), the oligonucleotides bound to the agarose beads are not complementary to the oligonucleotides bound to the QD-micelle. In (C), they are complementary. (D) Fluorescence image of aggregates of DNA-QD-micelles obtained by mixing equal amounts of two batches of QD-micelles conjugated with complementary single-stranded oligonucleotides. (E) TEM image of the same sample as in (D). The fluorescence images were obtained with Chroma filter set 41015 (wild-type GFP longpass emission with a 50-nm-wide band-pass excitation centered at 450 nm) mounted on a Zeiss fluorescence microscope. The samples were excited with a 50-W mercury lamp. Images were recorded with a color digital camera (AxioCam HR, Zeiss) and AxioVision Viewer software (Zeiss). In all experiments the QDs had a 3.5-nmdiameter CdSe core and ZnS outer layer. These QDs absorb light with wavelengths ~515 nm and emit light at ~550 nm. Their extinction coefficient is $8.4 \times 10^5 \text{ M}^{-1} \text{ cm}^{-1}$ (29).

To verify further the efficiency of the hybridization of DNA-QD-micelle conjugates to complementary sequences, we also performed directed assembly (Alivisatos, Johnsson et al. 1996; Mirkin, Letsinger et al. 1996). We mixed equal amounts of two batches of QD-micelles, each conjugated with a complementary oligonucleotide. After one-hour incubation at room temperature, fluorescent aggregates were visible under the microscope (Figure 15D). TEM confirmed that these aggregates, which ranged in size from 0.2 to 2 μ m, were formed from QD-micelles (Figure 15E).

In Vivo lineage Tracing Using QD's

The successful experiments *in vitro* prompted us to investigate QD-micelles *in vivo*. Synthetic fluorophores or fluorescent proteins are currently used as tracers for *in vivo* imaging. However, these approaches are restricted by photobleaching and the limited availability of different colors. QD-micelles offer an attractive alternative, but two criteria must be met. The QD-micelles must be biologically neutral (i.e., no biological activity or toxicity), and stable for long periods of time. To address these issues, we performed *in vivo* imaging with QD-micelles by microinjecting early *Xenopus* embryos (Figure 16A). An embryo is a sensitive test environment for biological activity and toxicity because cellular perturbances translate into measurable biological phenotypes. We chose *Xenopus* since a large number of embryos could be easily obtained, allowing a statistical analysis of different parameters. Figure 16 shows QD-micelles injected into individual cells of an early embryo. Several key results are noted: First, the QD-micelles are cell-autonomous. When one cell from a two-cell embryo was injected, the QD fluorescence was confined to the progeny of the injected cell (i.e., only half of the embryo was fluorescently labeled). If injected later in embryogenesis into individual blastomeres, the QD's were similarly confined only to the progeny of the injected cells during development (Figure 16 B through E). Second, the QD-micelles seem to have very little activity or toxicity. The toxicity is sufficiently low that cell lineage could be traced using fluorescence visualization. We found that for typical QD injections (2×10^9 QD's/cell), injected embryos display an unaltered phenotype and their health is statistically similar to uninjected embryos (Figure 17 Table1). At higher injection

FIGURE 16

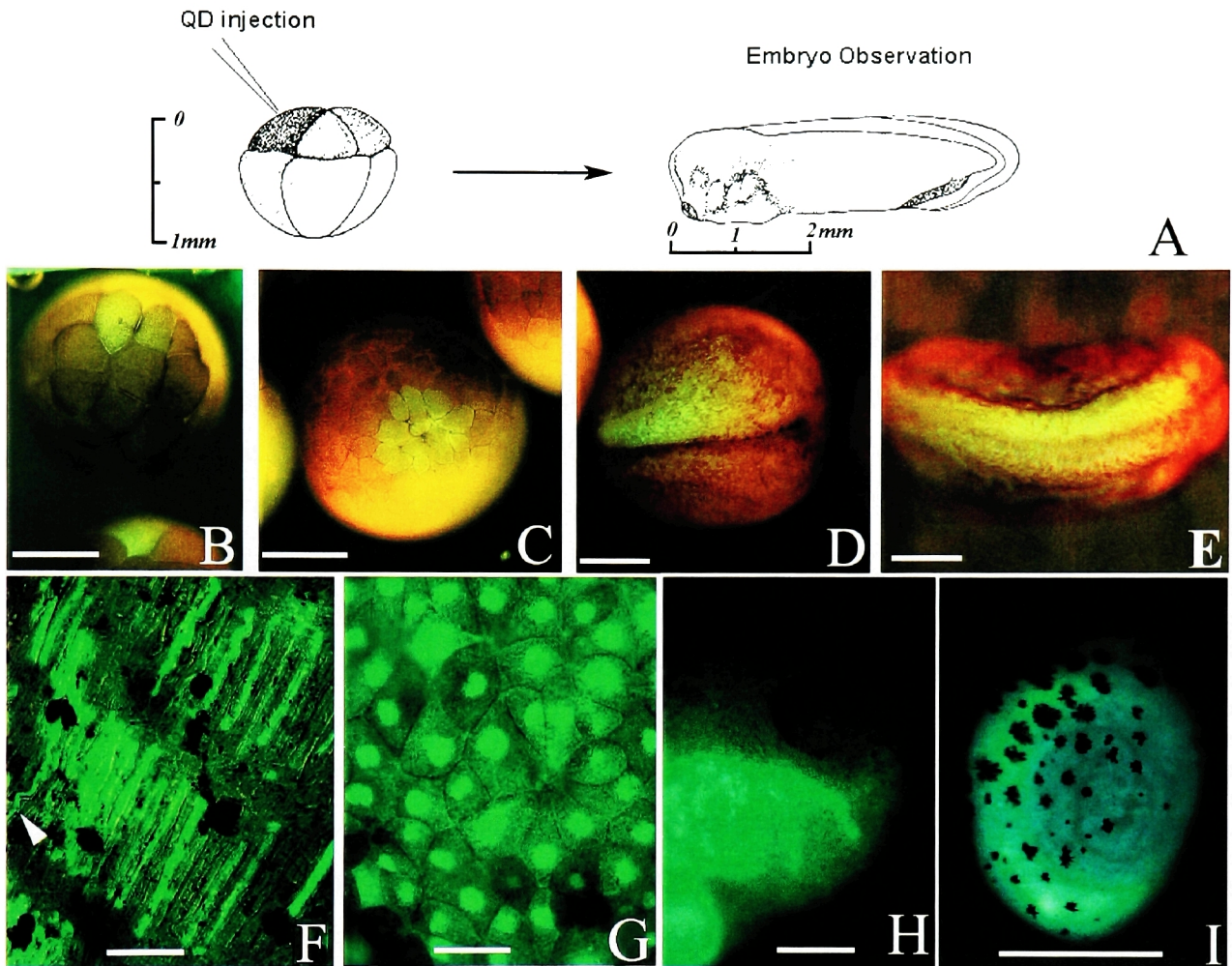


Figure16. QD labeling of *Xenopus* embryos at different stages and specific QD intracellular localizations. (A) Schematic showing the experimental strategy. QD-micelles, as in Fig. 2, were injected into an individual blastomere during very early cleavage stages. Between 1.5 and 3 nl of a 2.3 M suspension of QDs were injected, corresponding to 2.1×10^9 to 4.2×10^9 injected particles per cell. Embryos were then cultured until they reached different stages of development, and imaging was done as in Fig. 2. In (B) to (E), transmission and fluorescence images have been superposed. (B) Injection of one cell out of an eight-cell-stage embryo resulted in labeling of individual blastomeres. (C) Same embryo shown 1 hour later. The daughter cells of the injected blastomere are labeled (D) and at a later stage (E) show two neurula embryos, which were injected into a single cell at the eight-cell-stage in the animal pole. The QDs can be visualized through the pigmented layer of the epidermis. (F) Intracellular labeling of an axon (arrow) and somites at tadpole stage 40. The QD-micelles migrate into axons all the way to growth cones. In the somites, the QD-micelle seems to localize in subcellular structures. (G) QDs localized in the nucleus during mid-blastula stages. This localization is reduced in later stages of the development. (H) Labeled neural crest cells migrating into the branchial arches. (I) QD fluorescence observed in the gut of an injected embryo. Bars: (B) to (E), (H), and (I), 0.5 mm. (F) and (G), 30 μm .

concentrations (larger than 5×10^9 QD's/cell), clear abnormalities become apparent. The cause of these defects is not yet known, but may result from changes in the osmotic equilibrium of the cell. Third, the QD-micelles are stable *in vivo*. The fluorescence signal remained detectable throughout the experiment despite a restriction of the signal after the tailbud stage (we observed up to late tadpole stages). In addition, after four days of embryonic development, the QD-micelles did not exhibit any visible aggregation. Fourth, the QD-micelle can label all embryonic cell types, including somites, neurons and axonal tracks (Figure 16F), ectoderm (Figure 16G), neural crest (Figure 16H) as well as endoderm (Figure 16 I) without visible segregation. Fifth, the QD fluorescence is visible very early during development (Figure 16B), despite pigmentation and strong background fluorescence. In contrast, injection of green fluorescent protein (GFP) as a tracer (e.g., by injection of RNA which encodes GFP) requires time for GFP to be expressed at levels detectable *in vivo*. Sixth, examination of the embryos at tadpole stages also showed that strong QD fluorescence is visible even in high background regions such as the embryo guts (Figure 16H and I). Finally, the QD-micelles are much more resistant to photobleaching than other fluorophores *in vivo*, which has been shown previously *in vitro* (Bruchez, Moronne et al. 1998). Figure 17 compares the *in vivo* fluorescence quenching of QD-micelles and rhodamine green-dextran (RG-D). QD-micelles and RG-D were microinjected into sibling embryos which were at similar stages of development and had progressed to late blastula when they were imaged using time-lapse microscopy. After 80 minutes of constant illumination (at 450nm) under the microscope, the QD fluorescence intensity remained unchanged (movie 16), whereas the dextran had photobleached. Experiments using a membrane-bound GFP (EGFP fused to the Ras farnesylation sequence) gave similar results with the QD's being significantly more stable.

Interestingly, despite the fact that at early embryonic stages QD's appear to be diffusely localized in the entire cell, at later stages they concentrate in the cell nuclei (Figure 16G). Time-lapse microscopy (movie 14, movie 17) revealed that this translocation to the nucleus occurs at a stage that phenotypically resembles the Mid-Blastula-Transition (MBT) (Newport and Kirschner 1982), a very important stage in

FIGURE 17

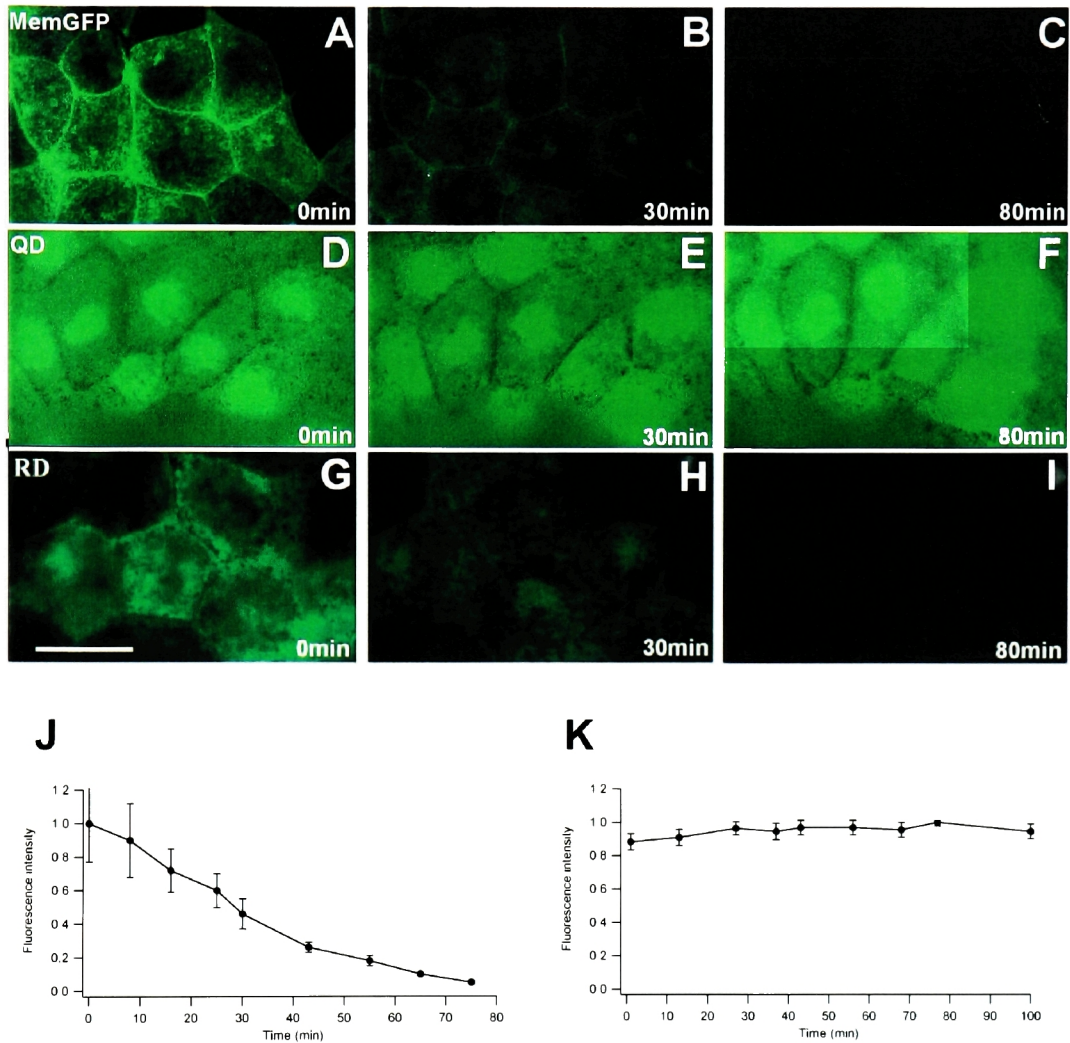


Table 1

Stage 19-20	n=55		n=39	
	1.5nl in 1 out of 8		Control	
Normal	38	69%	27	70%
Defects	15	27%	12	30%
Dead	2	4%	0	0%

Figure 17. Comparison of QD, RG-D (Rhodamine Green Dextran, Molecular Probes) and memGFP for resistance to photobleaching. QDs and injection amounts are similar to those used in Fig. 16. For RG-D, 1 nl of a 25 mg/ml solution was injected. (A to C) Consecutive images of RG-D–injected Xenopus animal pole blastomeres. (D to F) Consecutive images of QDinjected Xenopus animal pole blastomeres. (G to I) Consecutive images of memGFP injected Xenopus animal pole blastomeres. During each experiment, the injected embryos were excited continuously at 450 nm. (J) Graph representing the variation of fluorescence intensity of one cell of the RG-D–injected embryo (dotted line) and of one cell of the QD-injected embryo (solid line). Bars, 30 μ m. The optical setup is as described in Fig. 15

amphibian development when zygotic gene transcription is initiated. The internalization of cells in [movie 14](#) is abnormal and is due to excess amounts of QD's injected to make the translocation easy to visualize but this result did not change at lower injection amounts. As QD-micelles do not bind to DNA directly, it would be interesting to explore the mechanism of this translocation. If the translocation proves to be concomitant with MBT, QD's will make observation of MBT *in vivo* with single-cell resolution (a detailed analysis in the following chapter). Another interesting observation resulting from the nuclear accumulation of the QD's was the fact that the nuclei in these cells exhibited rapid movements that have not been described before ([movie 16](#)). The nuclei rotate and move within the cytoplasm and the role, if any, of these movements warrants further investigation.

Lineage Tracing and Labeling in Other Model Systems

The successful experiments in the frog lead to experiments where QD micelles were used to label cells and organs in other biological model systems as well as experiments in tadpoles. In one such experiment the vasculature of a living *Xenopus* tadpole was labeled by injecting QD's in the heart ([Figure 18A](#) and [B](#)). These tadpoles showed no evidence of toxicity and were just as viable as water-injected controls, further demonstration that QD-micelles are not toxic to living organisms. Furthermore, the labeling of the vasculature lasted much longer than what could be achieved with other fluorophores and was significantly brighter offering exceptional resolution of the individual vessels of the vasculature ([Figure 18A](#) and [B](#)). The QD's were also injected and used to successfully label adherent cells in culture as well as cells in a mouse blastocyst ([Figure 18D](#) and [E](#)). Multiple color labeling was also performed by using three different colors of QD's to inject an eight cell *Xenopus* embryo. These embryos could be visualized with a single QD filter at the same time ([Figure 18F](#)). Clearly three colors can be easily distinguished but the narrow emission spectra of the QD's makes the identification of many more colors at the same time possible. Countless shades of each color can be produced by varying the QD size and these shades can be positively identified and distinguished. These experiments demonstrate that QD's can be used in a

FIGURE 18

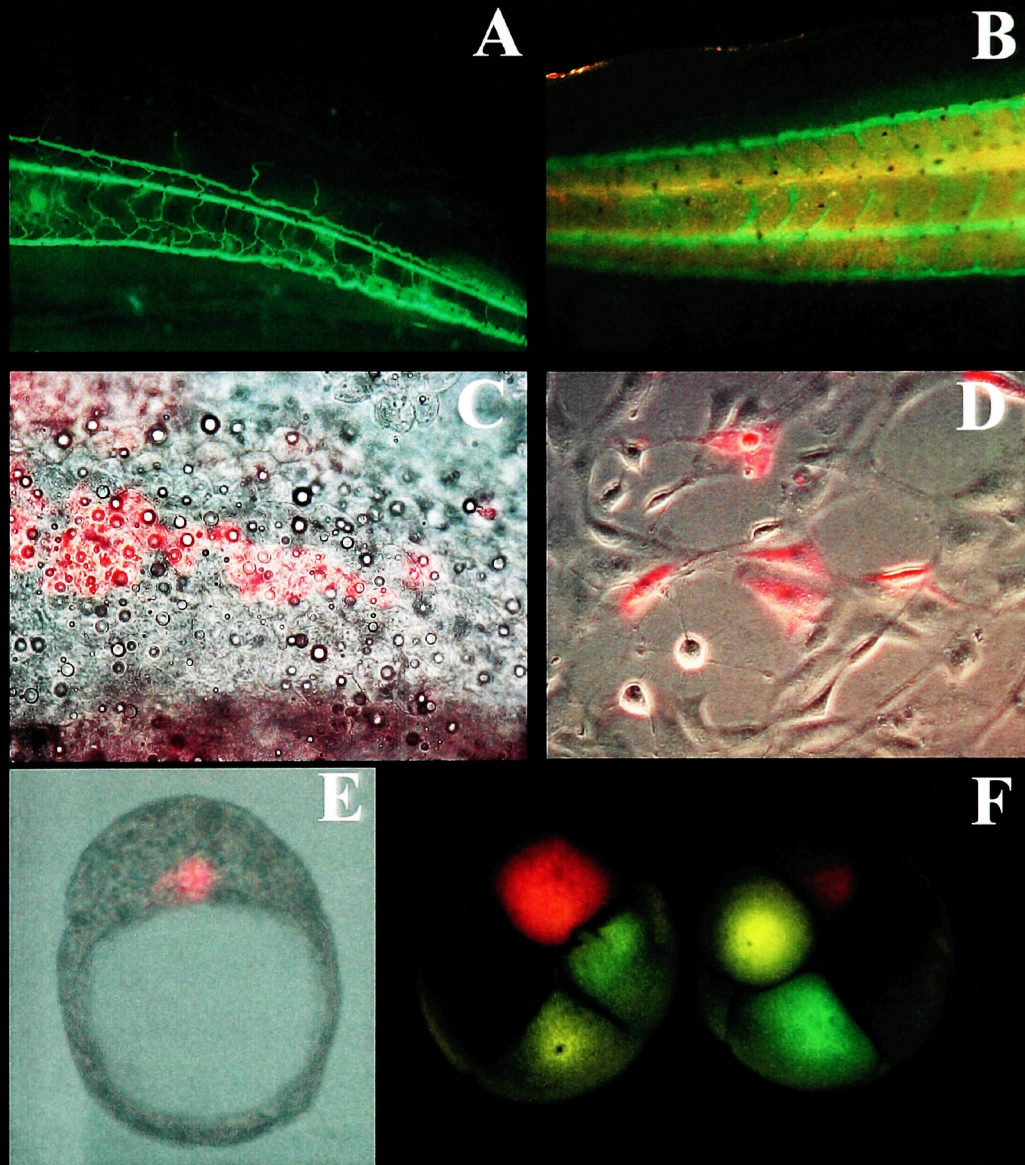


Figure 18. QD labeling in *Xenopus* cultured cells and a mouse blastocyst. (A-B) Labeling of the *Xenopus* vasculature by injection of QD-micelle solution in the heart of a tadpole. A is a fluorescent image of the tail of an injected tadpole and B is an image taken using both epifluorescence and transmitted light at the same time. The labeling of the vasculature is bright, detailed and lasts longer than labeling using organic fluorophores. (C) Labeling of epidermal cells with red QD's a week after injection. (D) Labeling of fibroblast cells in culture with red QD's. The fluorescently labeled cells were injected one at a time using an adherent cell injection setup. (E) Red QD labeling of a cell in a mouse blastocyst. (F) Multi color QD labeling of an eight cell stage embryo.

variety of biological models for lineage tracing and labeling and their use offers distinct advantages over current methods of labeling and lineage tracing.

QD Micelle Stability

Despite the great advantages and the easy method of solubilization the use of micelles presents some problems. The most serious problem is long-term stability. Although QD micelles proved to be extremely stable in solution for months and in a variety of buffers they always fall apart in the presence of detergents. The QD-Micelle stability is also extremely reduced when the micelles are inside the cells of an embryo, where they last up to four days, but a significant reduction in fluorescent intensity is gradually observed after that as well as restriction of the signal distribution. This reduction cannot be attributed to dilution (due to the embryos growth) alone and could be due to a number of reasons. The cells could be degrading the micelles actively, the micelles might be recognized and expelled from labeled cells or the micelles might break down gradually in the presence of membranes, which could act as traps for the phospholipids. The restriction of the signal also suggests that QD-micelles are more stable in some cells than in others. Imaging of resulting tadpoles more than a week after injection in the two-cell embryo offers the first clue for the fate of the QD-micelles. The QD's appear to be concentrated in round clumps outside of the cells. These clumps range in size with the bigger ones being about the size of cells ([movie 15](#)). The great majority of the QD's injected are found in such structures while there still are labeled cells with normal morphology even after a week ([Figure 18C](#)). The QD's within these clumps appear to be aggregated, which suggests that the micelles have either fused or they were degraded releasing the QD nanocrystals which in turn aggregate. We wanted to explore the reasons behind the differences in stability in buffers versus the stability inside the cells further. If the phospholipid molecules making up the micelles occasionally come off, then we would expect a much higher stability in a solution where there is no "sink" for these molecules, and they are going to eventually end up in another micelle, effectively creating a constant exchange of phospholipids between the micelles. To test this hypothesis, two glass capillaries were filled with the same QD-micelle solution. In

one of the capillaries a hydrophobic sink was created by layering mineral oil at the surface of the QD solution. The mineral oil/buffer interface would offer a place where the hydrophobic heads of the phospholipids could be trapped. As shown in [Figure 19](#) after 24 hours there was a clear reduction of fluorescence intensity in the capillary with the mineral oil sink. This result confirms that phospholipids do come off the micelles and suggests that the reduced stability of the QD-micelles within cells is at least partially due to this phenomenon.

Increasing the QD-Micelle Stability

The experiment described above demonstrated that the limited *in vivo* stability of the QD-micelles is at least partially due to an exchange of phospholipids from the micelle surface. Despite the increase in stability of QD-micelles compared to empty micelles derived from both the presence of a solid hydrophobic core as well as the PEG on the phospholipids it is clear that further stabilization would be required in order to make the QD-micelles an effective long term lineage tracer and to enable their use *in vitro* in solutions containing detergents and surfactants. Use of crosslinkable phospholipids followed by UV cross-linking, as well as use of much larger PEG chains to improve stability, were met with some success, but both approaches resulted in a much lower efficiency of micelle formation. UV crosslinking led to a formation of QD micelles solution that lasted up to twelve hours (defined as the time by which there was no detectable fluorescence in the solution) in 0.1% triton PBS vs two hours without crosslinking. The efficiency of solubilization using this method was only 10% of the original that was near 100%. Future work will show if crosslinking is the answer to the micelle stability problems.

QD-Micelle Toxicity

Despite the fact that sufficiently high amounts of QD's could be injected in the embryos to enable visualization of the labeling at the earliest stages of development toxicity issues arose with the injection of more than 5×10^9 QD's/cell. This number is

FIGURE 19

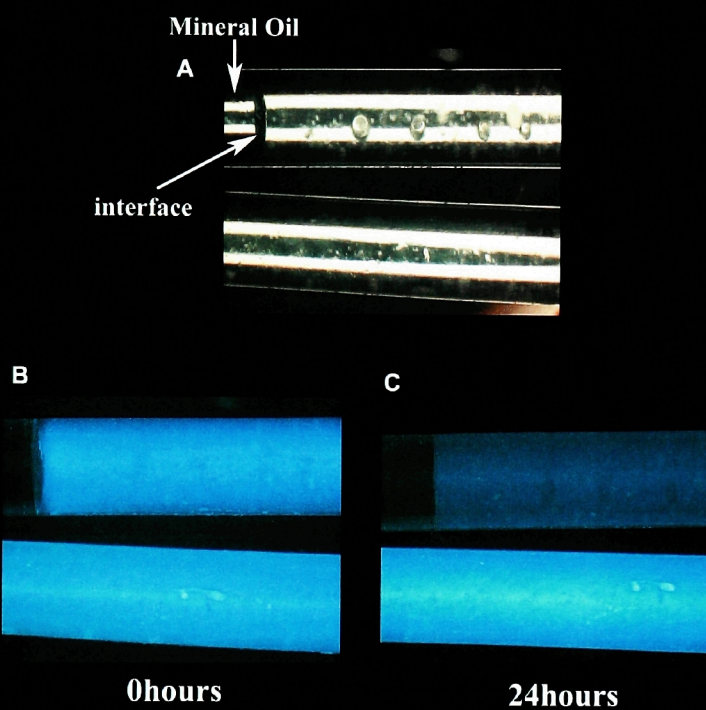


Figure 19. QD micelles suffer from poor stability in the presence of a hydrophobic sink. An aqueous solution of QD-micelles was used to fill two glass capillaries. In one of the two capillaries the QD solution was layered with a drop of mineral oil(A). The two capillaries were sealed at both ends and imaged under a fluorescent microscope. The rate of fluorescence decay was assessed by imaging the two capillaries every hour. Despite the fact that at time 0 the signal intensity from both was comparable(B) after 24 hours the fluorescence was significantly reduced in the capillary with the hydrophobic sink(C).

relatively low when compared to the toxicity of other fluorophores. In an effort to identify the source of toxicity, we injected unincorporated phospholipids into *Xenopus* embryos at different concentrations and observed the effects of these injections. It was determined that unincorporated phospholipids were several thousand-fold more toxic than incorporated ones. More surprisingly phospholipid micelles that did not contain QD's were also several hundred-fold more toxic than QD-micelles. This is probably due to their reduced stability compared to QD-micelles, which leads to the release of toxic free phospholipid in the cells when micelles break down. In an effort to further reduce the toxicity, QD-micelles were purified by ultracentrifugation in a sucrose gradient twice to eliminate empty micelles, free phospholipids, and potential traces of chlorophorm (see materials and methods). This purification lead to consistently lower toxicity and persistence of labeling in one week old tadpoles in areas where labeling had been lost when using QD-micelles derived with the original protocol. Labeling was present at the epidermis ([Figure 20A](#)), muscle somites ([Figure 20B](#)) anterior structures including the brain ([Figure 20C and D](#)), the eye lens ([Figure 20](#) inset of D) and fin mesenchymal cells ([Figure 20E and F](#)). Although this purification leads to QD-micelle toxicity levels that are acceptable for lineage tracing purposes, we believe the remaining toxicity to be stemming from the instability of the micelles, which inadvertently leads to the release of free phospholipids irrespective of the extent of the initial purification. This issue would be addressed if efforts to improve the stability were successful.

Discussion

These results indicate that micelle-encapsulated QD's fulfill the promise of fluorescent semiconductor nanocrystals for both *in vitro* and *in vivo* studies. Compared to other systems, they simultaneously provide efficient fluorescence, a great reduction in photobleaching, colloidal stability in a variety of bio-environments, and low non-specific adsorption. Although the QD-micelle stability is an issue that will have to be dealt with, even the current stability allows their use in a variety of ways. While here we demonstrated *in vitro* DNA hybridization and *in vivo* imaging during embryogenesis,

FIGURE 20

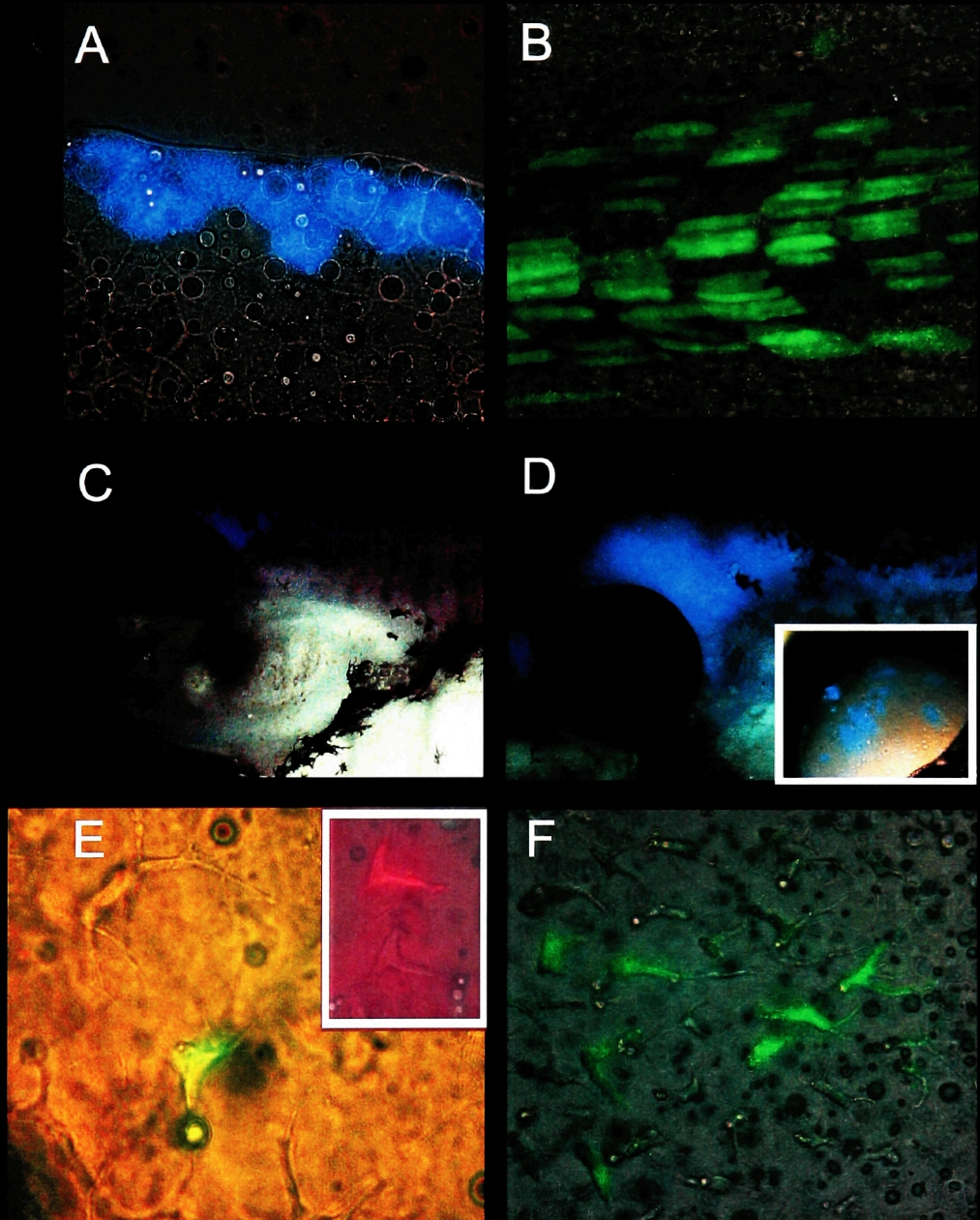


Figure 20. Sucrose gradient purification of QD-micelles leads to lower toxicity and longer persistence of QD-staining in *Xenopus* embryos. (A) Labeling of epidermal cells using green QD's 8days after the injection into the animal cap of a two cell embryo. The labeling appears blue due to the balancing of the digital color camera for maximum detection sensitivity and rejection of background fluorescence (see materials and methods). (B) Muscle somite staining using green QD's 7days after injection at the dorsal marginal zone of a four cell embryo. (C-D) Labeling of anterior structures including the brain and the eye lens(inset of D) seven days after injection at the dorsal marginal zone. (E-F) Labeling of mesenchymal cells on the fins of ten day old *Xenopus* tadpoles with green and red(inset of E) QD-micelles.

QD-micelles exhibit properties that should impact a much larger area from genomics to proteomics.

QD's offer numerous advantages over all current fluorophores available to biologists. In some ways, they are the ideal fluorophore and are bound to become part of mainstream biological research. Since our publication of successful *in vivo* use of soluble QD's for labeling and lineage tracing, QD's were successfully solubilized using amphipathic polymers that were directly coated onto them (Wu, Liu et al. 2003). Although these QD's are asymmetrical and their size is not easily controlled resulting in a non-homogeneous mixture they are extremely stable both *in vitro* and *in vivo* (Skourides, et al. unpublished data). These QD's are now available commercially and make the QD-micelles a less attractive method of solubilization purely based on stability. The geometric symmetry and precise size control of the resulting water soluble QD's are the advantages offered by the method we describe, but an increase in stability will be essential for this method to be a viable alternative to the current commercial process.

CHAPTER 2

QD accumulation in the nucleus at Mid Blastula Transition

Lineage tracing experiments using micelle encapsulated QD's lead to the observation that these QD's would accumulate to the nucleus at a stages equivalent to MBT. Given the importance of this stage during amphibian development, this property of the QD's raised the possibility that they could be used as *in vivo* markers for the resolution of the spatial and temporal aspects of MBT with single cell resolution.

One of the first issues that needed to be addressed was the timing of the translocation and whether it did indeed coincide with MBT. For this purpose, time-lapse movies were taken of whole embryos, as well as dissociated cells, in order to establish the exact number of divisions before the QD's became nuclear ([movie 18](#), [movie 19](#), [movie 19b](#)). QD's became concentrated in the cell nuclei after the 12th division, this matches the onset of MBT (Newport and Kirschner 1982). Another hallmark of MBT are cell movements and membrane blebbing (Newport and Kirschner 1982). Careful observation of individual cells shows that QD nuclear accumulation is seen right after blebbing begins to occur ([movie 19](#), [movie 19b](#)). These results established the temporal coincidence between QD translocation and MBT.

A Nuclear Localization Signal containing GFP protein accumulates in the nucleus at MBT.

In order to test whether the QD's were actively being transported to the nucleus, an inhibitor of active nuclear transport was used. Initial experiments where active nuclear transport was blocked indicated that when this process is blocked (using the previously characterized, active nuclear transport inhibitor Wheat Germ Agglutinin or WGA) the QD's nuclear accumulation is also blocked (Yoneda, Imamoto-Sonobe et al. 1987). This raised the surprising possibility that active transport was either not taking place or was limited before MBT in *Xenopus*. To test this hypothesis purified GFP protein containing a

nuclear transport signal (NLS) was injected into two cell embryos and its localization was monitored using time-lapse video microscopy. NLS-GFP was seen accumulating in the nucleus only after the 12th cell division at MBT giving support to the hypothesis that nuclear transport might indeed be inhibited prior to MBT ([movie 20](#)). At the same time, this result raised the suspicion that the extreme opacity of the blastula cells prior to MBT might be responsible for the sudden appearance of nuclear accumulation right after the 12th cell division. Staining of nuclei with a cell permeable Hoechst dye precluded this from being the case because nuclei were clearly visible well before MBT and nuclear accumulation in intact embryos ([Figure 21](#)).

QD nuclear accumulation is due to passive diffusion through the nuclear pore

A fortuitous observation that fluorescent dextran would also accumulate to the nucleus at MBT, albeit to a much lesser extent, prompted the question of whether the QD accumulation to the nucleus was indeed due to active transport. A series of experiments were carried out where WGA (+Texas red as an indicator of the cells which have received WGA) was injected in one out of two cells where QD's were previously injected. Cell permeable Hoechst was also used to stain the nuclei after MBT. These experiments demonstrated that WGA was unable to block the nuclear accumulation of QD's in nucleated cells ([Figure 22](#)). The original observation was false due to the fact that high WGA concentrations causes many cells to become anucleated, as seen in [figure 22](#). Every cell that is positive for Hoechst nuclear staining and WGA also has QD accumulation in the nucleus. This experiment demonstrated that active transport was not responsible for the QD accumulation in the nuclei and prompted experiments to test whether the QD's were actually passively diffusing into the nucleus and getting trapped. This was likely due to their ~10nm size, which was close to the limit for passive diffusion through a nuclear pore (Paine, Moore et al. 1975). To test this, QD-micelles of different sizes were injected into *Xenopus* embryos and their localization after MBT was determined. Red QD which are substantially larger than the original green QD's (14-16nm) failed to become nuclear at MBT and the same was true for green QD's that were made slightly larger (11nm-14nm) by using a longer PEG phospholipid in the micelle ([Figure 23](#)).

FIGURE 21

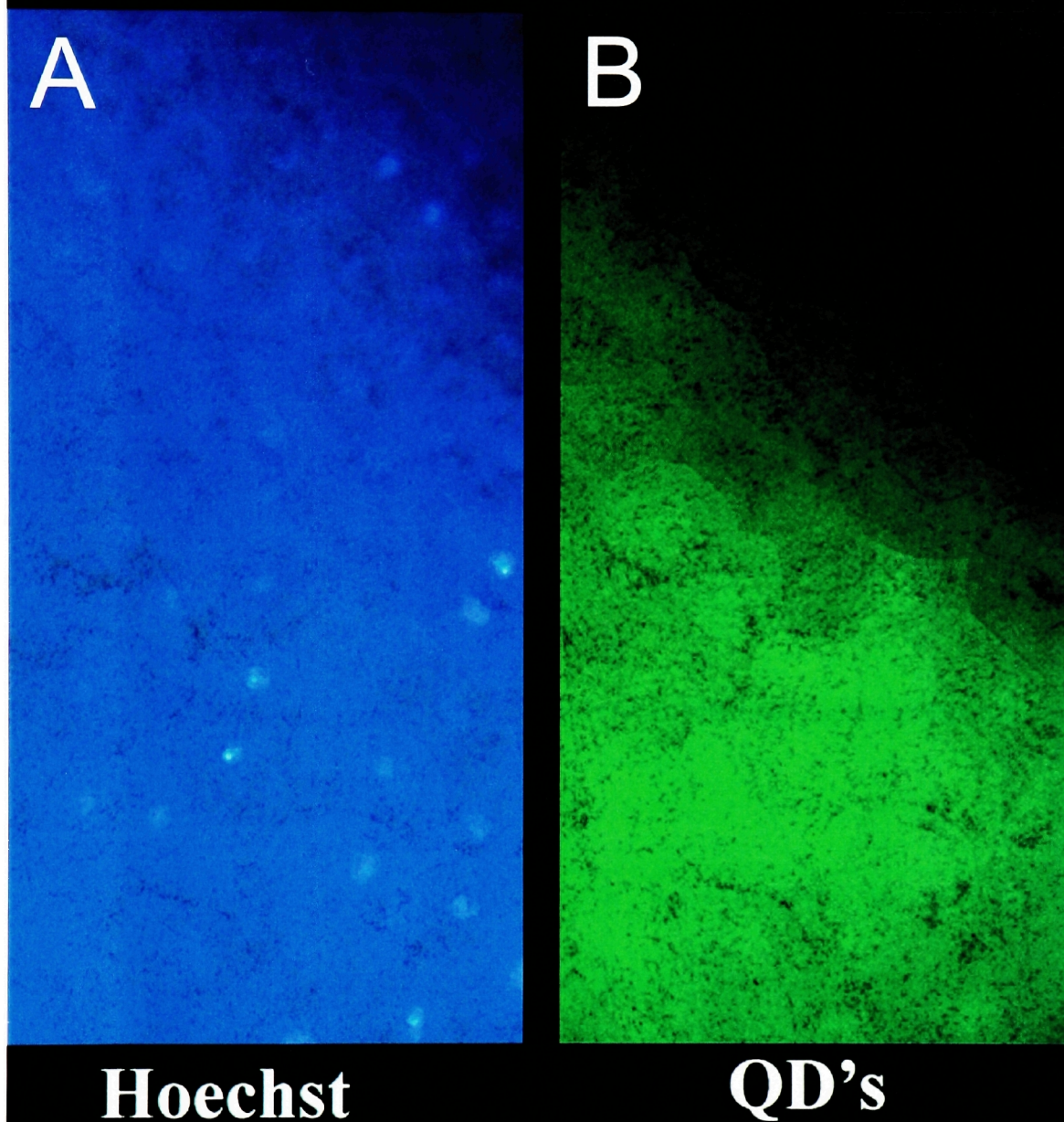
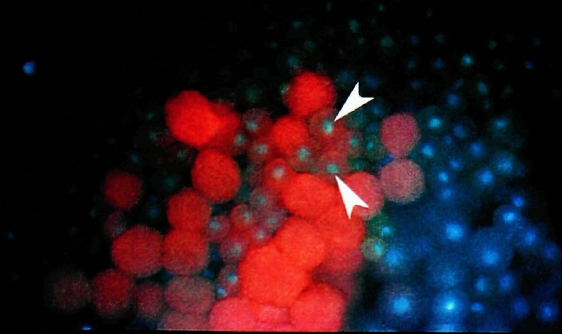


Figure 21. The nuclei of *Xenopus* embryos can be visualized prior to the nuclear accumulation of QD-micelles. (A) Hoechst staining of nuclei in the marginal zone of a living embryo after the tenth division which has been injected with QD's. The nuclei are readily visible. (B) The same area as in A viewed with a QD filter. There is no accumulation of QD-micelles in the nuclei of any of the cells.

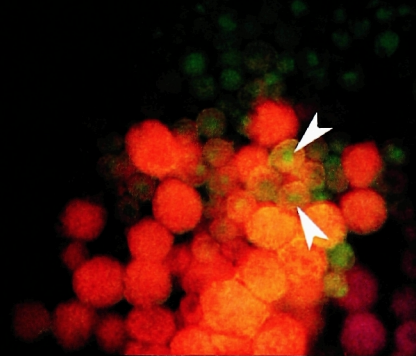
FIGURE 22

A



WGA+Hoechst

B



WGA+QD's

Figure 22. Use of WGA to block active transport does not inhibit the nuclear accumulation of QD-micelles after MBT. (A) Many WGA injected cells (red) are annealed as seen using a nuclear stain (Hoechst-Blue). (B) Cells which have received WGA and do have a nucleus (arrow heads A and B) have nuclear accumulation of green QD-micelles after MBT suggesting that passive diffusion and trapping are most likely responsible for the observed translocation.

FIGURE 23

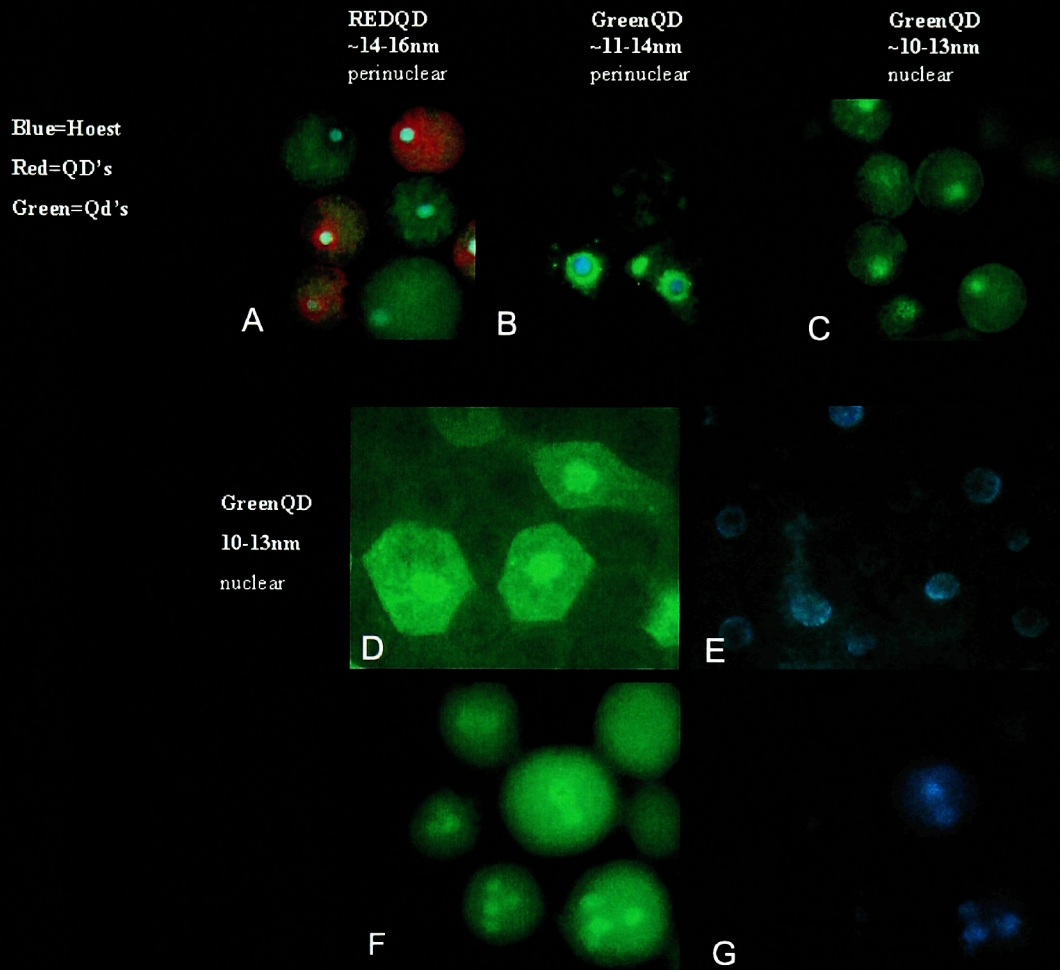


Figure 23. Size dependence of QD-micelle nuclear accumulation. (A-E) Red QD-micelles(A) as well as green QD-micelles(B) which are larger than the diffusion limit of the nuclear pore fail to become nuclear after MBT. The original QD-micelles with a size close to the diffusion limit of the nuclear pore become nuclear after MBT(C-E). (F-G) Use of CytochalasinD to block cell division leads to multi nucleated cells in which nuclear QD accumulation is observed after MBT.

These results are important because they conclusively show that QD nuclear accumulation is impossible if the QD size is above the 9nm diffusion limit of the nuclear pore, but well below the 39nm limit of active transport (Paine, Moore et al. 1975; Pante and Kann 2002). It is safe to conclude that since inhibition of active transport does not affect the QD nuclear accumulation and only QD's of a size permissive to passive diffusion can translocate to the nucleus that the QD nuclear accumulation is due to passive diffusion and trapping.

Timing of nuclear accumulation

The fact that the QD nuclear accumulation was due to passive diffusion did not explain why it took place at MBT. Neither did it explain why the NLS-GFP protein failed to accumulate in the nucleus prior to MBT. At this time, another hypothesis emerged. Cell cycles prior to MBT are very short (~20m at room temperature) and synchronous. At MBT the cell cycles become asynchronous and longer (Newport and Kirschner 1982). It is attractive to postulate that the reason QD's as well as NLS-GFP do not accumulate in the nucleus prior to MBT is the short cell division cycle that does not allow enough time for the accumulation to become visible. Every time the cell divides the nucleus dissolves and the accumulated NLS-GFP or QD's are released into the cytoplasm and have to start accumulating once again. When the accumulation reaches a certain threshold and the nuclear fluorescence intensity becomes sufficiently higher than the cytoplasmic one the nuclear accumulation becomes visible. The timing should be less of an issue with the NLS-GFP which should theoretically accumulate faster, since its being actively transported, than for the QD's. Because of this the NLS-GFP was selected to measure the time interval from a cell division to visible accumulation. These measurements had to be performed in cells after MBT and were obtained by using time-lapse videomicroscopy ([movie 21](#)). The average time required for nuclear accumulation to be clearly visible was 12m at room temperature (n=20). This amount of time should be sufficient since the cell cycle was measured to average 20 minutes prior to MBT. Nuclear envelope breaks down long before the actual cell division takes place. On average, the nuclear envelope was measured to break down 6 minutes prior to cytokinesis. This means that the time left for

visible accumulation is 14 minutes because that is the amount of time an intact nucleus is present during the pre MBT period. This is still theoretically long enough for such an accumulation to occur if the rate of accumulation is the same before and after MBT.

Use of cell division inhibitors cytochalasinD, nocodazole and hydroxyurea failed to conclusively resolve the timing issue MBT. CytochalasinD blocked the cell divisions but nuclear divisions proceeded because it only inhibits actin filament formation resulting in multinucleated cells, which showed nuclear QD accumulation at MBT like controls (Figure 23 F and G). The lack of nuclear accumulation prior to MBT in this case does not provide any new information since the time period the nuclear envelope is intact does not change. In the case of nocodazole cells are blocked during mitosis, and thus in these cells no nuclear QD accumulation was seen prior or after MBT. Use of hydroxyurea blocks DNA replication and as a result blocks the blastomeres at S phase. Using this inhibitor there was a failure to observe nuclear accumulation both before and after MBT. This result is puzzling but the use of inhibitors could be affecting other processes resulting in defective nuclear import.

Discussion

The data presented attempt to describe and explain the phenomenon observed during lineage tracing experiments, that QD's accumulate in the nuclei of *Xenopus* embryos at the onset of MBT. Our aim was to determine whether the nuclear accumulation of the QD's and of the NLS-GFP protein at MBT is due to a link between the two events, or a temporal coincidence.

Our results suggest that the nuclear accumulation of QD's is due to passive diffusion through the nuclear pore complex. Inhibition of active transport does not block QD accumulation and QD's with sizes above the diffusion limit of the nuclear pore fail to accumulate in the nucleus. Passive diffusion alone could not possibly account for any accumulation in the nucleus, but could only lead to an equilibration of the concentrations

inside and out of the nucleus unless the QD's are somehow trapped once they enter the nucleus.

The fact that QD's might get trapped in the nucleus does not explain why an accumulation does not become visible prior to MBT. It has been suggested that MBT is triggered by the titration of a factor or factors that bind DNA because an increase of the DNA amount in *Xenopus* and zebrafish by the introduction of exogenous DNA can trigger an early MBT (Almouzni and Wolffe 1995; Zamir, Kam et al. 1997). Other studies show that prior to MBT there is a competition between transcription complex assembly and chromatin assembly prior to MBT (Prioleau, Huet et al. 1994). Gene inactivation was shown to correlate with chromatin assembly, and titration of chromatin components was shown to relieve repression and permit the establishment of stable transcription during early development (Prioleau, Huet et al. 1994). Methylation of DNA has also been shown to play a role in the silencing observed prior to MBT and depletion of the maternal DNA methyltransferase was recently shown to allow zygotic transcription two cell divisions prior to MBT (Stancheva and Meehan 2000). In all these cases proteins involved in DNA organization or modification are titrated out by the DNA present in the embryo which is increasing fast during the first 12 cell divisions. This titration is what triggers zygotic transcription. So what is determinant for triggering MBT is the DNA to cytoplasm ratio per cell and more specifically the capacity of the DNA to titrate factors responsible for the observed gene "silencing". Since NLS-GFP is actively transported into the nucleus, it does not depend on the capacity of the nucleus to titrate it out of the cytoplasm. We conclude that a direct link between the ratio of the DNA to cytoplasm and the nuclear accumulation of NLS-GFP is improbable.

Our experiments have also addressed the possibility that the fast cell cycles prior to MBT do not allow sufficient time for accumulation to reach such levels that it would become visible. We show that the nucleus of the *Xenopus* blastomeres remains intact for approximately 16m each cell cycle while visible NLS-GFP accumulation takes 12m at post MBT stages. This rules out the timing factor for NLS-GFP if we assume that, the protein's transport rate is the same pre- and post-MBT, and that the time required for

sufficient build up of NLS-GFP in the nucleus is the same pre- and post-MBT. Although the first assumption might be correct the second is most likely incorrect. In order for the nuclear accumulation of NLS-GFP to become visible, the concentration of NLS-GFP needs to be sufficiently higher in the nucleus than in the surrounding cytoplasm. The smaller the cytoplasm to nuclear volume ratio, the faster such concentration differential will arise. So more time would be required for nuclear accumulation to become visible prior to MBT when the cytoplasm to nuclear ratio is higher. Given the very tight window for such an accumulation to take place, NLS-GFP fails to visibly accumulate in the nucleus prior to MBT partly due to the lack of sufficient time during the fast pre MBT division cycles.

CHAPTER 3

***QD in Situs* and other applications**

Introduction

With the advent of cell type specific molecular markers the description and analysis of the developmental morphogenesis in a number of biological systems has become possible. The use of RNA probes prepared from specific genes to visualize the expression patterns (by hybridizing the probes to the target RNA's) is now extensively used and is one of the techniques that from the foundation of molecular developmental biology. This type of experiment can provide valuable information about the role of specific genes during development, as well as information on the placement and movements of a particular cell type at different stages of development. The technique called *whole mount in situ hybridization* was initially carried out using radioactive probes, but it was radically simplified when for the first time non-radioactive probes were used successfully (Tautz and Pfeifle 1989). It is now widely used in several biological systems including *Drosophila* (Tautz and Pfeifle 1989), *Xenopus* (Hemmati-Brivanlou, Frank et al. 1990), quail (Coutinho, Morris et al. 1992) *Dictyostelium* (Escalante and Loomis 1995) and *Zebrafish* (Jowett and Yan 1996). Not long after its introduction, *in situ hybridization* protocols allowing the detection of more than one transcript at the same time by using two different labels for the RNA probes and two color substrates were described (O'Neill and Bier 1994).

A major limitation of the chromogenic multi-labeling techniques is that the overlapping regions of expression are very difficult to discern. The solution to this problem was use of fluorescent detection methods. Despite the widespread use of *in situ* hybridization use of fluorophores for visualization has only been extensively used in the fly both for single as well as double transcript visualization (Hughes and Krause 1998) and to some extent in zebrafish (Jowett and Yan 1996). Work done on other systems

failed to produce fluorescent images of sufficient quality to rival the staining obtained with normal chromogenic substrates. The successful implementation of current fluorescent protocols is vary rare, especially in *Xenopus laevis*, and even when it is successfully performed, imaging the signal is complicated by the high autofluorecence of the embryos even when confocal microscopy is used (Davidson and Keller 1999).

The high autofluorescence background makes the use of enzymatic amplification necessary for signal detection especially in *Xenopus*. Amplification is also used for chromogenic reactions and it undermines the resolving ability of the method. Amplification reactions create a precipitate which is deposited at the area surrounding the RNA. This precipitate has a diffusion radius and does not remain localized within the particular intracellular region or compartment were the RNA in question is localized. It often diffuses thought the cell and sometimes even leaks outside of the cell being labeled. The solution to this limitation is direct labeling of the probe which would allow single cell as well as intracellular resolution of the localization of a particular mRNA. Despite successful implementation of direct labeling of messenger RNA's in cell culture (Wilson, Velcich et al. 2002) this has not been possible in embryos due to the low fluorescent intensities of organic flurophores. Direct labeling of probes has other advantages besides the high resolution it offers. It allows the simultaneous hybridization for as many messages as one wants as long as the fluorophore colors can be resolved. It is also extremely simple and can be quantitative since the fluorescence of the probe can be calibrated.

Fluorescent detection of any part of the biological machinery at the molecular level offers a number of important advantages when compared to a chromogenic one. The use of fluorescent detection enables the imaging of the molecule in question in 3D and makes the use of multiple fluorophores easier because overlapping patterns can be clearly identified. When chromogenic reactions are used for double in situs the overlapping area is not clear due to the fact that the precipitates mix and there is no clear color change at the site of overlap but rather a very dark looking site. Using a green and a red fluorophore regions of overlap appear yellow, if the two signals are of comparable intensity. This

makes it clear if there is overlap. Furthermore equally abundant messages are the only kind that can be effectively visualized with a chromogenic reaction because if one is of significantly higher intensity than the other, then the overlap region becomes impossible to discern from a region of higher expression of the abundant mRNA. Using fluorescent visualization though independent genes can be visualized using different fluorescent filters, eliminating issues arising from different expression levels. Images acquired independently can then be reassembled to determine the exact areas of overlap.

As mentioned before two of the main problems preventing the widespread use of fluorescence detection for *in situ* hybridization are the high endogenous background fluorescence of many embryos as well as the limited brightness of organic fluorophores. A new type of inorganic fluorophore namely Quantum Dots (QD's) have been used recently in several systems *in vitro* for detection of proteins as well as *in vivo* for labeling and lineage tracing. QD's have ideal optical properties for use in biology and one of those properties is their extremely high fluorescence, due to very low extinction coefficients compared to organic and protein fluorophores (Bruchez, Moronne et al. 1998; Chan and Nie 1998). The high fluorescence intensity of the QD's raised the possibility of using them to perform non amplified RNA detection. Previous efforts to do this were plagued with aggregation problems and the detection had to be done with the RNA covalently linked to hydroxylated QD's making the process complex and time consuming (Pathak, Choi et al. 2001). Since then hydrophilic QD-avidin conjugates have become commercially available. We produced biotin labeled RNA probes and used QD-avidin conjugates to visualize the probe. Our experiments show that QD detection of biotinylated RNA is an extremely sensitive assay that improves the detection limit for RNA several thousand fold over a common reagent used to detect RNA EtBr. We also used QD's to visualize several RNA probes that had been used to perform *in situ hybridization* in *Xenopus* embryos. We demonstrate that QD detection of endogenous messenger RNA's is effective and that it can be used to provide *in situ* hybridization data of higher resolution than current technologies. The successful implementation of QD's to perform non-amplified direct fluorescent *in situs* in *Xenopus*, one of the most highly

autofluorescent (and thus demanding) developmental organisms, suggests that QD *in situ* will find application in most developmental models.

RESULTS

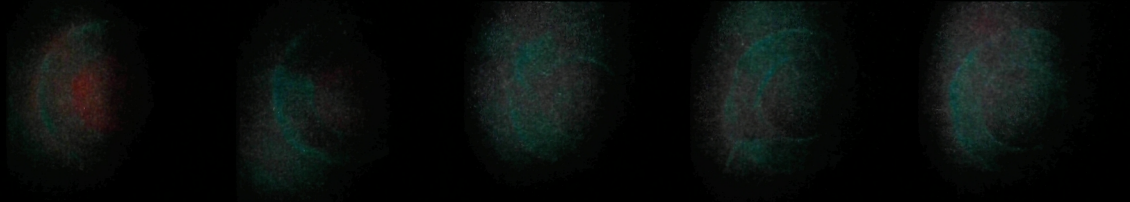
QD labeling of biotinylated RNA

Figure 24 presents individual images of a range of RNA amounts labeled with EtBr (top row) or QD's (bottom two rows). Each image was acquired using the same fluorescent filter set (which is ideal for exciting both EtBr as well as QD's), the same excitation intensity as well as the same acquisition time (exposure). It is clear from this that using QD's increases the signal intensity immensely and the detection sensitivity by more than a thousand-fold (Figure 25A). Even though the background using QD's is higher even after extensive washes, this can be substantially reduced by blocking using an avidin biotin blocking kit and eliminated by labeling the RNA in solution. As shown in the graph of Figure 25B, the signal to noise ratio of QD is significantly improved by using A/B blocking, making detection of lower amounts than the tested 3pg feasible. We have also successfully labeled RNA in solution by introducing saturating amounts of QD's in the RNA and then removing all free QD's by phenol-chlorophorm extraction. The QD labeled RNA can then be quantified without background being an issue. The extreme sensitivity and low detection levels achievable due to the high fluorescence intensity of the QD's in conjunction with detection in a two dimensional matrix instead of in solution has the potential to improve both RNA detection as well as quantitation. More importantly, this extremely efficient detection raises the possibility of non-amplified detection of RNA probes used for *in situ* hybridization.

Imaging QD's Fluorescence in the Embryo

FIGURE 24

EtBr >33ng >3.3ng >0.3ng >30pg >3pg



QD



QD 55 Degree Wash in PBT



Figure 24. Labeling of blotted RNA using QD's can increase the detection limit significantly when compared to EtBr. The stated amounts of biotinylated RNA were blotted on nitrocellulose membrane, crosslinked using UV and then the membranes were incubated with a QD-avidin solution(1:1000 in PBS) or EtBr. The membranes were then washed briefly with PBS and each dot was visualized independently under a fluorescent microscope. The same exposure was used to capture each dot. For the bottom row of dots an additional 10 minute 55 degree wash was performed prior to the imaging.

FIGURE 25

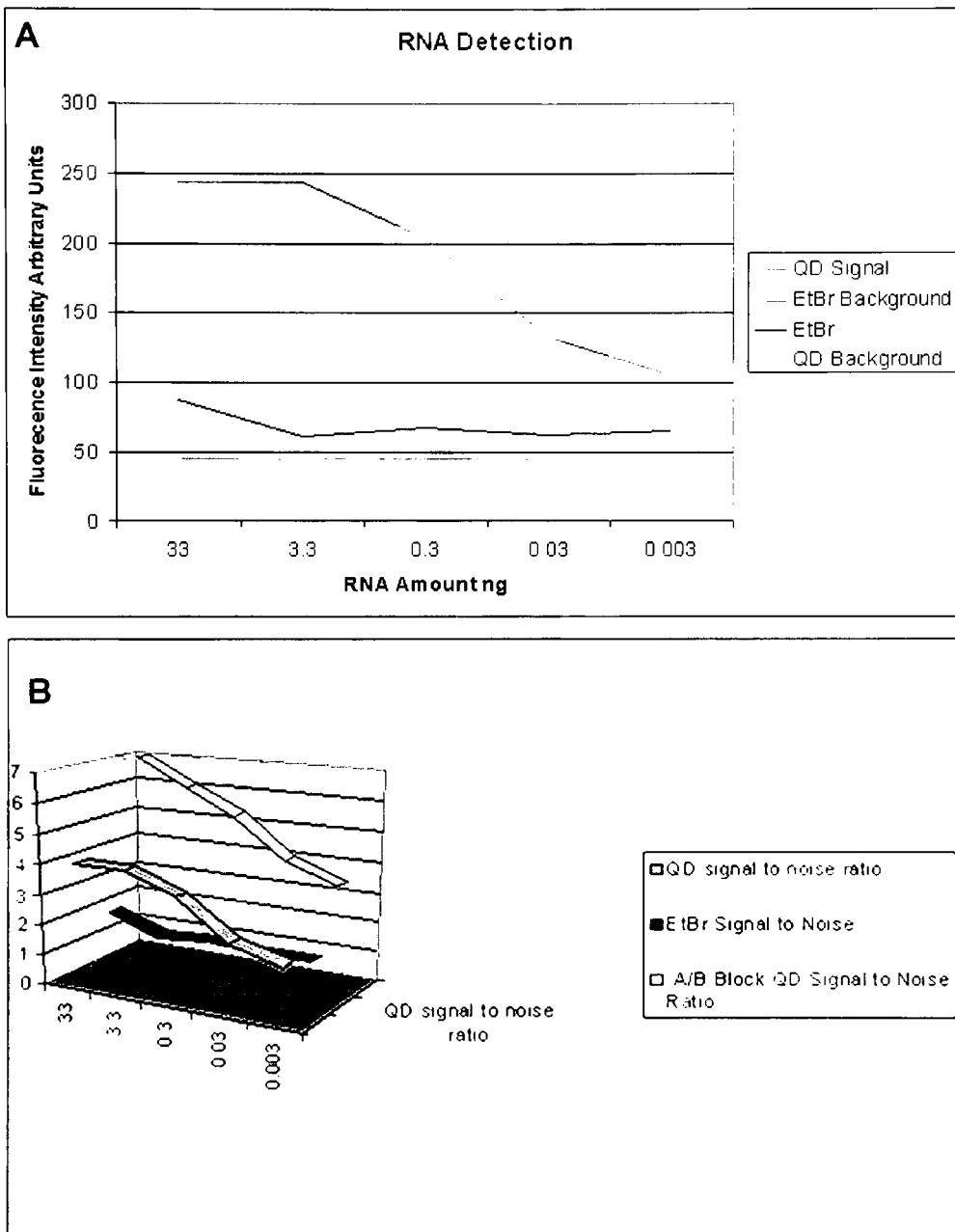


Figure 25. Signal intensity and signal to noise ratios of QD detections versus EtBr. (A) The fluorescence intensities from Figure 24 were quantified using the Zeiss axiovision software and then plotted on a common graph including the background from each type of labeling. Despite the higher background of the QD-avidin staining there is detectable signal even using RNA amounts below 3pg. (B) Comparison of signal to noise ratios achieved using QD-avidin versus EtBr for detection of RNA. The significantly higher signal to noise ratio using QD-avidin is improved even further if the membrane is blocked prior to the blotting using an avidin/biotin blocking kit to reduce background staining.

As mentioned previously, the very high sensitivity of RNA detection using QD's raised the possibility that QD's could be used to visualize biotinylated RNA used to perform *in situ* hybridization experiments without the need for enzymatic amplification. Current methods of visualizing mRNA in cells use enzymatic amplification in order to achieve detectable signal levels and reasonable noise to signal ratios. Both chromogenic and fluorescent *in situ* protocols are currently available but current fluorescent *in situ* protocols are complicated and offer poor results compared to chromogenic reactions. The superior optical properties of QD's could potentially improve fluorescent *in situ* protocols and alleviate the need for enzymatic signal amplification that leads to loss of resolution. By modifying the *in situ* hybridization protocol first reported by Brivanlou et. al and implementing the improvements reported by Harland RM., we were able to effectively hybridize biotinylated RNA probes against a number of previously characterized *Xenopus* mRNA's. Despite initial problems with the visualization of the staining due to excessive background fluorescence, we found out that bleaching of the autofluorescence of the embryos by UV irradiation before or after the hybridization can help to alleviate this problem. In [Figure 26](#), an embryo stained for the latent transforming growth factor-beta binding protein-1 (LTBP) mRNA is shown as increasing doses of near UV excitation light, are administered. Due to the extreme photostability of the QD's the endogenous autofluorescence is gradually quenched and the QD signal strength becomes more and more prominent. Avoiding the dehydration step and using a sodium borohydrite bleaching step prior to the hybridization also helps reduce endogenous autofluorescence. Despite the use of these methods, autofluorescence still remains as a major issue for QD *in situs* because very long exposures to near UV excitation light will also photobleach the QD's themselves if the process is carried out post staining. If the photobleaching is carried out prior to the staining, long exposures break down the structure of the embryo and make it much more fragile in the sensitive hybridization steps. We found that using 2% peroxide in the solution where the embryo is photobleached accelerates this process substantially. In the inset of [Figure 26](#) (bottom right) small areas of the *Xenopus* vegetal and animal pole are shown before and after a one minute exposure to near UV light in the presence of hydrogen peroxide. The reduction in autofluorescence is substantial and helps

FIGURE 26

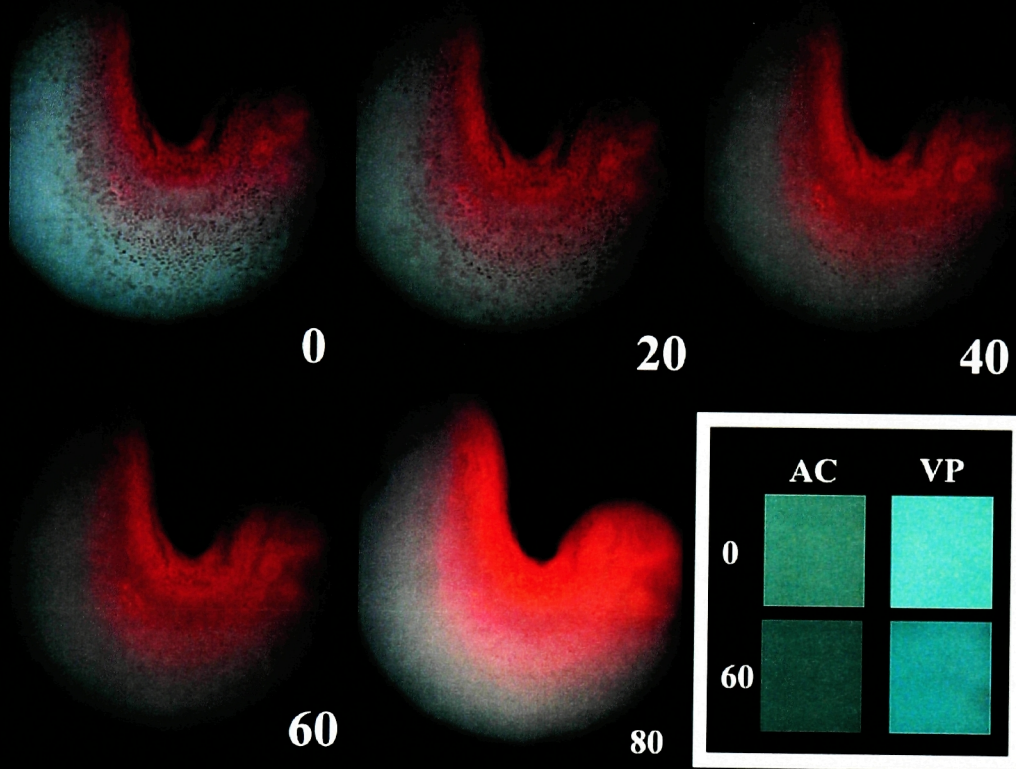


Figure 26. Quenching of endogenous autofluorescence using near UV excitation light from a mercury epifluorescence source is necessary for the detection of endogenous mRNA's using QD-avidin. Images were taken during the continuous exposure of an embryo on which in situ hybridization was performed against LTBP. Eighty seconds of exposure reveals the staining of the QD's which was previously obscured by endogenous autofluorescence. The inclusion of hydrogen peroxide in the solution prior to the photobleaching accelerates the process(inset).

a lot to raise the detection limit of the technique. Photobleaching using H₂O₂ has to be performed prior to any staining because it also eliminates QD fluorescence.

QD labeling of Specific Transcripts in *Xenopus* Embryos

Probes for *Xenopus* amylase (a gene encoding a digestive enzyme made by the pancreas) and LTBP and were hybridized to their respective target mRNA's and were subsequently directly or indirectly visualized with QD's using the protocol we describe. In [Figure 27](#), comparisons between the QD staining and chromogenic reactions using a probe against *Xenopus* LTBP are made. Overall, the staining pattern using QD's is very similar to the one obtained by a chromogenic reaction ([Figure 27](#) compare A and B, C and D). The labeling of the head expression (shown in the inset of [Figure 27D](#)) and the somites is present using both the QD *in situ* protocol as well as the chromogenic protocol. The comparable staining patterns show that the use of QD's can result to specific non amplified staining of endogenous mRNA's. Furthermore as seen in the close-ups of [Figure 27E](#) and [F](#) the resolution of the QD staining is very high and the signal strength high enough for easy detection using a regular fluorescence microscope. In [Figure 28A](#) and [B](#) a comparison of the staining using chromogenic reaction versus QD's is made in this case using sections of stained embryos. The two patterns match further proof of the successful and specific staining obtained using our protocol. The sections also demonstrate that the QD's under the conditions we have described can penetrate deep into the embryo and stain structures independently of their proximity to the free QD's in solution. Finally [Figure 28C](#) shows a lateral section of the head of an embryo stained using the chromogenic protocol. A clear demonstration of the potential of fluorescent *in situ* lies in the series of images (taken from a z-stack [movie 22](#)) following in the same figure. These are optical sections using a regular fluorescent microscope. The QD staining, unlike the staining of other fluorescent *in situ* technique, survives the clearing protocol used to render *Xenopus* embryos transparent for at least one hour, which is long enough to perform imaging on stained samples. The series of images starts at the head region and moves posteriorly. These optical sections demonstrate that the staining seen in the chromogenic sections was not originating from the notochord but rather somitic

FIGURE 27

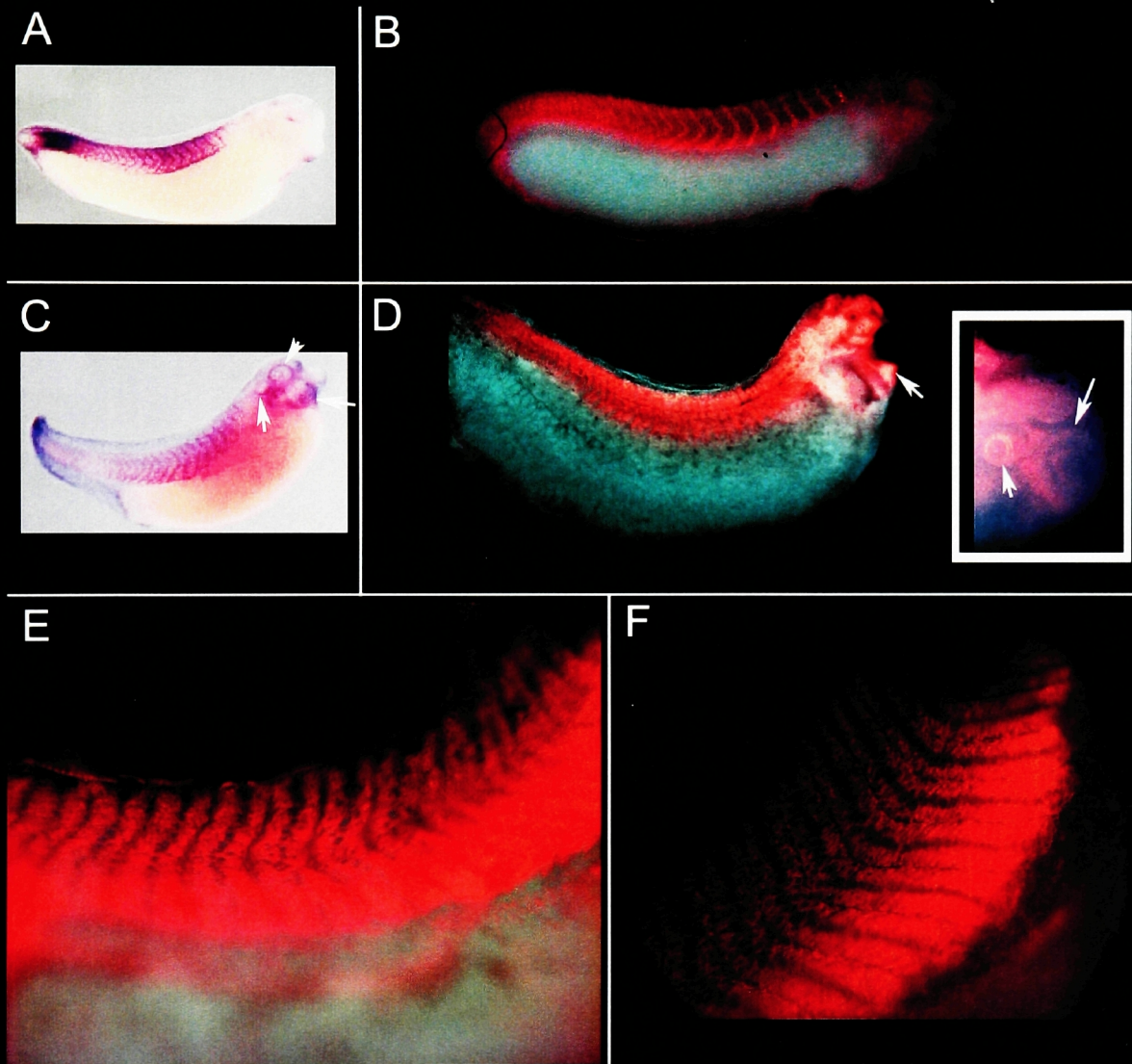


Figure 27. QD-avidin detection of the mRNA transcript for LFBP compares favorably with that obtained using a chromogenic reaction protocol. (A-D) Comparison of chromogenic (left) versus QD-avidin (right) whole mount in situ hybridization for LFBP mRNA. The staining pattern between the two methods is almost identical in the trunk region (compare A with B and C with D) as well as in the head (inset of D). (E-F) Close ups of the labeling of the muscle somites from in situ performed against LFBP using QD-avidin conjugates. The signal intensity and resolution attainable is sufficiently high to clearly distinguish each individual somite.

FIGURE 28

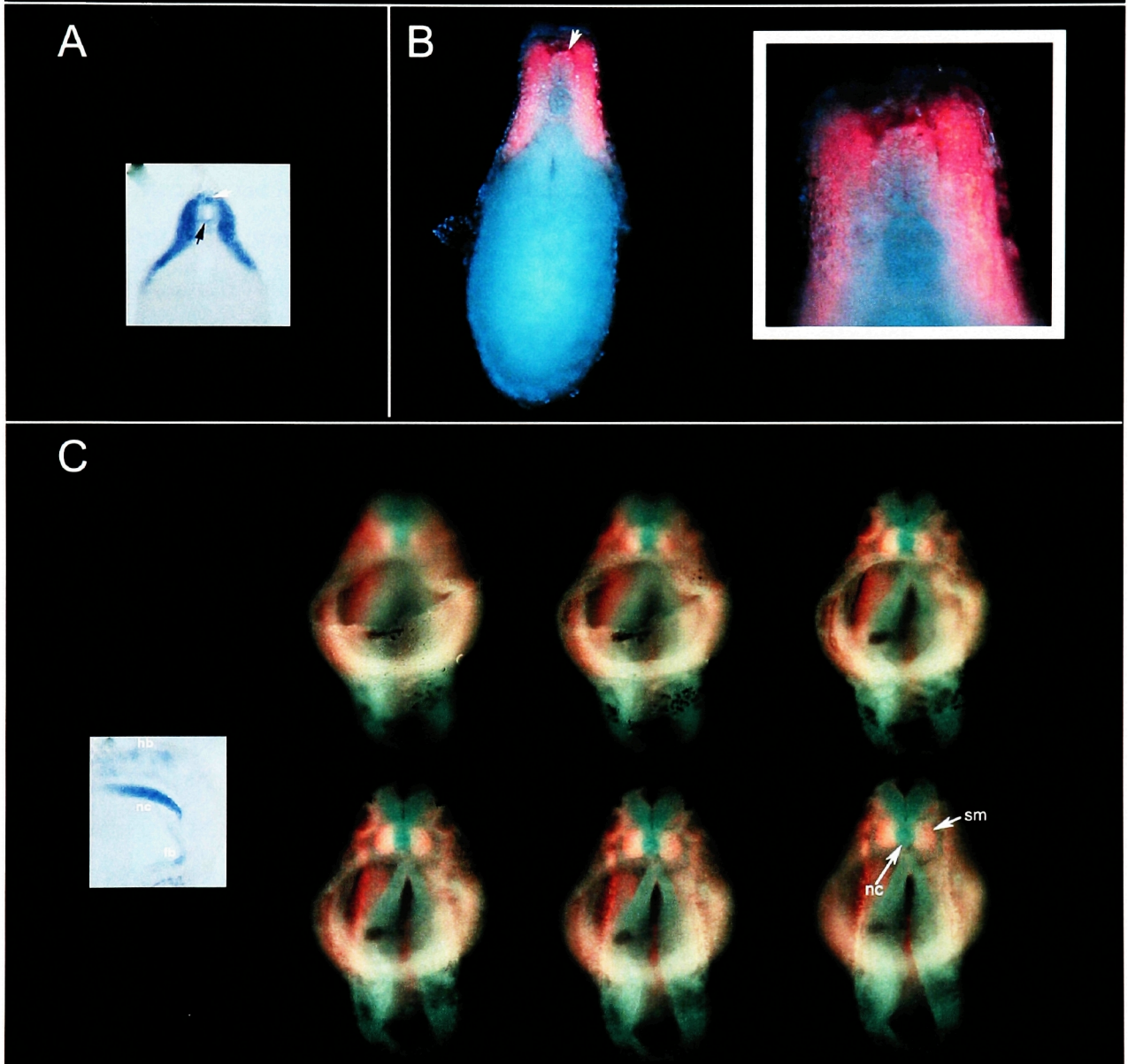


Figure 28. QD-avidin staining of TTBP compares favorably with the staining achieved using standard chromogenic protocols in the deeper structures of the embryo. (A-B) A transverse section of an embryo stained in whole mount for TTBP using a standard chromogenic protocol (A) is compared with a transverse section from a whole mount in situ using QD-avidin. The somatic staining is identical between the two showing that the QD-avidin solution can penetrate and stain the deep areas of the somites and not just the superficial. The neural tube staining is weaker using the QD's and in this section visible only on the upper part of the neural tube where the expression appears to be stronger. (C) A sagittal section of the head region of an TTBP stained embryo (left) using a chromogenic protocol is compared with a series of transverse optical sections of a QD-avidin stained embryo for the same message. The optical sections reveal that the staining seen in the chromogenic image was falsely identified as notochord. This staining is clearly flanking somitic mesoderm, notochord, sm = somatic mesoderm, hb, hindbrain, fb, forebrain.

mesoderm flanking the notochord. The fact that this type of imaging can be done without the need of time consuming sectioning (and actually results in better data quality) further emphasizes the advantages of QD labeling of RNA for *in situ* hybridization.

In Figure 29A the QD staining for amylase is compared to the staining obtained by the chromogenic reaction. This type of *in situ* is done on a dissected *Xenopus* gut and the staining using QD's is identical to that using a chromogenic reaction. Non stained areas appear white and due to background fluorescence that is present in all visible wavelengths but is more pronounced in the green. Use of long wavelength fluorophores (ranging from 600nm to 700nm) is more appropriate and with the eventual use of near infra red QD's background autofluorescence should become irrelevant. Despite high background and use of only a short post staining photobleaching step we obtained an acceptable signal to noise ratio and good contrast in the most highly autofluorescent organ of the *Xenopus* tadpoles. Amylase RNA is expressed in the pancreas and both the QD and the chromogenic staining are restricted to this morphologically identifiable organ.

We went on to test whether detection of digoxigenin labeled probes was possible, by using three well known mRNA's those of Endodermin (Edd a pan-endodermal marker), Xbra (an early mesodermal marker) and myoD (a gene encoding a DNA-binding protein that can activate muscle gene expression) which stain the gut the mesodermal belt and the muscle somites respectively. To perform these *in situ* we performed a non-enzymatic amplification step, which does not reduce the resolution of the method. A Dig labeled probe was used followed by a primary monoclonal biotinylated a-dig antibody and a secondary biotinylated a-mouse antibody. As seen in Figure 29 our method gives staining patterns that closely match the ones obtained using standard enzymatically amplified chromogenic reaction methods while maintaining high resolution. Depending on the case the QD staining can offer higher resolution like in the case of MyoD (Figure 29D) where the posterior somites look fused using the chromogenic protocol but are distinct using our method or less sensitive like the case of

FIGURE 29

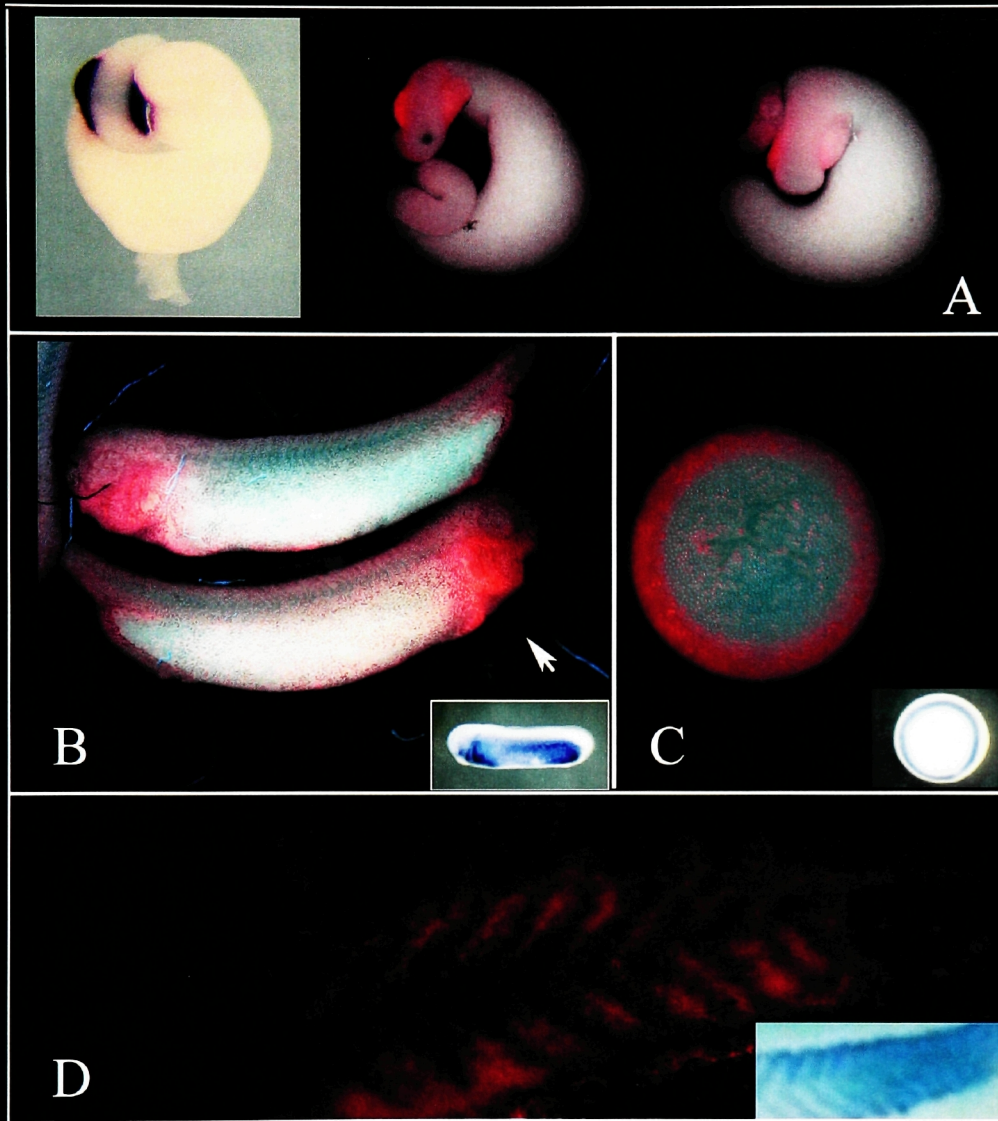


Figure 29. In situ hybridization using QD-avidin compares favorably with chromogenic in situ hybridization staining for a number of well characterized mRNAs. (A) QD staining for amylase is compared to the staining obtained by chromogenic reaction (left). These in situs were done on dissected *Xenopus* guts and the staining using QD's is identical to that using a chromogenic reaction. Amylase mRNA is expressed in the pancreas and both the QD and the chromogenic staining are restricted to this morphologically identifiable organ which is extremely autofluorescent making detection of fluorescent staining hard. (B) Comparison of QD versus chromogenic staining for the message for Edd an endodermal marker expressed through the tadpoles gut at varying levels. The staining using a chromogenic protocol is significantly stronger in this case and the QD-avidin seems restricted to the high expression regions (arrow). Careful observation reveals that the staining is present throughout the gut region but its masked by the intense autofluorescence of the gut. This autofluorescence proved harder to quench than that of other regions of the embryo. (C) Comparison of the QD-avidin staining versus the chromogenic staining for Xbra a widely used mesodermal marker. The marker is known to label the mesodermal belt at gastrula stages and both the chromogenic as well as the QD-avidin protocols result in the same staining pattern consistent with the mesodermal belt. (D) Comparison of the staining for MyoD a muscle marker. The QD-avidin and the chromogenic staining are similar but the QD-avidin staining gives slightly better resolution of the posterior somites.

Edd, which due to the fact that its expressed in the highly autofluorescent gut the QD staining appears weak except at the anterior, where the gene is expressed at higher levels (Figure 29B arrow). The autofluorescence of the *Xenopus* gut proved hard to quench unlike that of other regions of the embryo. After about two minutes of continuous exposure to excitation light the quenching reached a plateau and no further reduction of autofluorescence was observed with increased exposure. In the case of Xbra the staining between the chromogenic and the QD *in situ* is almost identical. Hoechst was used to stain the nuclei blue in this experiment and the embryo was visualized from the animal pole while the chromogenic one was visualized from the vegetal pole. The fact that dig labeled probes can also be visualized using QD's raises the possibility of performing double in situ in which one probe is biotinylated and the other is dig labeled. Our efforts to perform double labeling were met with no success due to the limited number of colors of QD's currently available. We were forced to use red and green QD's for double in situ and were unable to successfully image green QD staining due to the high background autofluorescence in this region of the spectrum.

Due to the direct nature of the QD *in situ* staining the resolving ability of this method is substantially higher than that of amplified protocols. In Figure 30A and B we present the intracellular mRNA localization for two transcripts. Hoechst was used to stain the nuclei of the cells. From these images it becomes apparent that QD labeling of transcripts results in an extremely high resolution of labeling capable of distinguishing intracellular localization patterns of mRNA. Despite the fact that we have no evidence proving, that the presented distribution of mRNA's coincides with the true intracellular localization of these transcripts the fact that there are noticeable differences in the signal patterns from different probes suggests that this is indeed the case. Future work will have to focus on closely examining the resolution of this method in model systems where non amplified *in situ*s can be performed using traditional fluorophores for comparison. Nevertheless it is clear that this level of resolution cannot be achieved with the existing methods for detection of RNA transcripts in *Xenopus* which are based on enzymatic amplification.

Despite our efforts we were unable to obtain specific staining for low abundance messenger RNA's at the blastula stages of *Xenopus*, especially for genes expressed in the vegetal pole. This might have to do with limitations in the permeability of red QD's in these tissues or simply the low signal to noise ratio stemming from the extremely high background autofluorescence in this region of the embryo. The vegetal pole is notoriously hard to permeate and stain even with the use of standard chromogenic protocols. The fact that QD's are large compared to organic fluorophores (roughly the

FIGURE 30

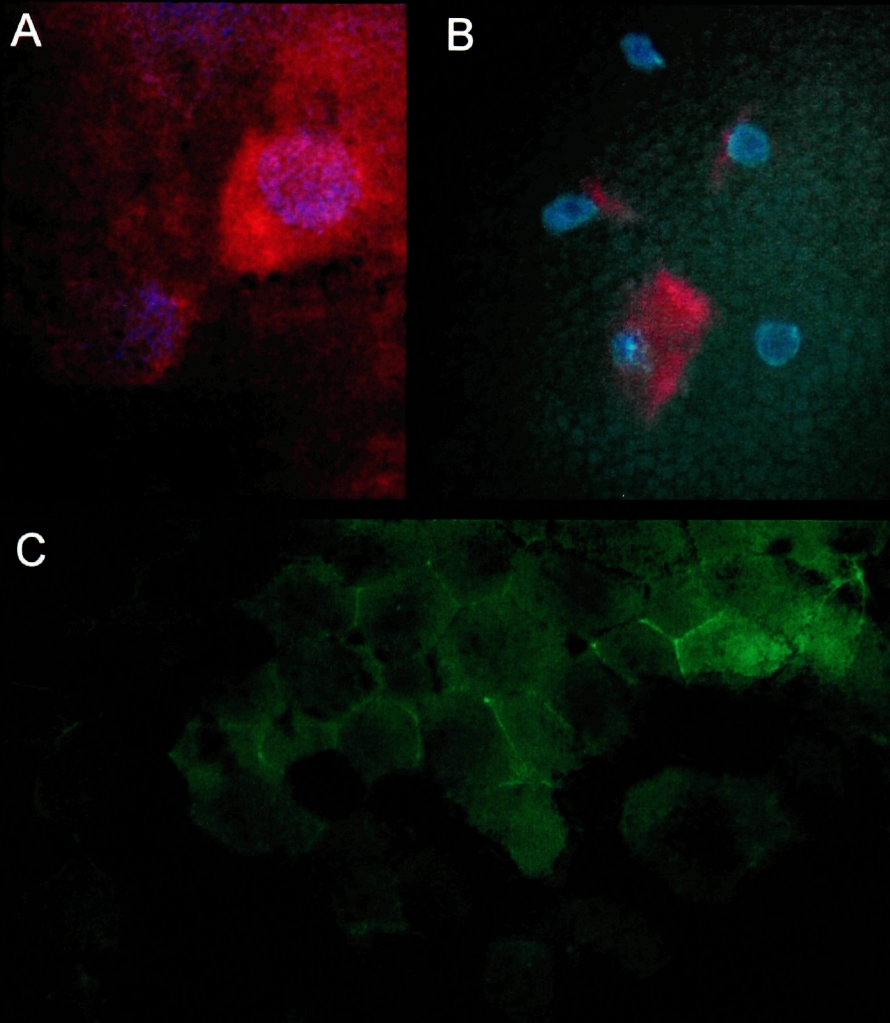


Figure 30. QD-avidin labeling of mRNA transcripts has the potential to reveal differences in the intracellular localization of messenger RNA's. (A-B) Due to the lack of an enzymatic amplification step the in situ hybridization protocol using QD-avidin results in direct labeling of the transcript in question. The intracellular mRNA patterns of two messages that of LTBP (A) and 212 (B) are shown. (C) Expression of an actin binding domain fused to GFP fails to reveal an organized actin cytoskeleton.

size of proteins) makes this region especially difficult for QD's to penetrate. Nevertheless we have seen QD penetration even at the deepest parts of the vegetal pole as well as specific staining. Further experiments will be needed to address this issue and determine the contributions of permeability versus signal to noise ratio that leads to the poor results observed in this region of the embryo.

In vivo labeling of Actin using QD avidin

QD's were effectively used to perform fluorescent *in situs*, immunofluorescent staining of a number of antigens and have also been used to target mice tumors in vivo (Akerman, Chan et al. 2002; Watson, Wu et al. 2003; Wu, Liu et al. 2003). In order to test whether intracellular *in vivo* labeling of a protein using QD nanocrystals is possible, biotinylated actin monomers were prepared in the appropriate buffer to prevent polymerization and were then injected into a two cell *Xenopus* embryo. The embryos were allowed to develop to four cell stage to allow time for integration of the biotinylated actin into actin filaments. This way, we were aiming to avoid binding of the QD's at areas which would block polymerization. By having some of the biotinylated actin polymerized it is ensured that the QD's would not interfere with polymerization. Unfortunately due to the multivalency of streptavidin and the fact that multiple streptavidin molecules are attached on each QD some aggregation is always observed in injected cells. This problem is specific to the avidin-biotin system and as such could be avoided by directly conjugating the QD's to the actin monomers. The aggregation, despite the fact that it probably alters the dynamics of the labeled actin, enabled the clear observation of the movement of the QD-actin within *Xenopus* cells. Due to the "disorganized nature" of the actin networks in *Xenopus* (no stress fibers or clear actin cables) and the high opacity of the cells, it is hard to observe actin dynamics or a discernable pattern even when using an actin binding domain fused to GFP (Figure 30C) which beautifully labels actin filaments in cells in culture (Pang, Lee et al. 1998). Due to the fairly large size of the aggregates in the injected cells their movement, which was clearly non-Brownian, could be observed by time-lapse videomicroscopy (movie 23). Aggregates would follow fast linear tracks and would display sudden bursts of motion

(movie 23 arrow tips). This is in contrast to QD's injected in cells that received purified biotin and QD's were aggregates remain stationary or display very limited random motion. The crude nature of this experiment prevents any speculation about how well QD-actin can polymerize and how its dynamics are affected, but it is the first demonstration of QD labeling of a protein *in vivo*.

Discussion

We describe a new method of performing non-amplified, fluorescent *in situ* detection of endogenous mRNA's taking advantage of the ideal optical properties of QD nanocrystals. Despite the fact that the *in situ* hybridization method has been available for more than a decade, the requirement for an enzymatic amplification step in the process has kept the level of resolution of this method low. At the same time, the limitations of current fluorescent protocols have kept fluorescent *in situ*s out of mainstream use in most developmental models with the exception of *Drosophila* and to some extent zebrafish. In the case of zebrafish, an enzymatic amplification step is necessary. ~~while~~ In the case of *Drosophila*, direct visualization of high-abundance transcripts is possible. Fluorescent detection of a messenger opens exciting possibilities in terms of imaging and it can eliminate the need for sectioning samples. It can also be used to create three-dimensional maps of expression at a previously unattainable resolution.

The intracellular localization of mRNA transcripts has started being investigated fairly recently (St Johnston 1995; Fages, Kaksonen et al. 1998; Palacios and St Johnston 2001; Yaniv and Yisraeli 2001). The study of mRNA localization is limited by the current *in situ* methods both fluorescent and chromogenic due to their low resolving ability. Chromogenic reactions have been used successfully to localize mRNA transcripts in cultured cells but only for transcripts of very high abundance (St Johnston 1995; Fages, Kaksonen et al. 1998; Palacios and St Johnston 2001; Yaniv and Yisraeli 2001). The method described is the first non-amplified fluorescent detection of mRNA *in situ* in *Xenopus*. Our protocol results in signal intensities sufficient for imaging on regular epifluorescence microscopes without the need for confocal microscopy. Of great

([movie 23](#) arrow tips). This is in contrast to QD's injected in cells that received purified biotin and QD's were aggregates remain stationary or display very limited random motion. The crude nature of this experiment prevents any speculation about how well QD-actin can polymerize and how its dynamics are affected, but it is the first demonstration of QD labeling of a protein *in vivo*.

Discussion

We describe a new method of performing non-amplified, fluorescent *in situ* detection of endogenous mRNA's taking advantage of the ideal optical properties of QD nanocrystals. Despite the fact that the *in situ* hybridization method has been available for more than a decade, the requirement for an enzymatic amplification step in the process has kept the level of resolution of this method low. At the same time, the limitations of current fluorescent protocols have kept fluorescent *in situ*s out of mainstream use in most developmental models with the exception of *Drosophila* and to some extent zebrafish. In the case of zebrafish, an enzymatic amplification step is necessary. ~~while~~ In the case of *Drosophila*, direct visualization of high-abundance transcripts is possible. Fluorescent detection of a messenger opens exciting possibilities in terms of imaging and it can eliminate the need for sectioning samples. It can also be used to create three-dimensional maps of expression at a previously unattainable resolution.

The intracellular localization of mRNA transcripts has started being investigated fairly recently (St Johnston 1995; Fages, Kaksonen et al. 1998; Palacios and St Johnston 2001; Yaniv and Yisraeli 2001). The study of mRNA localization is limited by the current *in situ* methods both fluorescent and chromogenic due to their low resolving ability. Chromogenic reactions have been used successfully to localize mRNA transcripts in cultured cells but only for transcripts of very high abundance (St Johnston 1995; Fages, Kaksonen et al. 1998; Palacios and St Johnston 2001; Yaniv and Yisraeli 2001). The method described is the first non-amplified fluorescent detection of mRNA *in situ* in *Xenopus*. Our protocol results in signal intensities sufficient for imaging on regular epifluorescence microscopes without the need for confocal microscopy. Of great

significance, in terms of *Xenopus* and other opaque embryos like the chick, is the fact that the QD *in situ* staining is capable of remaining localized and fluorescent for more than an hour after the embryo is cleared.

Another important advantage that QD *in situs* offer is the intracellular resolution of mRNA expression that the method can achieve. Even in the case of *C. Elegans*, where background is not a major issue, use of fluorescent antibodies to detect labeled RNA probes has to be carried out in conjunction with chromogenic amplified detection of the probes in order to get a comprehensive picture of the overall expression of a gene (Seydoux and Fire 1995). The amplified reaction is used to detect low expressing regions and overall expression whereas the fluorescent antibodies to resolve intracellular localization. The fact that our protocol can do both in what is possibly the most demanding model system for fluorescent detection of RNA transcripts makes us confident that the implementation of QD *in situs* in other less demanding model systems will be met with equal success. Overall our results demonstrate that QD *in situs* are a viable alternative to current *in situ* protocols and together with the demonstration for the first time of *in vivo* protein labeling using QD's it expands the current frontier of QD's in biology.

Materials and Methods

Embryos and explants

Xenopus laevis embryos from induced spawning (Winklbauer, 1990) were staged according to Nieuwkoop and Faber (1967). Operation techniques and buffer (MMR, Ubbels, 1983) have been described (Winklbauer, 1990). *Xenopus* embryos were injected with RNA at the 2 and 4-cell stage according to established protocols (Smith and Harland, 1991). For elongation assays, animal cap explants were prepared from stage 8 (all stages according to Nieuwkoop) embryos and treated with activin protein (Piccolo et al., 1996) containing 0.2% bovine serum albumin (BSA).

Antibodies and surface labeling

Indirect immunofluorescence assays were carried out as described previously (Skourides et al., 1999) with modifications. Cells were plated on glass coverslips (the coverslips were first coated with 5 μ g/ml fibronectin for 1 h, washed three times with ice cold phosphate buffered saline (PBS) containing 0.5 mM MgCl₂ and 0.5 mM CaCl₂ (PBS²⁺) and then fixed for 10 min in 4% paraformaldehyde solution in PBS. Fixation was followed by addition of 50 mM glycine solution in PBS and then the cells were permeabilized using 0.2% triton solution in PBS for 10 min. Permeabilized cells were blocked using 10% normal donkey serum (Jackson Immunoresearch, West Gove, PA, USA) for 30 min. Primary antibodies were added in 5% normal donkey serum solution in PBS and were incubated for 30 min. Embryos and explants were fixed in 3.7% formaldehyde in phosphate-buffered saline (PBS) for 2 hours at room temperature and vitelline envelopes removed manually. Following vitelline envelope removal embryos were permeabilised and blocked for 2 hours in 0.5% triton, 5% BSA and 1% Normal Goat or Normal Donkey serum. Primary antibody staining followed using Upstate Biotechnology α -FAK rabbit polyclonal, α -Phospho-FAK rabbit polyclonal, Covance α -HA monoclonal and Phospho-Specific FAK [Tyr397] Polyclonal Antibody, Santa Cruz α -FAK rabbit polyclonal (A17), and Transduction Laboratories α -paxillin-FITC one at a time or in combinations as mentioned. Secondary antibodies were added after overnight PBS + 0.1% triton washes. For focal adhesion visualization after Texas-red goat anti-mouse was used as a secondary antibody (Jackson Immunoresearch) and Texas-red donkey anti-goat (Jackson Immunoresearch) as a tertiary after a two hour wash of the secondary antibody.

Plasmids and Cloning

HA-FAK and HA-FRNK constructs in the mammalian pCDNA3.1 vector (Hauck et al., 2001) were transferred to the CS2++ vector and transcribed into RNA for injections. EGFP fused to a Ras farnesylation sequence (mem-GFP) in the CS2++ vector. Xdd1 as described (Wallingford JB et al., 2000). Full length human Rap1b (V12) or Rap1b (N17) cDNAs in pGBT9 (Bertoni, Tadokoro et al. 2002) were transferred to CS2++

vector and then were transcribed into RNA for injections as above. The fusions of the Akt PH domain to the COOH terminus of enhanced GFP were made by cloning into the pEGFP-C1 vector (Clontech). The AKT-PH-GFP was subsequently transferred to CS2++ and transcribed into RNA for injections.

Explant spreading and Cell Migration assays

The schematic of Figure 1 is a general outline of the way the assays were performed. Dorsal marginal zone explants or animal caps were dissociated in CMFM (Sato and Sargent, 1989) with the addition of 1mM EDTA for 10 minutes and were induced using activin protein in solution. Cells or explants were then placed in four well plates from which the plastic bottom had been removed and a glass cover slip was attached using Silicone Grease. The glass had been previously coated with fibronectin. In the cases where more than one cell population was filmed at the same time small Petri dishes were coated with a thin film of agarose and then small wells were created by punching through the agarose with a cut pipette tip. The individual wells were then coated with FN and cells were placed in them after being dissociated. Explants and dissociated cells were then observed under a Zeiss Axiophot and time lapse movies were made using a Zeiss AxioCam and the Axiovision software and the average speed of migration each batch of cells was calculated.

For the conditioning of substrates and directional migration, animal caps were dissected at stage 8.5 and were then placed face down on a plastic dish in 0.5MMR (The use of 0.5MMR aims at reducing the speed of healing). After an explant is on the dish, a glass coverslip with silicon grease in each of the four corners was gently placed over the explant and pushed down until the explant was flat being careful to not damage in or press too hard. The flat animal cap was then cultured till stage 10 and allowed to condition the underlying plastic. Using a marker, the area over which the cap was cultured was marked as well as the orientation of the explant(dorso-ventral). Furthermore, the location of the top of the animal cap was also marked. After conditioning the coverslip and the explant were both removed and 1X MMR was used to wash the dish twice. FN was used to coat the entire dish and was then followed by treatment with BSA to block any non-specific binding. Explants were placed at the periphery of the conditioned area as well as in other positions within and outside the conditioned area and the behaviour of the explants was monitored using time-lapse video microscopy.

QD Micelle preparation

A simple, 10 minute method was used to encapsulate QDs in PEG-PE/PC micelles. Typically, 100 μ L of ZnS-overcoated CdSe QDs in hexane (170 mg/mL), synthesized according to standard methods (Murray, Norris et al. 1993; Hines and Guyot-Sionnest

1996), were precipitated with methanol and dried under vacuum. The QDs were then suspended in 1mL chloroform with 5.5×10^{-6} moles of phospholipids containing 40% 1,2-dipalmitoyl-*sn*-glycero-3-phosphoethanolamine-N-[methoxy(polyethylene glycol)-2000] (mPEG-2000 PE) and 60% of 1,2-dipalmitoyl-glycero-3-phosphocholine (DPPC), both from Avanti Polar Lipids, Inc., Alabaster, AL. After complete evaporation of the chloroform, the residue was heated at 80C and 1mL of water was added to obtain an optically clear suspension containing PEG-PE/PC micelles. Since this suspension contained both empty micelles and those containing QDs, the empty micelles were removed with ultracentrifugation at 500,000g for two hours. The micelles containing QDs formed a pellet while the empty micelles stayed suspended. The supernatant was discarded and the QD-micelles were resuspended in water.

All of the micelles used in this work contained 60% DPPC due to the initial belief that the DPPC would allow better packing of the PEG chains on the surface of the micelle. However, preliminary results also indicate that QD-micelles made from 100% mPEG-2000 PE are similar in behavior.

Conjugation of QD-micelles with DNA was obtained by replacing 50% of the mPEG-2000 PE with an amino PEG-PE (1,2-distearoyl-*sn*-glycero-3-phosphoethanolamine-N-[amino(polyethylene glycol)2000] (Avanti Polar Lipids, Inc, Alabaster, AL). The DNA (purchased from Midland Certified Reagent Company, Midland, TX) contained a disulfide group at the 5' end. The disulfide bond was cleaved with dithiothreitol (DTT) and the oligonucleotide was purified of excess DTT. The coupling of the DNA to the QD-micelle was performed using Sulfosuccinimidyl 4-(N-maleimidomethyl)cyclohexane-1-carboxylate (Sulfo-SMCC) (Pierce, Rockford, IL).

To determine the number of QDs injected into the embryo, the absorbance of an aqueous suspension of QD-micelles was measured in a cuvette of known path length. From recently reported values for the extinction coefficient of CdSe QDs (Leatherdale, Woo et al. 2002), the concentration of QDs could be obtained.

RNA Labeling and Detection in Vitro

Biotin labeled RNA was transcribed using the BioArray High Yield RNA transcript labeling kit. This kit results in RNA transcripts containing bio-UTP and bio-CTP. The manufacturers protocol was followed with a modification in the total reaction volume which was scaled down to 20 μ l. Two independent genes were transcribed, *Xenopus* amylase (in pCR4Blunt-TOPO) and *Xenopus* LTBP (in CS2++) using the T3 polymerase. RNA from these reactions was purified using Quick Spin columns from Roche to eliminate free nucleotides. Different dilutions of RNA were used to dot blot a nylon membrane and the membrane was then incubated (after thirty minute blocking with 2%BSA) with QD-streptavidin conjugates or with EtBr. After PBS washes individual dots were visualized using a Zeiss Axiophot and a Zeiss Axiocam and the signal intensities compared. To label RNA in solution saturating amounts of QD's were added to the RNA and after phenol extraction free QD's were all removed while QD labeled

RNA remained in the aqueous phase. The supernatant was carefully removed and it contained QD labeled RNA.

Specific Transcript Detection and Visualization in Vivo

Biotinylated RNA was transcribed like above and then used to perform in situ hybridization using the protocol reported by Harland RM (Harland RM, In situ hybridization: an improved whole-mount method for *Xenopus* embryos. *Methods Cell Biol.* 1991;36:685-95.) with modifications. Methanol was substituted with Ethanol and 4% paraformaldehyde in PBS was used to fix the embryos instead of Formaldehyde. After proteinase K treatment embryos were blocked with avidin solution followed by biotin and then washes were performed in PBS. After blocking embryos were refixed for one hour in 4% paraformaldehyde followed by prehybridization at 65C. The original protocol was followed up to the post hybridization washes and then as described below. After the last 0.2X SSC wash at 65C the embryos were blocked with PBS + 2%BSA + 0.2% Triton for one hour and then transferred to a new vial which contained 1ml of a 1:500 dilution of Qdot 605 Streptavidin conjugate in Qdot Incubation Buffer (Quantum Dot Corporation). 1% BSA and 0.1% Triton were added in the incubation buffer and significantly improved penetration and background without appreciably affecting t QD colloidal stability or the signal intensity. After the incubation the embryos were washed in PBS 0.1% Triton 5ml each time for four times half hour each at room temperature. Following the washes the embryos were imaged using a custom filter set (excitation 300-460nm, emission 500nm longpass, dichroic 475nm). Bleaching of endogenous fluorescence by exposure to near UV excitation light immensely improves the signal to noise ratio. Bleached embryos could then be dehydrated in Methanol and clarified by immersion in benzyl benzoate. The fluorescent signal remains localized and allows data acquisition from different planes within the embryo without the need for sectioning. The image acquisition was done using a Zeiss Axiocam and the Axiovision software. The axiovision software allowed careful balancing of the camera in such a way that the green background appears white resulting in a major boost of the red QD signal extreme decrease of the threshold of detection and significantly better contrast. If the calibration of the camera is done properly control embryos that are not labeled with QD's appear completely white under UV excitation without any traces or Red. This color separation method has to be performed carefully and control embryos need to appear white otherwise the risk of creating false staining increases significantly. Due to the fact that the embryo has several distinct regions where the background fluorescence changes not only in terms of intensity but also in terms of spectral balance the region chosen for assignment of "white" was the region in which the background had the longest average wavelength. In this manner we ensured that long average wavelength background regions would appear white and shorter average wavelength regions would appear blue. A similar technique was used for achieving the best color separation using green QD's. In this particular case assigning the average background green as white shifts the QD green to blue. The reason is the lower wavelength of average emission of the QD's compared to the average wavelength of the background fluorescence. Such shift is not observed using

red QD's because removal of the green autofluorescence only leads to a deeper perceived red.

REFERENCES

- Akerman, M. E., W. C. Chan, et al. (2002). "Nanocrystal targeting in vivo." Proc Natl Acad Sci U S A **99**(20): 12617-21.
- Aldana, J., Y. A. Wang, et al. (2001). "Photochemical instability of CdSe nanocrystals coated by hydrophilic thiols." J. Am. Chem. Soc. **123**: 8844-8850.
- Alivisatos, A. P. (1996). "Semiconductor clusters, nanocrystals, and quantum dots." Science **271**: 933-937.
- Alivisatos, A. P., K. P. Johnsson, et al. (1996). "Organization of 'nanocrystal molecules' using DNA." Nature **382**: 609-611.
- Almouzni, G. and A. P. Wolffe (1995). "Constraints on transcriptional activator function contribute to transcriptional quiescence during early *Xenopus* embryogenesis." Embo J **14**(8): 1752-65.
- Amaya, E., T. J. Musci, et al. (1991). "Expression of a dominant negative mutant of the FGF receptor disrupts mesoderm formation in *Xenopus* embryos." Cell **66**(2): 257-70.
- Asha, H., N. D. de Ruyter, et al. (1999). "The Rap1 GTPase functions as a regulator of morphogenesis in vivo." Embo J **18**(3): 605-15.
- Belousov, L. V., N. N. Luchinskaia, et al. (1999). "[Tensotaxis--a collective movement of embryonic cells up along the gradients of mechanical tensions]." Ontogenez **30**(3): 220-8.
- Belousov, L. V., N. N. Louchinskaia, et al. (2000). "Tension-dependent collective cell movements in the early gastrula ectoderm of *Xenopus laevis* embryos." Dev Genes Evol **210**(2): 92-104.
- Belsito, S., R. Bartucci, et al. (2000). "Molecular and mesoscopic properties of hydrophilic polymer-grafted phospholipids mixed with phosphatidylcholine in aqueous dispersion: interaction of dipalmitoyl N-poly(ethylene glycol)phosphatidylethanolamine with dipalmitoylphosphatidylcholine studied by spectrophotometry and spin-label electron spin resonance." Biophys. J. **78**: 1420-1430.
- Boguski, M. S. and F. McCormick (1993). "Proteins regulating Ras and its relatives." Nature **366**(6456): 643-54.
- Bos, J. L., J. de Rooij, et al. (2001). "Rap1 signalling: adhering to new models." Nat Rev Mol Cell Biol **2**(5): 369-77.
- Bruchez, M., M. Moronne, et al. (1998). "Semiconductor nanocrystals as fluorescent biological labels." Science **281**: 2013-2016.
- Burridge, K. and M. Chrzanowska-Wodnicka (1996). "Focal adhesions, contractility, and signaling." Annu Rev Cell Dev Biol **12**: 463-518.
- Burridge, K., K. Fath, et al. (1988). "Focal adhesions: transmembrane junctions between the extracellular matrix and the cytoskeleton." Annu Rev Cell Biol **4**: 487-525.
- Chan, P. Y., S. B. Kanner, et al. (1994). "A transmembrane-anchored chimeric focal adhesion kinase is constitutively activated and phosphorylated at tyrosine residues identical to pp125FAK." J Biol Chem **269**(32): 20567-74.
- Chan, W. C. W. and S. Nie (1998). "Quantum dot bioconjugates for ultrasensitive nonisotopic detection." Science **281**: 2016-2018.

- Chang, F., J. T. Lee, et al. (2003). "Involvement of PI3K/Akt pathway in cell cycle progression, apoptosis, and neoplastic transformation: a target for cancer chemotherapy." Leukemia **17**(3): 590-603.
- Chung, C. Y., G. Potikyan, et al. (2001). "Control of cell polarity and chemotaxis by Akt/PKB and PI3 kinase through the regulation of PAKa." Mol Cell **7**(5): 937-47.
- Coutinho, L. L., J. Morris, et al. (1992). "Whole mount in situ detection of low abundance transcripts of the myogenic factor qmf1 and myosin heavy chain protein in quail embryos." Biotechniques **13**(5): 722-4.
- Crawford, B. D., C. A. Henry, et al. (2003). "Activity and distribution of paxillin, focal adhesion kinase, and cadherin indicate cooperative roles during zebrafish morphogenesis." Mol Biol Cell **14**(8): 3065-81.
- Dahan, M., T. Laurence, et al. (2001). "Time-gated biological imaging by use of colloidal quantum dots." Opt. Lett. **26**: 825-827.
- Davidson, L. A., B. G. Hoffstrom, et al. (2002). "Mesendoderm extension and mantle closure in *Xenopus laevis* gastrulation: combined roles for integrin alpha(5)beta(1), fibronectin, and tissue geometry." Dev Biol **242**(2): 109-29.
- Davidson, L. A. and R. E. Keller (1999). "Neural tube closure in *Xenopus laevis* involves medial migration, directed protrusive activity, cell intercalation and convergent extension." Development **126**(20): 4547-56.
- de Gunzburg, J. (1993). "[Are rap genes anti-oncogenes?]." Bull Cancer **80**(8): 723-7.
- Du, Q. S., X. R. Ren, et al. (2001). "Inhibition of PYK2-induced actin cytoskeleton reorganization, PYK2 autophosphorylation and focal adhesion targeting by FAK." J Cell Sci **114**(Pt 16): 2977-87.
- Dubertret, B., P. Skourides, et al. (2002). "In vivo imaging of quantum dots encapsulated in phospholipid micelles." Science **298**(5599): 1759-62.
- Escalante, R. and W. F. Loomis (1995). "Whole-mount in situ hybridization of cell-type-specific mRNAs in *Dictyostelium*." Dev Biol **171**(1): 262-6.
- Fages, C., M. Kaksonen, et al. (1998). "Regulation of mRNA localization by transmembrane signalling: local interaction of HB-GAM (heparin-binding growth-associated molecule) with the cell surface localizes beta-actin mRNA." J Cell Sci **111** (Pt 20): 3073-80.
- Fox, G. L., I. Rebay, et al. (1999). "Expression of DFak56, a *Drosophila* homolog of vertebrate focal adhesion kinase, supports a role in cell migration in vivo." Proc Natl Acad Sci U S A **96**(26): 14978-83.
- Furuta, Y., D. Ilic, et al. (1995). "Mesodermal defect in late phase of gastrulation by a targeted mutation of focal adhesion kinase, FAK." Oncogene **11**(10): 1989-95.
- Gerhart, J. and R. Keller (1986). "Region-specific cell activities in amphibian gastrulation." Annu Rev Cell Biol **2**: 201-29.
- Gerion, D., W. J. Parak, et al. (2002). "Sorting fluorescent nanocrystals with DNA." J. Am. Chem. Soc. **124**: 7070-7074.
- Gerion, D., F. Pinaud, et al. (2001). "Synthesis and properties of biocompatible water-soluble silica-coated CdSe/ZnS semiconductor quantum dots." J. Phys. Chem. B **105**: 8861-8871.
- Gilmore, A. P. and L. H. Romer (1996). "Inhibition of focal adhesion kinase (FAK) signaling in focal adhesions decreases cell motility and proliferation." Mol Biol Cell **7**(8): 1209-24.

- Golander, C. G., J. N. Herron, et al. (1992). Poly(ethylene glycol) Chemistry. J. M. Harris. New York, Plenum Press: 221-245.
- Goldman, E. R., G. P. Anderson, et al. (2002). "Conjugation of luminescent quantum dots with antibodies using an engineered adaptor protein to provide new reagents for fluoroimmunoassays." Anal. Chem. **74**: 841-847.
- Hardin, J. and R. Keller (1988). "The behaviour and function of bottle cells during gastrulation of *Xenopus laevis*." Development **103**(1): 211-30.
- Haugh, J. M., F. Codazzi, et al. (2000). "Spatial sensing in fibroblasts mediated by 3' phosphoinositides." J Cell Biol **151**(6): 1269-80.
- Heidkamp, M. C., A. L. Bayer, et al. (2002). "GFP-FRNK disrupts focal adhesions and induces anoikis in neonatal rat ventricular myocytes." Circ Res **90**(12): 1282-9.
- Hemmati-Brivanlou, A., D. Frank, et al. (1990). "Localization of specific mRNAs in *Xenopus* embryos by whole-mount in situ hybridization." Development **110**(2): 325-30.
- Henry, C. A., B. D. Crawford, et al. (2001). "Roles for zebrafish focal adhesion kinase in notochord and somite morphogenesis." Dev Biol **240**(2): 474-87.
- Hens, M. D. and D. W. DeSimone (1995). "Molecular analysis and developmental expression of the focal adhesion kinase pp125FAK in *Xenopus laevis*." Dev Biol **170**(2): 274-88.
- Hines, M. A. and P. Guyot-Sionnest (1996). "Synthesis and characterization of strongly luminescing ZnS-capped CdSe nanocrystals." J. Phys. Chem. **100**: 468-471.
- Hristova, K. and D. Needham (1995). "Phase behavior of lipid/polymer-lipid mixture in aqueous medium." Macromol. **28**: 991-1002.
- Hughes, S. C. and H. M. Krause (1998). "Double labeling with fluorescence in situ hybridization in *Drosophila* whole-mount embryos." Biotechniques **24**(4): 530-2.
- Hynes, R. O. (1992). "Integrins: versatility, modulation, and signaling in cell adhesion." Cell **69**(1): 11-25.
- Hynes, R. O., E. L. George, et al. (1992). "Toward a genetic analysis of cell-matrix adhesion." Cold Spring Harb Symp Quant Biol **57**: 249-58.
- Johnson, K. E., T. Darribere, et al. (1993). "Mesodermal cell adhesion to fibronectin-rich fibrillar extracellular matrix is required for normal *Rana pipiens* gastrulation." J Exp Zool **265**(1): 40-53.
- Johnsson, M., P. Hansson, et al. (2001). "Spherical micelles and other self-assembled structures in dilute aqueous mixtures of poly(ethylene glycol) lipids." J. Phys. Chem. B **105**: 8420-8430.
- Jones, M. C. and J. C. Leroux (1999). "Polymeric micelles - a new generation of colloidal drug carriers." Eur. J. Pharm. Biopharm. **48**: 101-111.
- Jowett, T. and Y. L. Yan (1996). "Double fluorescent in situ hybridization to zebrafish embryos." Trends Genet **12**(10): 387-9.
- Kataoka, K., G. S. Kwon, et al. (1993). "Block-copolymer micelles as vehicles for drug delivery." J. Controlled Release **24**: 119-132.
- Keller, R. (1991). "Early embryonic development of *Xenopus laevis*." Methods Cell Biol **36**: 61-113.
- Keller, R., J. Shih, et al. (1992). "The cellular basis of the convergence and extension of the *Xenopus* neural plate." Dev Dyn **193**(3): 199-217.

- Keller, R. E. (1980). "The cellular basis of epiboly: an SEM study of deep-cell rearrangement during gastrulation in *Xenopus laevis*." J Embryol Exp Morphol **60**: 201-34.
- Keller, R. E. (1981). "An experimental analysis of the role of bottle cells and the deep marginal zone in gastrulation of *Xenopus laevis*." J Exp Zool **216**(1): 81-101.
- Keller, R. E., M. Danilchik, et al. (1985). "The function and mechanism of convergent extension during gastrulation of *Xenopus laevis*." J Embryol Exp Morphol **89 Suppl**: 185-209.
- Kitayama, H., Y. Sugimoto, et al. (1989). "A ras-related gene with transformation suppressor activity." Cell **56**(1): 77-84.
- Kuhl, M. and D. Wedlich (1996). "Xenopus cadherins: sorting out types and functions in embryogenesis." Dev Dyn **207**(2): 121-34.
- Kurth, T. and P. Hausen (2000). "Bottle cell formation in relation to mesodermal patterning in the *Xenopus* embryo." Mech Dev **97**(1-2): 117-31.
- Lasic, D. D., M. C. Woodle, et al. (1991). "Phase-behavior of stealth-lipid-lecithin mixtures." Period. Biol. **93**: 287-290.
- Lauffenburger, D. A. and A. F. Horwitz (1996). "Cell migration: a physically integrated molecular process." Cell **84**(3): 359-69.
- Leu, T. H. and M. C. Maa (2002). "Tyr-863 phosphorylation enhances focal adhesion kinase autophosphorylation at Tyr-397." Oncogene **21**(46): 6992-7000.
- Maher, P. A., E. B. Pasquale, et al. (1985). "Phosphotyrosine-containing proteins are concentrated in focal adhesions and intercellular junctions in normal cells." Proc Natl Acad Sci U S A **82**(19): 6576-80.
- Marsden, M. and D. W. DeSimone (2001). "Regulation of cell polarity, radial intercalation and epiboly in *Xenopus*: novel roles for integrin and fibronectin." Development **128**(18): 3635-47.
- Material, S.
- Mattoussi, H., J. M. Mauro, et al. (2000). "Self-assembly of CdSe-ZnS quantum dot bioconjugates using an engineered recombinant protein." J. Am. Chem. Soc. **122**: 12142-12150.
- McLeod, S. J., A. H. Li, et al. (2002). "The Rap GTPases regulate B cell migration toward the chemokine stromal cell-derived factor-1 (CXCL12): potential role for Rap2 in promoting B cell migration." J Immunol **169**(3): 1365-71.
- Meili, R., C. Ellsworth, et al. (1999). "Chemoattractant-mediated transient activation and membrane localization of Akt/PKB is required for efficient chemotaxis to cAMP in *Dictyostelium*." Embo J **18**(8): 2092-105.
- Mikulec, F. (1999). Semiconductor nanocrystal colloids: manganese-doped cadmium selenide, (core)shell composites for biological labeling, and highly fluorescent cadmium telluride. chemistry. Cambridge, Massachusetts Institute of Technology.
- Mirkin, C. A., R. L. Letsinger, et al. (1996). "A DNA-based method for rationally assembling nanoparticles into macroscopic materials." Nature **382**: 607-609.
- Murray, C. B., D. J. Norris, et al. (1993). "Synthesis and characterization of nearly monodisperse CdE (E = S, Se, Te) semiconductor nanocrystallites." J. Am. Chem. Soc. **115**: 8706-8715.
- Nagata, K., H. Itoh, et al. (1989). "Purification, identification, and characterization of two GTP-binding proteins with molecular weights of 25,000 and 21,000 in human

- platelet cytosol. One is the rap1/smg21/Krev-1 protein and the other is a novel GTP-binding protein." J Biol Chem **264**(29): 17000-5.
- Nagel, M. and R. Winklbauer (1999). "Establishment of substratum polarity in the blastocoel roof of the *Xenopus* embryo." Development **126**(9): 1975-84.
- Nakatsuji, N., A. C. Gould, et al. (1982). "Movement and guidance of migrating mesodermal cells in *Ambystoma maculatum* gastrulae." J Cell Sci **56**: 207-22.
- Nakatsuji, N. and K. E. Johnson (1982). "Cell locomotion in vitro by *Xenopus laevis* gastrula mesodermal cells." Cell Motil **2**(2): 149-61.
- Nakatsuji, N. and K. E. Johnson (1983). "Conditioning of a culture substratum by the ectodermal layer promotes attachment and oriented locomotion by amphibian gastrula mesodermal cells." J Cell Sci **59**: 43-60.
- Newport, J. and M. Kirschner (1982). Cell **30**: 675.
- Niehrs, C., R. Keller, et al. (1993). "The homeobox gene gooseoid controls cell migration in *Xenopus* embryos." Cell **72**(4): 491-503.
- Noda, M. (1993). "Structures and functions of the K rev-1 transformation suppressor gene and its relatives." Biochim Biophys Acta **1155**(1): 97-109.
- Noda, M., H. Kitayama, et al. (1989). "Detection of genes with a potential for suppressing the transformed phenotype associated with activated ras genes." Proc Natl Acad Sci U S A **86**(1): 162-6.
- O'Neill, J. W. and E. Bier (1994). "Double-label in situ hybridization using biotin and digoxigenin-tagged RNA probes." Biotechniques **17**(5): 870, 874-5.
- Paine, P. L., L. C. Moore, et al. (1975). "Nuclear envelope permeability." Nature **254**(5496): 109-14.
- Palacios, I. M. and D. St Johnston (2001). "Getting the message across: the intracellular localization of mRNAs in higher eukaryotes." Annu Rev Cell Dev Biol **17**: 569-614.
- Palecek, S. P., C. E. Schmidt, et al. (1996). "Integrin dynamics on the tail region of migrating fibroblasts." J Cell Sci **109** (Pt 5): 941-52.
- Palmer, R. H., L. I. Fessler, et al. (1999). "DFak56 is a novel *Drosophila melanogaster* focal adhesion kinase." J Biol Chem **274**(50): 35621-9.
- Pang, K. M., E. Lee, et al. (1998). "Use of a fusion protein between GFP and an actin-binding domain to visualize transient filamentous-actin structures." Curr Biol **8**(7): 405-8.
- Pante, N. and M. Kann (2002). "Nuclear pore complex is able to transport macromolecules with diameters of about 39 nm." Mol Biol Cell **13**(2): 425-34.
- Parak, W. J., R. Boudreau, et al. (2002). "Cell motility and metastatic potential studies based on quantum dot imaging of phagokinetic tracks." Adv. Mater. **14**: 882-885.
- Pathak, S., S. K. Choi, et al. (2001). "Hydroxylated quantum dots as luminescent probes for in situ hybridization." J. Am. Chem. Soc. **123**: 4103-4104.
- Pizon, V., I. Lerosey, et al. (1988). "Nucleotide sequence of a human cDNA encoding a ras-related protein (rap1B)." Nucleic Acids Res **16**(15): 7719.
- Prioleau, M. N., J. Huet, et al. (1994). "Competition between chromatin and transcription complex assembly regulates gene expression during early development." Cell **77**(3): 439-49.

- Ramos, J. W. and D. W. DeSimone (1996). "Xenopus embryonic cell adhesion to fibronectin: position-specific activation of RGD/synergy site-dependent migratory behavior at gastrulation." J Cell Biol **134**(1): 227-40.
- Ramos, J. W., C. A. Whittaker, et al. (1996). "Integrin-dependent adhesive activity is spatially controlled by inductive signals at gastrulation." Development **122**(9): 2873-83.
- Richardson, A. and T. Parsons (1996). "A mechanism for regulation of the adhesion-associated proteintyrosine kinase pp125FAK." Nature **380**(6574): 538-40.
- Ridyard, M. S. and E. J. Sanders (1999). "Potential roles for focal adhesion kinase in development." Anat Embryol (Berl) **199**(1): 1-7.
- Ridyard, M. S. and E. J. Sanders (2000). "Comparison between the in vivo and in vitro expression of three adhesion-signaling proteins in embryonic cells." Cell Biol Int **24**(10): 669-80.
- Ridyard, M. S. and E. J. Sanders (2001). "Inhibition of focal adhesion kinase expression correlates with changes in the cytoskeleton but not apoptosis in primary cultures of chick embryo cells." Cell Biol Int **25**(3): 215-26.
- Rosenthal, S. J., A. Tomlinson, et al. (2002). "Targeting cell surface receptors with ligand-conjugated nanocrystals." J. Am. Chem. Soc. **124**: 4586-4594.
- Sasaki, K., M. Sato, et al. (2003). "Fluorescent indicators for Akt/protein kinase B and dynamics of Akt activity visualized in living cells." J Biol Chem **278**(33): 30945-51.
- Schaller, M. D., C. A. Borgman, et al. (1993). "Autonomous expression of a noncatalytic domain of the focal adhesion-associated protein tyrosine kinase pp125FAK." Mol Cell Biol **13**(2): 785-91.
- Scheid, M. P. and J. R. Woodgett (2003). "Unravelling the activation mechanisms of protein kinase B/Akt." FEBS Lett **546**(1): 108-12.
- Selchow, A. and R. Winklbauer (1997). "Structure and cytoskeletal organization of migratory mesoderm cells from the Xenopus gastrula." Cell Motil Cytoskeleton **36**(1): 12-29.
- Servant, G., O. D. Weiner, et al. (2000). "Polarization of chemoattractant receptor signaling during neutrophil chemotaxis." Science **287**(5455): 1037-40.
- Seydoux, G. and A. Fire (1995). "Whole-mount in situ hybridization for the detection of RNA in Caenorhabditis elegans embryos." Methods Cell Biol **48**: 323-37.
- Skourides, P. A., S. A. Perera, et al. (1999). "Polarized distribution of Bcr-Abl in migrating myeloid cells and co-localization of Bcr-Abl and its target proteins." Oncogene **18**(5): 1165-76.
- Smith, J. C., K. Symes, et al. (1990). "Mesoderm induction and the control of gastrulation in Xenopus laevis: the roles of fibronectin and integrins." Development **108**(2): 229-38.
- Sokol, S. Y. (1996). "Analysis of Dishevelled signalling pathways during Xenopus development." Curr Biol **6**(11): 1456-67.
- Song, B. H., S. C. Choi, et al. (2003). "Local activation of protein kinase A inhibits morphogenetic movements during Xenopus gastrulation." Dev Dyn **227**(1): 91-103.
- St Johnston, D. (1995). "The intracellular localization of messenger RNAs." Cell **81**(2): 161-70.

- Stancheva, I. and R. R. Meehan (2000). "Transient depletion of xDnmt1 leads to premature gene activation in *Xenopus* embryos." Genes Dev **14**(3): 313-27.
- Tada, M. and J. C. Smith (2000). "Xwnt11 is a target of *Xenopus* Brachyury: regulation of gastrulation movements via Dishevelled, but not through the canonical Wnt pathway." Development **127**(10): 2227-38.
- Tautz, D. and C. Pfeifle (1989). "A non-radioactive in situ hybridization method for the localization of specific RNAs in *Drosophila* embryos reveals translational control of the segmentation gene hunchback." Chromosoma **98**(2): 81-5.
- Torchilin, V. P. (2002). "PEG-based micelles as carriers of contrast agents for different imaging modalities." Adv. Drug Delivery Rev. **54**: 235-252.
- Valencia, A., P. Chardin, et al. (1991). "The ras protein family: evolutionary tree and role of conserved amino acids." Biochemistry **30**(19): 4637-48.
- Wacker, S., A. Brodbeck, et al. (1998). "Patterns and control of cell motility in the *Xenopus* gastrula." Development **125**(10): 1931-42.
- Wallingford, J. B. and R. M. Harland (2001). "*Xenopus* Dishevelled signaling regulates both neural and mesodermal convergent extension: parallel forces elongating the body axis." Development **128**(13): 2581-92.
- Watson, A., X. Wu, et al. (2003). "Lighting up cells with quantum dots." Biotechniques **34**(2): 296-300, 302-3.
- Watton, S. J. and J. Downward (1999). "Akt/PKB localisation and 3' phosphoinositide generation at sites of epithelial cell-matrix and cell-cell interaction." Curr Biol **9**(8): 433-6.
- Weinstein, D. C., J. Marden, et al. (1998). "FGF-mediated mesoderm induction involves the Src-family kinase Laloo." Nature **394**(6696): 904-8.
- Weliky, M., S. Minsuk, et al. (1991). "Notochord morphogenesis in *Xenopus laevis*: simulation of cell behavior underlying tissue convergence and extension." Development **113**(4): 1231-44.
- Whiteman, E. L., H. Cho, et al. (2002). "Role of Akt/protein kinase B in metabolism." Trends Endocrinol Metab **13**(10): 444-51.
- Wilson, A. J., A. Velcich, et al. (2002). "Novel detection and differential utilization of a c-myc transcriptional block in colon cancer chemoprevention." Cancer Res **62**(21): 6006-10.
- Wilson, P. and R. Keller (1991). "Cell rearrangement during gastrulation of *Xenopus*: direct observation of cultured explants." Development **112**(1): 289-300.
- Winklbauer, R. (1990). "Mesodermal cell migration during *Xenopus* gastrulation." Dev Biol **142**(1): 155-68.
- Winklbauer, R. and R. E. Keller (1996). "Fibronectin, mesoderm migration, and gastrulation in *Xenopus*." Dev Biol **177**(2): 413-26.
- Winklbauer, R. and M. Nagel (1991). "Directional mesoderm cell migration in the *Xenopus* gastrula." Dev Biol **148**(2): 573-89.
- Winklbauer, R., M. Nagel, et al. (1996). "Mesoderm migration in the *Xenopus* gastrula." Int J Dev Biol **40**(1): 305-11.
- Winklbauer, R. and M. Schurfeld (1999). "Vegetal rotation, a new gastrulation movement involved in the internalization of the mesoderm and endoderm in *Xenopus*." Development **126**(16): 3703-13.

- Winklbauer, R. and A. Selchow (1992). "Motile behavior and protrusive activity of migratory mesoderm cells from the *Xenopus* gastrula." Dev Biol **150**(2): 335-51.
- Winklbauer, R., A. Selchow, et al. (1992). "Cell interaction and its role in mesoderm cell migration during *Xenopus* gastrulation." Dev Dyn **195**(4): 290-302.
- Winter, J. O., T. Y. Liu, et al. (2001). "Recognition molecule directed interfacing between semiconductor quantum dots and nerve cells." Adv. Mater. **13**: 1673-1677.
- Wu, X., H. Liu, et al. (2003). "Immunofluorescent labeling of cancer marker Her2 and other cellular targets with semiconductor quantum dots." Nat Biotechnol **21**(1): 41-6.
- Yamanaka, H., T. Moriguchi, et al. (2002). "JNK functions in the non-canonical Wnt pathway to regulate convergent extension movements in vertebrates." EMBO Rep **3**(1): 69-75.
- Yaniv, K. and J. K. Yisraeli (2001). "Defining cis-acting elements and trans-acting factors in RNA localization." Int Rev Cytol **203**: 521-39.
- Yap, A. S., B. R. Stevenson, et al. (1995). "Vinculin localization and actin stress fibers differ in thyroid cells organized as monolayers or follicles." Cell Motil Cytoskeleton **32**(4): 318-31.
- Yoneda, Y., N. Imamoto-Sonobe, et al. (1987). "Reversible inhibition of protein import into the nucleus by wheat germ agglutinin injected into cultured cells." Exp Cell Res **173**(2): 586-95.
- Zamir, E., Z. Kam, et al. (1997). "Transcription-dependent induction of G1 phase during the zebra fish midblastula transition." Mol Cell Biol **17**(2): 529-36.
- Zhang, X., C. V. Wright, et al. (1995). "Cloning of a *Xenopus laevis* cDNA encoding focal adhesion kinase (FAK) and expression during early development." Gene **160**(2): 219-22.